

Revista **ALCONPAT**

Latin American Journal of Quality Control, Pathology and Construction Recovery

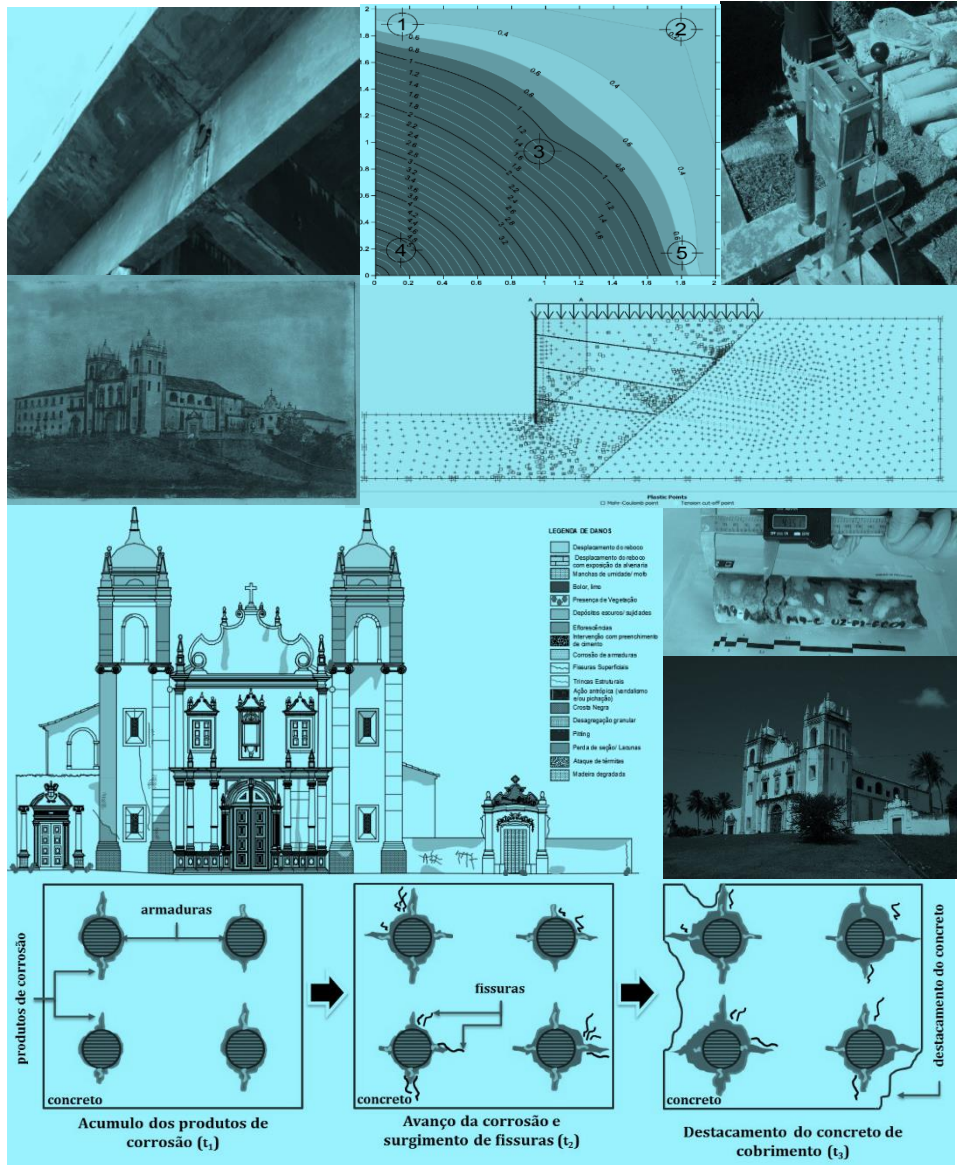
DOI: <http://dx.doi.org/10.21041/ra.v8i1>
editorial@revistaalconpat.org

eISSN: 2007-6835

Volume 8

January - April 2018

Issue 1



Latin American Journal of Quality Control, Pathology and Construction Recovery

<http://www.revistaalconpat.org>



ALCONPAT International

Founders members:

Liana Arrieta de Bustillos – **Venezuela**
Antonio Carmona Filho - **Brazil**
Dante Domene – **Argentina**
Manuel Fernández Cánovas – **Spain**
José Calavera Ruiz – **Spain**
Paulo Helene, **Brazil**

Board of Directors International:

President of Honor

Angélica Ayala Piola, **Paraguay**

President

Carmen Andrade Perdrix, **Spain**

General Director

Pedro Castro Borges, **Mexico**

Executive Secretary

José Iván Escalante García, **Mexico**

Technical Vice President

Enio Pazini Figueiredo, **Brazil**

Administrative Vice President

Luis Álvarez Valencia, **Guatemala**

Manager

Paulo Helene, **Brazil**

Revista ALCONPAT

Editor in Chief:

Dr. Pedro Castro Borges
Centro de Investigación y de Estudios Avanzados del Instituto
Politécnico Nacional, Unidad Mérida (CINVESTAV IPN –
Mérida)
Merida, Yucatan, **Mexico**

Co-Editor in Chief:

Arch. Margita Kliwer
Universidad Católica “Nuestra Señora de la Asunción”
Asuncion, Paraguay

Executive Editor:

Dr. José Manuel Mendoza Rangel
Universidad Autónoma de Nuevo León, Facultad de Ingeniería
Civil
Monterrey, Nuevo Leon, **Mexico**

Associate Editors:

Dr. Manuel Fernandez Canovas Universidad
Politécnica de Madrid. Madrid, **Spain**

Ing. Raúl Husni

Facultad de Ingeniería Universidad de Buenos Aires. Buenos
Aires, **Argentina**

Dr. Paulo Roberto do Lago Helene

Universidade de São Paulo.

São Paulo, **Brazil**

Dr. José Iván Escalante García

Centro de Investigación y de Estudios Avanzados del
Instituto Politécnico Nacional (Unidad Saltillo) Saltillo,
Coahuila, **Mexico**.

Dr. Mauricio López.

Departamento de Ingeniería y Gestión de la Construcción,
Escuela de Ingeniería,
Pontificia Universidad Católica de Chile
Santiago de Chile, **Chile**

Dra. Oladis Troconis de Rincón Centro de Estudios de

Corrosión Universidad de Zulia

Maracaibo, **Venezuela**

Dr. Fernando Branco Universidad

Técnica de Lisboa

Lisboa, **Portugal**

Dr. Pedro Garcés Terradillos

Universidad de Alicante

San Vicente, **Spain**

Dr. Andrés Antonio Torres Acosta

Instituto Mexicano del Transporte / Universidad Marista de
Querétaro

Querétaro, **Mexico**

Dr. Luiz Fernández Luco

Universidad de Buenos Aires – Facultad de Ingeniería –
INTECIN

Buenos Aires, **Argentina**

**JOURNAL OF THE LATIN-AMERICAN
ASSOCIATION OF QUALITY CONTROL,
PATHOLOGY AND RECOVERY OF
CONSTRUCTION**

<http://www.revistaalconpat.org>

With great satisfaction, we present the first issue of the eighth year of the ALCONPAT journal.

The aim of the journal is to publish case studies within the scope of the Association, namely quality control, pathology and recovery of constructions, including basic and applied research, reviews and documentary research.

The V8 N1 issue begins with a research from **Brazil**, in which Emerson Felix et al analyze and numerically model the corrosion process, estimating the service life of concrete structures. The modelling process was divided in two stages, initiation and propagation. The modeling of the initiation phase was carried out by Artificial Neural Networks (ANN), and the modeling of the propagation phase was done by means of Finite Element Method (FEM). The results show the efficiency of the model generated by the coupling of ANN to the FEM to analyze and study the durability of reinforced concrete structures under uniform corrosion, as well as the numerical model applicability to estimate the service life of reinforced concrete structures.

The second paper comes from **Mexico**, where Tezozomoc López et al discuss about the electrochemical behavior of reinforced concrete elements without and with addition of sodium chloride (NaCl) in the mixing water. They were exposed in a marine/tropical environment and the monitoring consisted of measuring corrosion potential (E_{corr}), carbonation front advance (xCO_2) and photographic record of the concrete/steel interface at different stages of the exposure time. The addition of NaCl in the mixing water favored the advancement of carbonation in the outdoor exposure, without showing the beginning of corrosion. The presence of chloride was decisive in the beginning and development of the process of corrosion for both, exposure to the outdoor and immersion.

In the third paper from **Brazil**, Romildo Alves et al present an experimental program to investigating the potential of the use of sugarcane bagasse ash as a partial replacement of cement in the production of mortars. Sugarcane bagasse ashes from two origins were studied - one from sugarcane industry and other from pizzerias that use this material in replacement of the wood in their ovens. The methodology followed the characterization of the material, where it was carried out through laboratory tests using X-ray diffraction (XRD) and X-ray fluorescence (WDXRF) and initial tests for the ideal quantification of cement substitution by residues. Results obtained indicated that both residues exhibited pozzolanic features presenting about 60% of amorphous material in their

composition. Compressive strength tests at different ages showed satisfactory results. The paper concludes that residues played an important role in increasing short and long term compressive strengths.

The fourth paper, by Othavio Toniasso Takeda and Wellington Mazer, from **Brazil**, discusses the potential of thermographic analysis in the evaluation of pathological manifestations in building façades. Its use can aid in identification and diagnosis, reducing the time and costs of these activities. To implement this technique, the calibration of the thermal sensor was performed, and the tests were performed in two different periods of sunlight. The results showed that the application of thermographic analysis allows the identification and measurement of the extent of hidden pathological manifestations in façade cladding systems, including difficult access sites, complementing the results of visual inspections and reducing their subjectivity.

The fifth work of this number is written by Eudes de Arimatéa Rocha et al from **Brazil**. They present the elaboration and implementation of a damage map in a 16th century building with the aim of promoting the preservation of this historical-cultural heritage. The study adopts the elaboration of the damage map from the damage identification sheets developed during the inspections, configuring itself as an important tool to register problems and guide the prophylaxis services. The complexity of the analysis of historical buildings is emphasized, since it is essential to know the techniques and materials used in these constructions. It is concluded that the use of the indicated stages, in the elaboration of the map of damages, provides subsidies that facilitate the analysis of the symptomatology and the correct diagnosis, guaranteeing a more reliable treatment.

In the sixth work, from **Brazil**, Alexandre Machado and Luiz Carlos Mendes investigate the load behavior on the tie rods of anchored curtain walls built to eliminate geological-geotechnical hazards on hillsides in the city of Rio de Janeiro. Taking into account increases in overload due to the growth in construction uphill of these structures and the end of their service lives, a simulation was conducted using the Plaxis computational system to estimate the loads on the tie rods of 20 anchored curtains after 50 years. Those results were compared with results obtained from residual load verification tests. The comparison shows that although the theoretical simulations indicate increases in loads over 50 years due to the additional overloads, the tie rods tend to lose load, even with increased overloads in the anchored curtains.

In the seventh work, from **Brazil**, Clayton José Gomes Silva et al discuss the structural and functional conditions of 332 bridges and viaducts of the Federal Highways of Pernambuco, adopting as methodology the database of the National Department of Infrastructure of Transportation (DNIT) and structural inspections that constitute the sample studied. The information obtained was analyzed according to criteria of the standard DNIT 010/2004 – PRO and standard ABNT NBR 9452/2016. It is the first survey in Brazil with such quantity of structures using two

normative systems. Although with the limitations of this type of study, the conclusions show that it means a contribution to improvement of the Brazilian's highways bridges that, in general, suffer from the same problems that exist in the analyzed bridges.

The article that closes the edition is from Erick Maldonado et al from **Mexico**. They present and discuss the results of a corrosion inspection, as well as a repair proposal for the external walls of a reinforced concrete tower which is in the southern coast of the Veracruz state. The inspection included a drone guided damage survey together with physical, chemical, mechanical and electrochemical tests that allowed the concrete characterization and corrosion damage. The governing deterioration mechanism of the structure was carbonation of concrete. However, the sulfate emission in this industrial environment was reflected on the compressive strength, cracks and delaminations. These conditions were taken into account on the proposed actions for repairing and extending the service life of the structure.

This first issue of the year opens with good news because we are launching a new version of the OJS platform where you can now consult statistics and other parameters that you did not have before. The portal is now fully translated into English and Portuguese and has English as the default language. As a result, our citation index increased considerably during 2017 in Google Scholar. Likewise, Revista ALCONPAT is already indexed in the SciELO Citation Index, a Web of Science integral database, which places us in the forefront of evaluation for our future incorporation to the WoS Journal Citation Reports (JCR).

We are confident that the articles in this issue will be an important reference for those readers involved with issues of modeling applications and service life, as well as inspections with modern and / or improved methodologies. We thank the authors participating in this issue for their willingness and effort to present quality articles and meet the established times.

For the Editorial Board

A handwritten signature in black ink, appearing to read 'Pedro Castro Borges', written over a circular stamp or seal.

Pedro Castro Borges
Editor in Chief



CONTENT

BASIC RESEARCH

E. F. Felix, T. J. Rodrigues Balabuch, M. Corrêa Posterli, E. Possan, R. Carrazedo: Useful life analysis of reinforced concrete structure under uniform corrosion through ANN model coupled to the FEM.

1

APPLIED RESEARCH

M. R. Sosa, T. Pérez, V. M. J. Moo-Yam, E. Chávez, J. T. Pérez-Quiroz: Analysis of the concrete-steel interface in specimens exposed to the weather and immersed in natural sea water.

16

R. A. Berenguer, F. A. Nogueira Silva, S. Marden Torres, E. C. Barreto Monteiro, P. Helene, A. A. de Melo Neto: On the influence of sugarcane bagasse ashes as a partial replacement of cement in compressive strength of mortars.

30

O. T. Takeda, W. Mazer: Potential of thermographic analysis to evaluate pathological manifestations in facade cladding systems.

38

E. A. Rocha, J. V. S. Macedo, P. Correia, E. C. Barreto Monteiro: Adaptation of damages map to historical buildings with pathological problems: Case study of the Carmo's Church in Olinda PE.

51

A. X. Machado, L. C. Mendes: Load check on anchored curtains located in geotechnical hazard areas in the city of Rio de Janeiro.

64

C. J. G. Silva, E. C. Barreto Monteiro, J. P. A. Vitória: Structural and functional conditions of bridges and viaducts of the federal highways of Pernambuco.

79

CASE STUDY

E. E. Maldonado-Bandala, D. Nieves-Mendoza, J. L. Vela-Jiménez, P. Castro-Borges: Evaluation of pathologies associated with carbonation and sulphates in a concrete tower with more than 50 years of service.

94



Service life analysis of reinforced concrete structure under uniform corrosion through ANN model coupled to the FEM

E. F. Felix^{*1}, T. J. Rodrigues Balabuch¹, M. Corrêa Posterlli¹, E. Possan², R. Carrazedo¹

*Corresponding author: emerson.felipe.felix@gmail.com

DOI: <http://dx.doi.org/10.21041/ra.v8i1.256>

Received: 24/08/2017 | Accepted: 15/12/2017 | Published: 30/01/2018

ABSTRACT

The present work intends to analyze and numerically model the corrosion process, estimating the service life of concrete structures. The modelling process was divided in two stages, initiation and propagation. The modeling of the initiation phase was carried out by Artificial Neural Networks (ANN), and the modeling of the propagation phase was done by means of Finite Element Method (FEM). The results show the efficiency of the model generated by the coupling of ANN to the FEM to analyze and study the durability of reinforced concrete structures under uniform corrosion, and the numerical model applicability to estimate the service life of reinforced concrete structures.

Keywords: reinforced concrete; reinforcement corrosion; service life; Artificial Neural Networks; Finite Element Method.

Cite as: E. F. Felix, T. J. Rodrigues Balabuch, M. Corrêa Posterlli, E. Possan, R. Carrazedo (2018), “*Service life analysis of reinforced concrete structure under uniform corrosion through ANN model coupled to the FEM*”, Revista ALCONPAT, 8 (1), pp. 1-15, DOI: <http://dx.doi.org/10.21041/ra.v8i1.256>

¹ Escola de Engenharia de Sao Carlos, Universidade de Sao Paulo, Brasil.

² Universidade Federal da Integração Latino-Americana, Brasil.

Legal Information

Revista ALCONPAT is a quarterly publication of the Latinamerican Association of quality control, pathology and recovery of construction- International, A. C., Km. 6, antigua carretera a Progreso, Mérida, Yucatán, C.P. 97310, Tel.5219997385893, alconpat.int@gmail.com, Website: www.alconpat.org

Editor: Dr. Pedro Castro Borges. Reservation of rights to exclusive use No.04-2013-011717330300-203, eISSN 2007-6835, both awarded by the National Institute of Copyright. Responsible for the latest update on this number, ALCONPAT Informatics Unit, Ing. Elizabeth Sabido Maldonado, Km. 6, antigua carretera a Progreso, Mérida, Yucatán, C.P. 97310.

The views expressed by the authors do not necessarily reflect the views of the publisher.

The total or partial reproduction of the contents and images of the publication without prior permission from ALCONPAT International A.C. is not allowed.

Any discussion, including authors reply, will be published on the third number of 2018 if received before closing the second number of 2018.

Análise da vida útil de estruturas de concreto armado sob corrosão uniforme por meio de um modelo com RNA acoplado ao MEF

RESUMO

O presente trabalho apresenta uma análise numérica da vida útil de estruturas de concreto armado sujeitas à corrosão uniforme. O processo de modelagem foi dividido em dois estágios, iniciação e propagação. A modelagem da fase de iniciação foi feita via Redes Neurais Artificiais (RNA) enquanto que a fase de propagação foi modelada através do Método dos Elementos Finitos (MEF). Os resultados demonstram que o modelo gerado pelo acoplamento das RNA ao MEF, possibilita de forma eficiente, a simulação da degradação de estruturas de concreto armado devido à ação da corrosão uniforme e, a aplicabilidade da ferramenta numérica quanto a previsão da vida útil destas estruturas.

Palavras chave: concreto armado; corrosão de armaduras; vida útil; Redes Neurais Artificiais; Método dos Elementos Finitos.

Análisis de la vida útil de estructuras de hormigón armado bajo la acción de corrosión uniforme a través del modelo con RNA acoplado al MEF

RESUMEN

Este estudio tiene como objetivo analizar y estimar la vida útil de estructuras de hormigón armado bajo la acción de corrosión uniforme. El modelado se dividió en dos etapas, iniciación y propagación. El modelado de la fase de iniciación fue realizado por medio de Redes Neuronales Artificiales (RNA) y el modelado de la fase de propagación fue hecho por medio del Método de los Elementos Finitos (MEF). El acoplamiento de la RNA en el MEF permitió analizar y estudiar la durabilidad de estructuras de hormigón armado bajo la acción de corrosión uniforme, presentándose como una metodología alternativa para la estimación del tiempo de vida útil de estas estructuras.

Palabras clave: hormigón armado; corrosión de las armaduras; vida útil; Redes Neuronales Artificiales; Método de los Elementos Finitos.

1. INTRODUCTION

Among the factors for the sustainable development and economic growth of modern society are the reliability and durability of structures and infrastructure facilities, especially reinforced concrete structures. However, such structural systems are vulnerable to deterioration processes resulting from chemical degradation and physical damage, which, over time, can lead to unsatisfying structural performance under service loads or accidental actions.

In the last years, there have been significant advances in modeling, analysis and design areas relate to the deterioration in structures, besides as new approaches have been proposed to evaluate the service life of structures (Ellingwood, 2016; Biondini et al., 2017, Andrade et al., 2017).

The corrosion of reinforcement is the pathological manifestation with the highest occurrence rate in reinforced concrete structures (KARI et al., 2014). In Brazil, for example, this rate varies from 14 to 64% depending on analysis zone (Carmona et al., 1988; Dal Molin, 1988; Andrade, 1992).

A precise and computationally efficient structural modeling of corrosion deterioration is an essential for structural reliability and service life analysis in order to reduce the maintenance costs of structures; especially reinforced concrete structures (Vu et al., 2000, Rao et al., 2017).

Corrosion of steel reinforcement in concrete is an electrochemical process caused by differences in the concentrations of dissolved ions, so that part of the metal becomes cathodic and another anodic, resulting in the loss of material volume and the formation of corrosion products, which is a secondary material with a volume of 3 to 10 times greater than the initial one (Mehta et al., 2014; Geiker et al., 2016).

Concrete damage modeling due to uniform corrosion has been used phenomenological processes that segment and synthesize steel corrosion, immersed in reinforced concrete, in two stages, initiation and propagation.

The initiation phase corresponds to the period that the transport of aggressive agents (CO₂) occurs in the porous matrix of concrete, resulting in reducing the pH (from approximately 12.5 to 8.5) and in the depassivation of steel reinforcement. Conversely, the propagation phase is characterized by the loss of steel mass and the formation of corrosion products, which causes cracking of concrete cover or, in advanced stages, the concrete spalling (Tuutti, 1982; Bakker, 1988; Rao et al. al., 2017).

The projects costs of reinforced concrete structures that consider only the initiation period for corrosion are not the most economical, precisely because they do not consider the maintenance costs caused during the corrosion propagation, an important consideration in the service life analysis of reinforced concrete structures (Yanaka et al., 2016).

Given the above, this work analyzes the service life of reinforced concrete structures through the coupling of two models, one responsible for the time estimation at which occurs the steel depassivation (design life - DL) and another referring to the time at which the concrete element reaches the serviceability limit state (service life - SL).

2. SERVICE LIFE OF CONCRETE STRUCTURES UNDER CORROSION

The service life, safety, reliability and risk of civil infrastructure systems have become emerging problems in recent years due to natural and human disasters, sustainability issues and global warming.

The durability management of civil infrastructure involves significant expenses and, in an era of limited public resources, requires difficult decisions to establish maintenance, rehabilitation, and replacement priorities. In this regard, the definition of service life stands out as an important concept, which serves as the basis for a holistic design approach. Structures should be designed for structural safety and maintenance for a specified period, which includes a design for durability and sustainability. With the aim of design a structure with a low-maintenance during its service life, measures must be taken in the early stages of design, and it is necessary to carry out the control during the structure service life (Ellingwood et al., 2016).

Corrosion is one of the main causes of reduced service life of reinforced concrete structures, since this involves the material loss from steel surface as a result of a chemical action. The material loss leads to an effective area reduction of cross section, and, consequently, decreased load-bearing capacity.

However, corrosion can be delayed by adopting a medium or high durability concrete (depending on the exposure environment) or by considering a suitable thickness for the concrete cover. Broomfield (2007) and Dyer (2015) report that the lower the concrete cover and quality, the greater the corrosion possibility and, consequently, its degradative effects, e.g., the cracking in concrete.

The concrete alkalinity is due to the high concentrations of soluble calcium, sodium and potassium oxides present in the concrete microscopic pores. These oxides form hydroxides, alkaline in the presence of water, creating an optimal pH condition (between 12 and 13). In this way, the concrete protects the steel from corrosion both physically by forming a protective layer

for the reinforcement, and chemically through of the alkaline condition that induces the formation of a passive film on the steel surface, very dense, thin layer of oxide, and leading to a very slow rate of corrosion (Broomfield, 2007; Köliö et al., 2017).

The uniform corrosion process, carbonation corrosion, can be segmented into two phases, initiation and propagation. The diffusion process of CO₂ characterizes the initiation phase. Carbon dioxide enters the concrete porous matrix reacting with the calcium hydroxides (Ca(OH)₂) present in the cement paste, leading to the formation of calcium carbonate (CaCO₃) (Figure 1). In the literature, this process is called carbonation, and is responsible for some alterations in carbonated concrete, e.g., permeability reduction (Neville, 1997). In addition, this process reduces the pH of concrete (approximately 12.5 to 8.5), resulting in the destruction of a chemical layer that protects steel from corrosion mechanisms (Chang et al., 2006) (Figure 1).

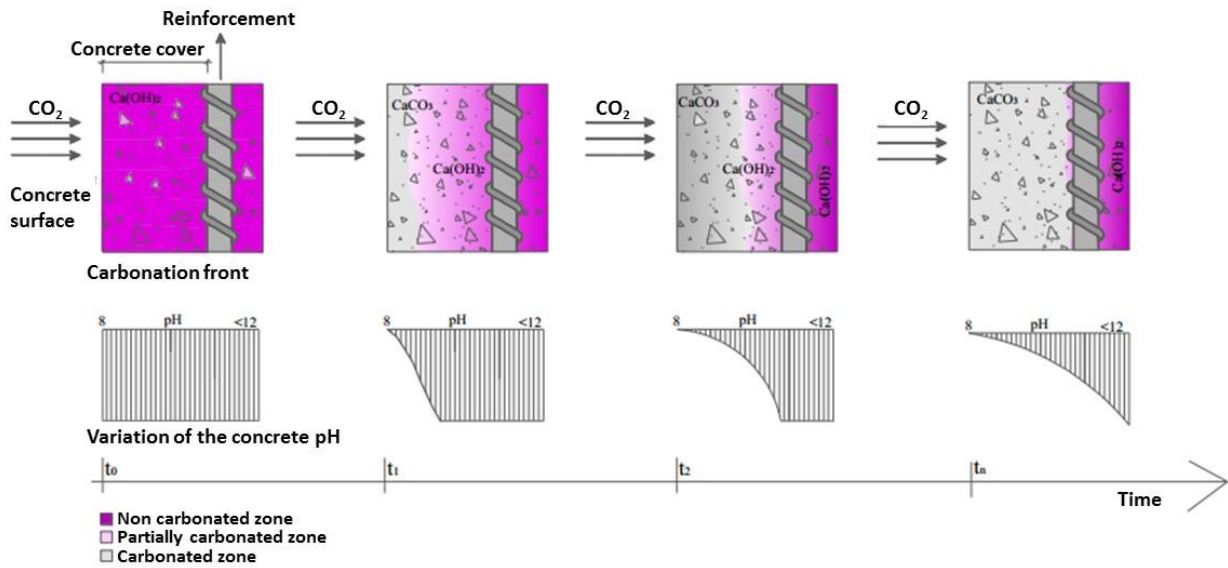


Figure 1. Advance of carbonation front vs pH reduction in concrete (Possan, 2010).

The carbonation reaction begins at the concrete surface progressing internally over time. As the carbonation front reaches the steel depth, the corrosion progression phase begins, with no actual damage to the structure to this point (Tuutti, 1982; Possan, 2010; Köliö et al., 2017).

In the propagation stage, for the corrosion products formation, it is necessary, firstly, the transformation of ferrous hydroxide into ferric hydroxide (1), and then, the transformation into hydrated ferric oxide, also called the corrosion product (2).



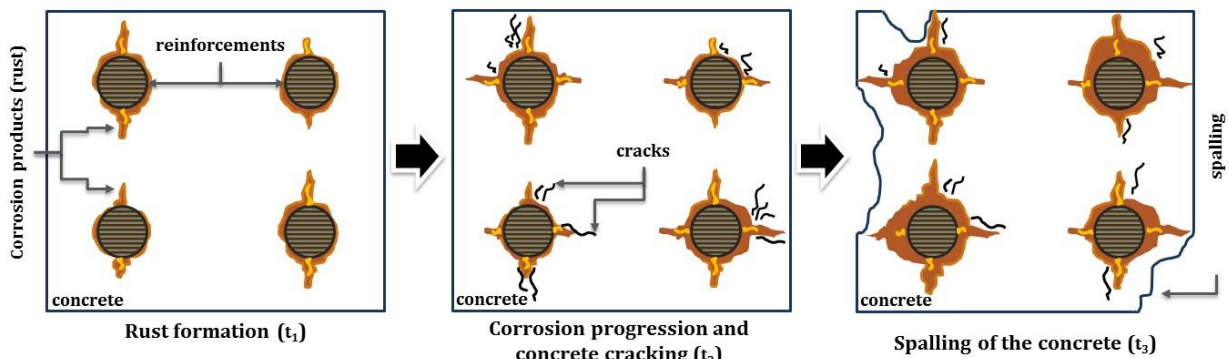


Figure 2. Stages of concrete damage during the period of corrosion progression.

Propagation is determined by the corrosion rate (governed by oxygen availability, relative humidity and temperature) and by the capacity of concrete cover to withstand internal stresses. The unhydrated ferric oxide (Fe_2O_3) has a volume of about twice that of steel it replaces when fully dense. Ferric oxide upon hydration expands further, becoming porous, increasing the volume at the steel-concrete interface about six to ten times, and causing loss of effective steel area.

The concrete expansion due to formation of corrosion products results in the cracking of concrete cover, this occurs when the stresses induced by the increasing layer of corrosion products exceed the tensile strength capacity of concrete, especially in structures with low concrete covers. The cracking in concrete facilitates and accelerates the diffusion of external agents, and may cause greater damages to the concrete, e.g., the concrete spalling (Figure 2), where a whole segment of concrete cover detaches from the structure surface. (Broomfield, 2007; Köliö et al., 2017).

3. CONCRETE STRUCTURES SERVICE LIFE

3.1 Description of the implemented model for the service life analysis

In order to determine the service life of reinforced concrete structures subjected to uniform corrosion, a FORTRAN code was developed. The code possibilities the geometric non-linear structure analysis of two-dimensional fibers composites solid based on the Positional Finite Element Method (PFEM) described in Coda (2003). To represent and simulate the effects and damages from the uniform corrosion propagation phase, an adaptation was made in the code, where the useful steel area of the reinforcement is actualized in function of the corrosion time progression as given in (3) and (4).

$$d(t_p) = d_0 - (2.0,0116 \cdot \eta \cdot t_p) \quad (3)$$

$$\eta = \left(\frac{37,8 \cdot (1 - a/c)^{-1,64}}{cob} \right) \cdot 0,85 \cdot (t_p)^{-0,29} \quad (4)$$

where $d(t_p)$ is the service steel reinforcement (mm) in function of the corrosion progression time t_p (years), d_0 is the initial bar diameter (mm), η is the rate corrosion ($\mu\text{A}/\text{cm}^2$), w/c is the water/cement ratio and cob is the concrete cover (mm).

To determine when occur the steel reinforcement depassivation (referent to the DL), a concrete carbonation depth predictive model based on Artificial Neural Network Model (ANN) and developed by Felix (2016), was coupled to the PFEM code. The Figure 3 present the model inputs and the ANN topology (the neural architecture) utilized to developed the concrete carbonation model.

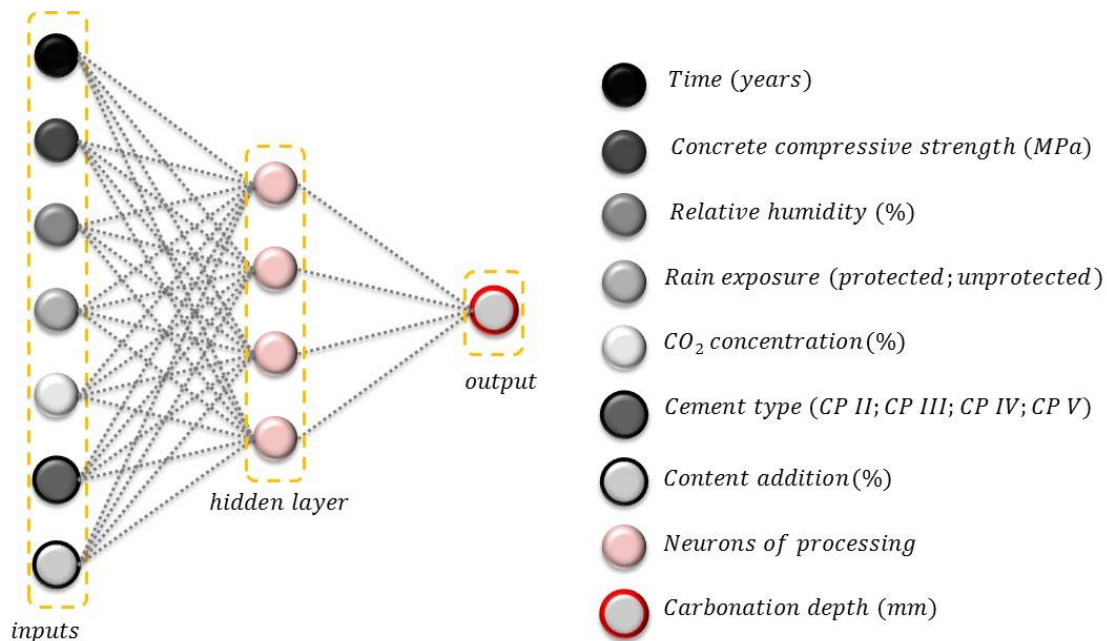


Figure 3. Model inputs and ANN topology (Félix et al., 2017).

The time corresponding to the service life (SL) was determined in this work as the instant of time in which the characteristic crack width (w) is greater than the value described on NBR 6118 (ABNT, 2014) or the maximum vertical beam displacement is greater than 250/beam length, also described on NBR 6118 (ABNT, 2014).

$$w \leq \begin{cases} w_1 = \frac{\phi_i}{12,5 \cdot \lambda_i} \cdot \frac{\sigma_{si}}{E_{si}} \cdot \frac{3 \cdot \sigma_{si}}{f_{ctm}} \\ w_2 = \frac{\phi_i}{12,5 \cdot \lambda_i} \cdot \frac{\sigma_{si}}{E_{si}} \cdot \left(\frac{4}{\rho_{ri}} + 45 \right) \end{cases} \quad (5)$$

where w is the characteristic crack width (mm), ϕ_i is the bar diameter (mm), λ_i is the surface conformation coefficient of the bar (1.0 to steel plain bar, 1.4 to steel notched bar e 2.5 to steel ribbed bar), σ_{si} is the tensile stress (kN/cm²), E_{si} is the steel elasticity modulus (kN/cm²), f_{ctm} is the concrete mean tensile (kN/cm²) e ρ_{ri} is the reinforcement ratio in relation to the surrounding concrete area.

The Figure 4 show the flowchart referent to the model code implemented to determine the service life of reinforced concrete structures subjected to the uniform.

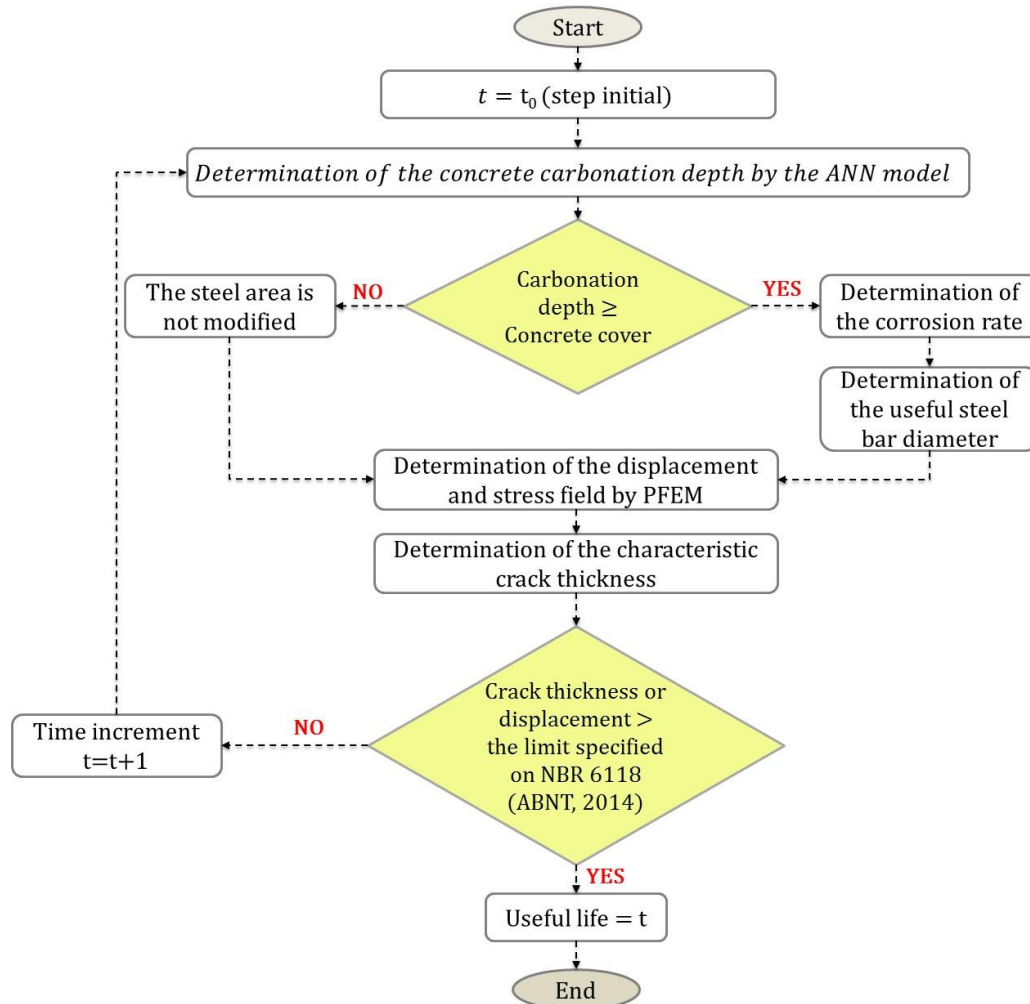


Figure 4. Flowchart of the calculation process for the implemented code.

3.2 Validation of the concrete carbonation depth predicting model

The Figure 5(a-d) presents the concrete carbonation depth in function of the time for concrete structures in four different environment conditions (sceneries). The environment conditions are detail in the Table 1. With the purpose to demonstrate the model applicability and accuracy, the results obtained by the model were compared to different analytical models (Smolczyk, 1976; Vesikari, 1988; Bob et al., 1993; EHE, 2008; Possan, 2010) and real data Mehta (2014). More details about the analytical and the numerical model can be obtained in Felix (2016).

Table 1. Environment sceneries.

Scenery	CO ₂ concentration (%)	Relative humidity (%)	Rain exposure	Cement type	Compressive strength (MPa)
I	0.04	70.00	Protected	CP II – E	30.00
II	0.04	70.00	Protected	CP III	40.00
III	0.04	65.00	Unprotected	CP IV	40.00
IV	0.04	65.00	Unprotected	CP V	40.00

OBS.: In all scenarios the addition content is zero and the analysis time is 60 years.

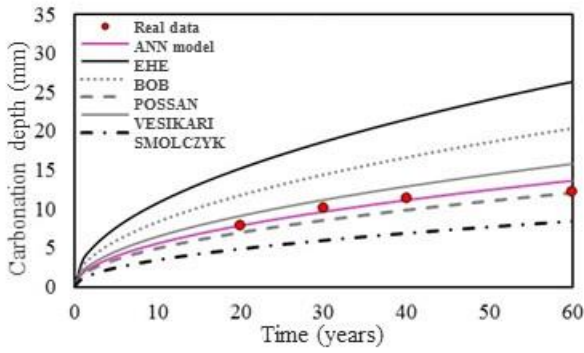


Figure 5(a). Carbonation scenery I.

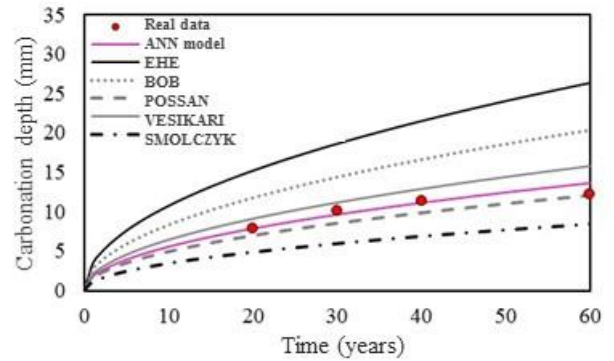


Figure 5(b). Carbonation scenery II.

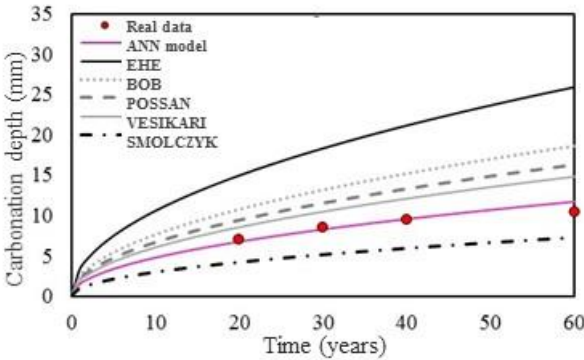


Figure 5(c). Carbonation scenery III.

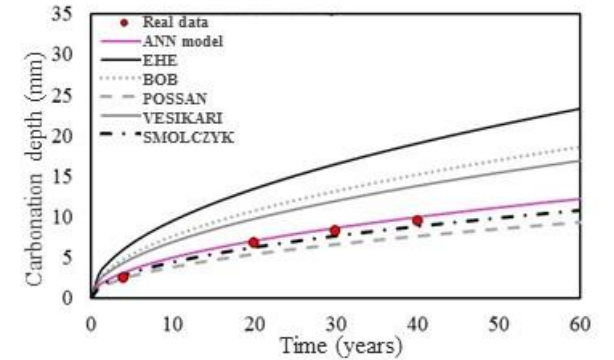


Figure 5(d). Carbonation scenery IV.

The results show the model applicability and that it presents as an efficient numerical tool to predict the carbonation concrete depth.

3.3 Validation of the reinforced concrete corrosion model

In order to validate the numerical model implemented and proposed in this work, a reinforced concrete beam subjected to the uniform corrosion was modeled, the results are compared with the experimental results obtained by Graeff (2007). The modeled structure consist in a reinforced concrete beam with a rectangular section. The beam dimensions is specified in the Figure 6.

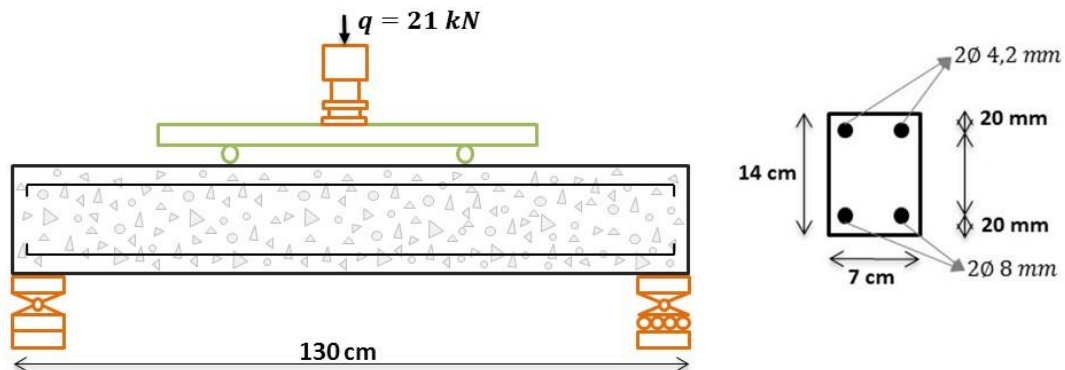


Figure 6. Construction and designing details of the reinforced concrete beam.

The concrete beam was discretized with two different mesh, where to represent the concrete matrix we used 134 triangular finite elements, and the reinforcements was represented with 120 simple bars elements.

Regarding the materials properties, the elasticity modulus of the concrete is 2600 kN/cm², the compressive strength is 2.5 kN/cm², the tensile strength adopted was 0.179 kN/cm² and the Poisson coefficient is 0.2. About the reinforcements, the elasticity modulus is 21000 kN/cm² and the tensile strength is 50 kN/cm². With the purpose to represent and modeling elastic-linear materials we used the Saint-Venant-Kirchhoff constitutive law.

A comparison between the experimental, realized by Graeff (2007), and numerical (obtained with the model proposed) results of the vertical beam displacements is shown in the Figure 7. It is possible verified that the numerical model proposed represent efficiently the beam displacement field in the elastic linear regime of the material.

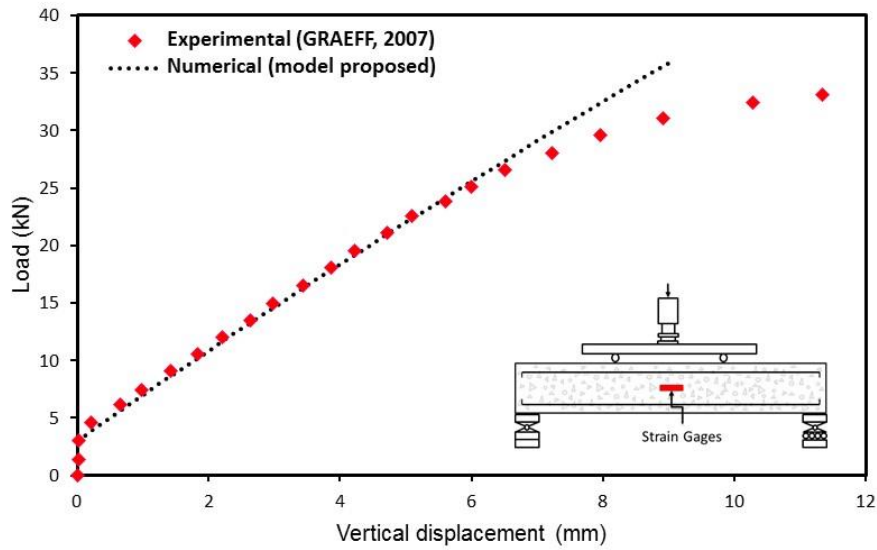


Figure 7. Comparison between experimental and numerical displacements.

With the purpose to verify the applicability of the model to the determination of the effects caused by corrosion to reinforced concrete structures, the rate of increase of the vertical displacement of the center of the beam was compared as the reinforcement suffered degradation (loss of area), with the one obtained numerically by Graeff (2007).

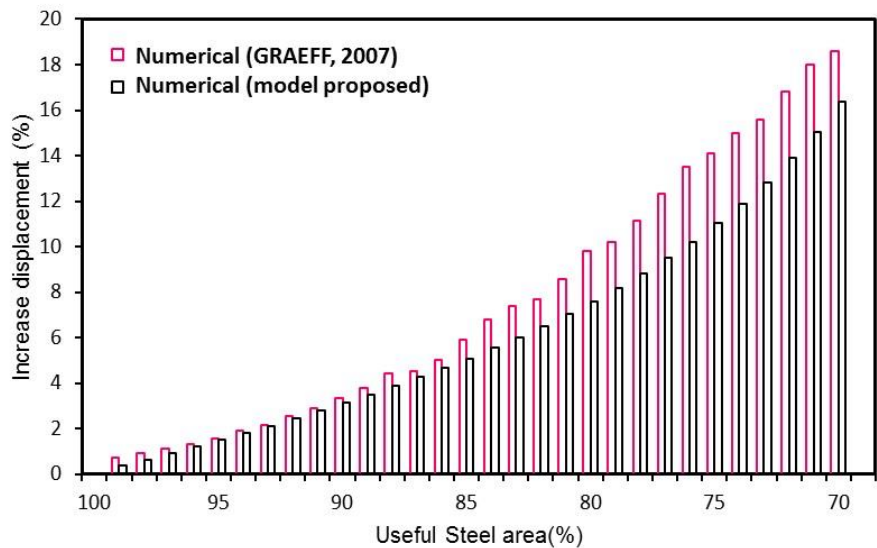


Figure 8. Comparison of the displacement increase rates.

It is observed in Figure 8, that the difference between the responses of the two models is increasing with the evolution of the deformation of the armature, this is due to Graeff (2007) adopting in its model a nonlinear constitutive law. However, the model proposed in this work obtains displacements equivalent to the Graeff (2007), presenting 3.20% of average deviation.

3.4 Description of the analyzed structure

The structure analyzed in this work consists of a reinforced concrete beam dimensioned according to the procedures of NBR 6118 (ABNT, 2014). The Figure 9 present the values of the loads utilized to design the reinforced concrete beam and analyze the service life. In the Figure 9 the construction and geometric details have also shown. In order to analyze the concrete structure durability exposed to a moderately aggressiveness environment, the structure was dimensioned with three different concrete cover (i.e., 20, 25 and 30 mm).

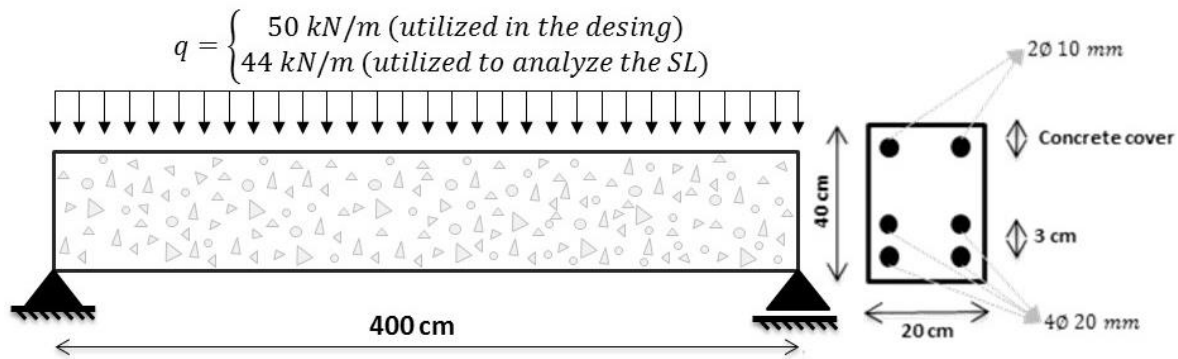


Figure 9. Simplified detailing of the reinforced concrete beam.

The concrete beam was discretized with two different mesh, where to represent the concrete matrix we used 486 triangular finite elements, and the reinforcements was represented with 900 simple bars elements. With the purpose to represent and modeling elastic-linear materials we used the Saint-Venant-Kirchhoff constitutive law.

The data relative to the properties of the materials are presented in Table 2(a), while in Table 2(b) the concrete and conditions exposure data are presented.

Table 2(a). Materials properties.

Material	Property (kN/cm ²)	Value
Concrete	Elasticity modulus	2607.16
	Poisson coefficient	0.20
	Compressive strength	3.00
	Tensile strength	0.21
Steel	Elasticity modulus	21000.00
	Tensile strength	50.00

Table 2(b). Exposure and concrete properties database.

Attribute	Condition
Cement type	CP III
Content additions (%)	0.00
Relative humidity (%)	60.00
Rain exposure	Outdoor
CO ₂ concentration (%)	0.04 (urban environment)

4. RESULTS

Initially, the concrete carbonation depth advance and the design life (DL) of the beams with different cover thicknesses (20, 25 e 30 mm) are presented in Figure 10. It is immediately noticeable the importance of using an adequate concrete cover due to the aggressiveness of the

medium to which the concrete structure is exposed, since adequate covering increases the DL and consequently the time required for the first human interventions and structural repairs.

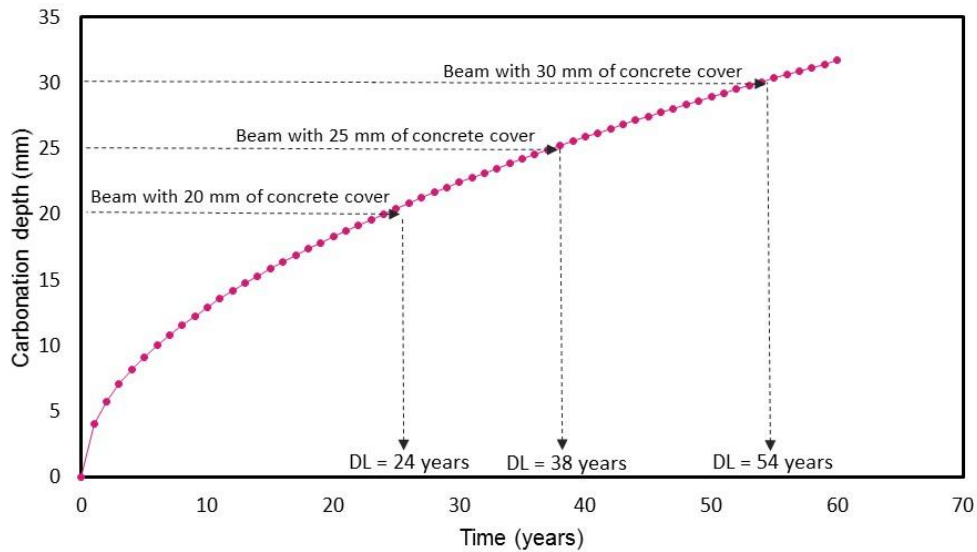


Figure 10. Carbonation advance and the DL of the beams with different concrete cover.

In Figure 11 it is possible to analyze the advance of the degradation of the reinforcement due to the action of corrosion (the graph shows the steel area of the longitudinal reinforcement). It is observed that during the corrosion initiation phase (DL) the steel area of the reinforcement is not reduced, and the section loss is more pronounced in the early years of the corrosion propagation period, in agreement with the study of Vu et al. (2000). The authors report that there is a tendency of greater loss of steel area in the initial period of corrosion because the corrosion rate of the reinforcement is higher during this period, decreasing over time with an exponential behavior.

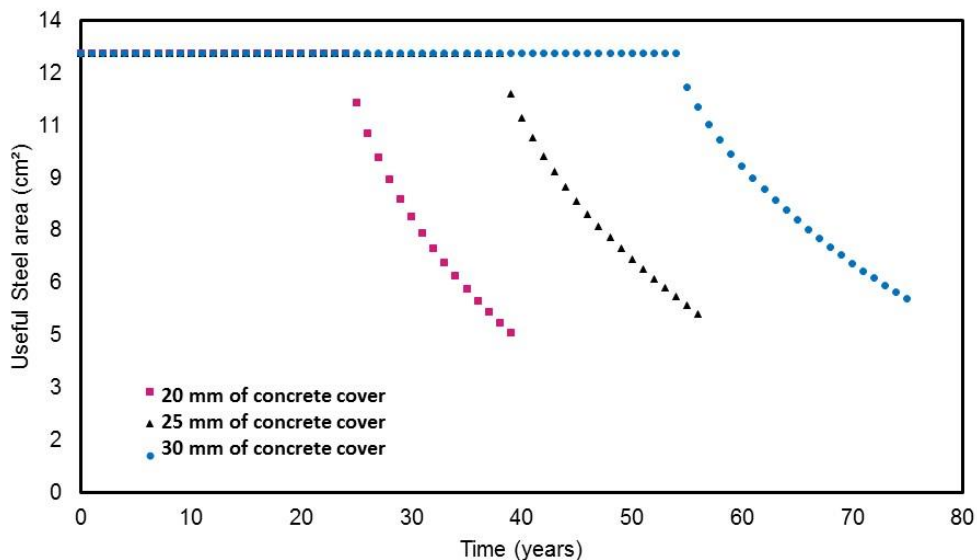


Figure 11. Loss of steel area on concrete beams under corrosion.

Figure 12 shows the DL of the reinforced concrete beams analyzed in this work. The crack width limit adopted was $w_{lim} = 0.3$ mm, as prescribed by NBR 6118 (ABNT, 2014) for concrete structures with class II of environmental aggression (moderate).

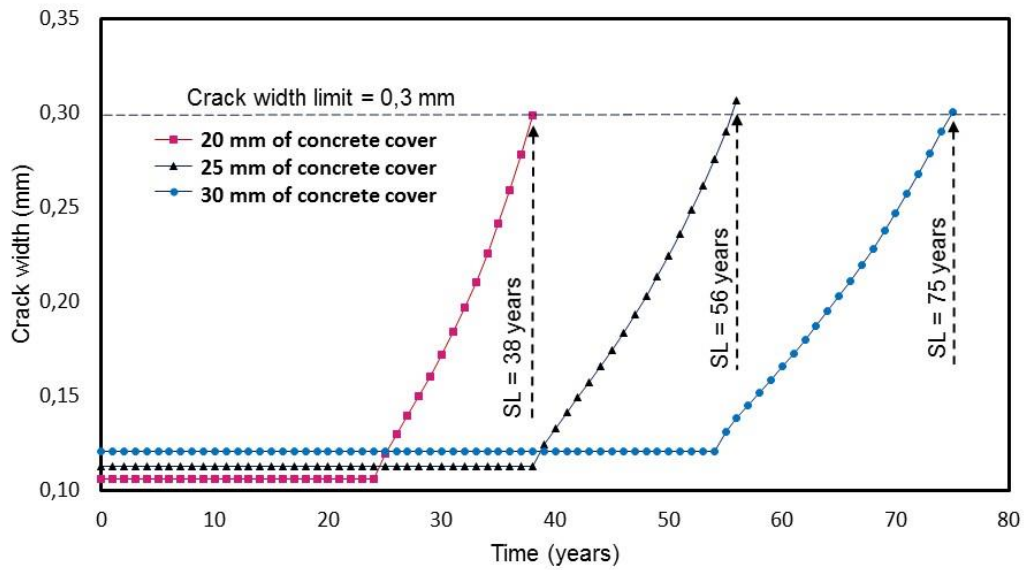


Figure 12. Progress of crack opening and the DL of the concrete beams.

It is observed that the slope of the crack opening curve decreases with the increase of the concrete cover, increasing the time required for the reinforced concrete structure to reach the cracking-opening limit state (relative to the SL).

Finally, Figures 13, 14 and 15 show the longitudinal tensions and vertical displacements of the reinforced concrete beam with 20, 25 and 30 mm of concrete cover, at the moment the cracks reach their limit value (DL).

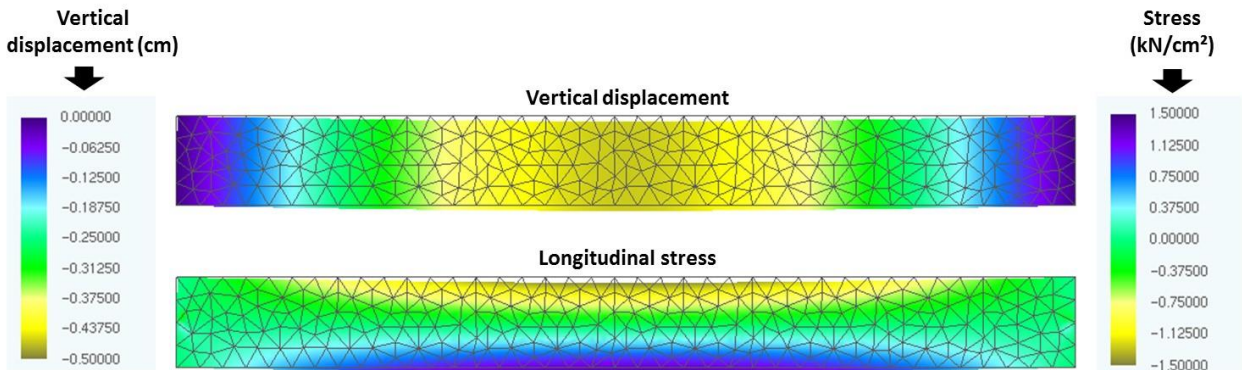


Figure 13. Deformed configuration of the beam with 20 mm of concrete cover at the end of the DL.

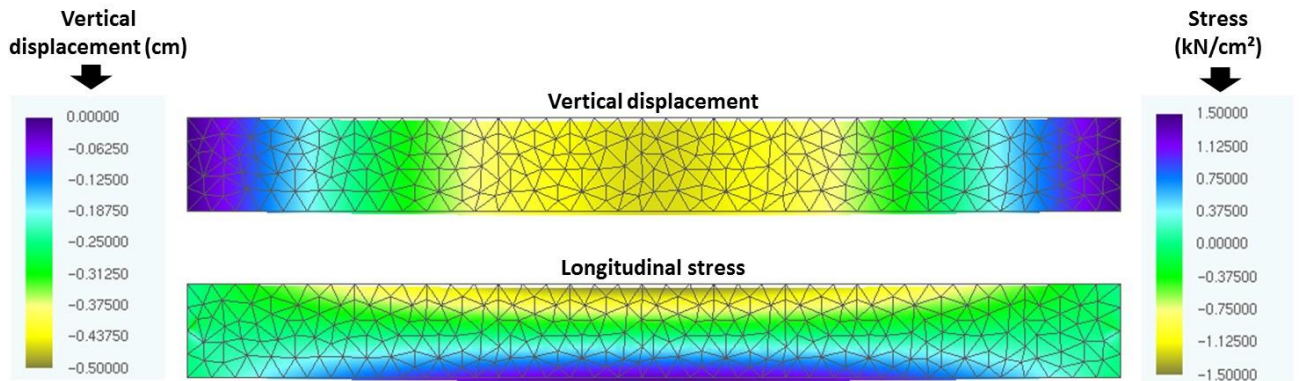


Figure 14. Deformed configuration of the beam with 25 mm of concrete cover at the end of the DL.

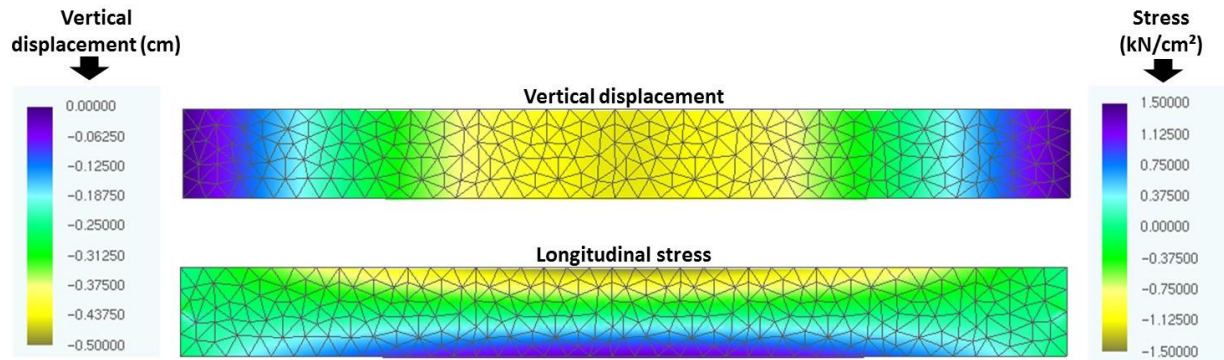


Figure 15. Deformed configuration of the beam with 30 mm of concrete cover at the end of the DL.

Thought the color maps presented in Figures 13, 14 and 15 it is possible to observe that the displacements of the beam decrease with the increase of the concrete cover because of the fact that there is a greater layer of concrete for the diffusion of CO_2 , delaying the corrosion beginning and, consequently, the degradation of the reinforcement, responsible for giving greater rigidity to the concrete beam. This result demonstrates the need to know correctly the environment to which the structure will be exposed, since the concrete elements will be designed with the required durability, guaranteeing the design life of the structures and the safety of their users.

5. CONCLUSÕES

From the analysis of the presented results regarding the validation of the developed model, it can be concluded that the formulation for the determination of the Design Life (DL) through the use of Artificial Neural Networks (ANN) and the formulation for the mechanical analysis of reinforced concrete structures under uniform corrosion based on the Finite Element Method (FEM) are consistently implemented and present consistent results when compared to literature data.

From the simulations performed with the model generated by the coupling of the MEF with the ANN, it was possible to conclude that:

- An adequate concrete cover (cover which takes into account the degree of aggressiveness to which the structure is exposed) guarantees not only a longer period to lead to the depassivation of the reinforcement, but also to reach the crack-opening limit recommended by NBR 6118 (ABNT, 2014);
- Consideration of the loss of steel mass as a consequence of corrosion results in the development of cracks larger than the recommendation of the NBR 6118 (ABNT, 2014), when the level of corrosion reaches 60 %;
- When the corrosion rate of the reinforcement reaches 50%, there is an increase of 30% in the beam vertical displacement, regardless of the concrete cover;
- By increasing the concrete cover, the maximum displacements and the deformation of the beam are reduced at the end of the DL, due to the lower degree of corrosion to which the reinforcement is subjected;
- Although all the beams at the end of the DL are with the concrete in the same state of cracking, the mechanical capacity of the beam with 30 mm of concrete cover is higher than the others beams, since the reinforcement has a lower degree of corrosion and a greater area of steel, demonstrating that a concrete cover coherent with the aggressiveness of the environment to which the structure is exposed provides durability and security for its users.

The results obtained indicate the applicability of the developed code as an efficient and alternative tool for the analysis of the design life of reinforced concrete structures subjected to uniform corrosion.

In addition, the developed program demonstrates the efficiency of the use of numerical tools in the development of models for the study and simulation of complex mechanisms of the degradation of reinforced concrete structures, corroborating with the studies of the pathology of constructions.

6. AGRADECIMIENTOS

Authors thanks the Coordination of Personal Improvement of Higher Education (CAPES) and to the National Council of Scientific and Technological Development (CNPq) by the financial support.

7. REFERENCES

- Andrade, C. (1992), *“Manual para diagnóstico de obras deterioradas por corrosão de armaduras”*, Tradução de Antônio Carmona e Paulo Helene, São Paulo: PINI, p. 104.
- Andrade, J. J. O., Possan, E., Dal Molin, D. C. C. (2017), *“Considerations about the service life prediction of reinforced concrete structures inserted in chloride environments”*, Journal of Building Pathology and Rehabilitation, V. 2, p. 1-8.
- Associação Brasileira de Normas Técnicas (2014), NBR 6118 - Projeto de estruturas de concreto, Rio de Janeiro, ABNT.
- Bakker, R. M. F. (1988), Initiation period. In: Schiess P. *“Corrosion of steel in concrete”*, London, Chapman and Hall, cap. 3, pp. 22-55.
- Biondini, F., Frangopol D. M. (2017), *“Time-variant redundancy and failure times of deteriorating concrete structures considering multiple limit states”*, Structure and Infrastructure Engineering, V.13, pp. 94-106.
- Bob, C., Afana, E. (1993), *“On-site assessment of concrete carbonation”*, Proceedings of the International Conference Failure of Concrete Carbonation, RILEM, Bratislava, pp. 84-87.
- Broomfield, J. P. (2007), *“Corrosion of steel in concrete: understanding, investigation and repair”*. 2. Ed. New York, Taylor & Francis, pp. 294.
- Carmona, A. F., Marega, A. (1988), *“Retrospectiva da patologia no Brasil: Estudo Estatístico”*, in: Jornadas em Espanhol y Portugués sobre Estructuras y Materiales, CEDEX, IETcc, pp. 325-348.
- Chang, C. F., Chen, J. W. (2006), *“The experimental investigation of concrete carbonation depth”*, Cement and Concrete Research, V.36, pp. 1760-1767.
- Coda, H. B. (2003), *“Análise não linear geométrica de sólidos e estruturas: uma formulação posicional baseada no MEF”*, Volume II, Departamento de Estruturas, Escola de Engenharia de São Carlos, Universidade de São Paulo, São Carlos.
- Comission Permanente del Hormigón, EHE (2008), *“Instrucción de Hormigón Estructural. Ministério de obras públicas e urbanismo”*. Madrid, Espanha.
- Dal Molin, D. C. C. (1988), *“Fissuras em estruturas de concreto armado: análise das manifestações típicas e levantamento de casos ocorridos no Estado do Rio Grande do Sul”*, Dissertação de Mestrado em Engenharia, Universidade Federal do Rio Grande do Sul, Porto Alegre.
- Dyer, T. (2015), *“A durabilidade do concreto”*. Rio de Janeiro, Editora Ciência Moderna, pp. 536.

- Ellingwood, B. R., Frangopol, D. M. (2016), “*Introduction to the state of the art collection: risk-based lifecycle performance of structural systems*”, Journal of Structural Engineering, V.142, pp. 1.
- Felix, E. F. (2016), “*Desenvolvimento de software para a estimativa da profundidade de carbonatação, vida útil e captura de CO₂ de estruturas de concreto empregando RNA's*”, Trabalho de conclusão de curso, Universidade Federal da Integração Latino-Americana, Foz do Iguaçu.
- Félix, E. F., Carrazedo, R., Possan, E. (2017), “*Análise Paramétrica da carbonatação em estruturas de concreto armado via Redes Neurais Artificiais*”, Revista ALCONPAT, V.7, N. 3, pp. 302-316.
- Geiker, M. R., Polder, R. B. (2016), “*Experimental support for new electro active repair method for reinforced concrete*”, Materials and Corrosion, V.67, pp. 600-606.
- Graeff, A. G. (2007), “*Avaliação experimental e modelagem dos efeitos estruturais da propagação da corrosão em elementos de concreto armado*”, Dissertação de Mestrado em Engenharia, Universidade Federal do Rio Grande do Sul, Porto Alegre.
- Kari, O. P., Puttonen, J., Skantz, E. (2014), “*Reactive transport modelling of long-term carbonation*”, Cement and Concrete Composites, V.52, pp. 42-53.
- Köliö, A., Pakkala, T. A., Hohti, H., Laukkarinen, A., Lahdensivu, J., Mattila, J., Pentti, M. (2017), “*The corrosion rate in reinforced concrete facades exposed to outdoor environment*”, Materials and Structures, V.50, pp. 1-16.
- Mehta, P. K., Monteiro, P. J. M. (2014), “*Concreto: microestrutura, propriedades e materiais*”. 2.ed. São Paulo, IBRACON, pp.751.
- Neville, A. M. (1997), “*Propriedades do concreto*”, São Paulo: PINI, pp. 828.
- Possan, E. (2010), “*Modelagem da carbonatação e previsão de vida útil de estruturas de concreto em meio urbano*”, Tese de Doutorado em Engenharia, Programa de Pós-Graduação em Engenharia Civil, Universidade Federal do Rio Grande do Sul, Porto Alegre.
- Rao, A. S., Lepech, M. D., Kiremidjian, A. S., Sun X. Y. (2017), “*Simplified structural deterioration model for reinforced concrete bridge piers under cyclic loading*”, Structure and Infrastructure Engineering, V.13, pp. 55-66.
- Smolczyk, H. G. (1969), “*Written Discussion*”, proceeding of the 1969 International Symposium on the Chemistry of Cement, Part III, v. II/4, pp. 369-384.
- Stewart, M. G., Rosowsky, D. V. (1998), “*Structural safety and serviceability of concrete bridges subject to corrosion*”, Journal of Infrastructure Systems V.4, pp. 146-155.
- Tuutti, K. (1982), “*Corrosion of steel in concrete*”. Stockholm, Swedish Cement and Concrete Research Institute.
- Val, D. V., Melchers, R. E. (1997), “*Reliability of deteriorating RC slab bridges*”, Journal of Structural Engineering, V.123, pp. 1638-1644.
- Vesikari, E. (1988), “*Service life prediction of concrete structures with regard to corrosion of reinforcement*”. Technical Research Centre of Finland, report No. 553, Finland p. 53.
- Vu, K. A. T., Stewart, M. G. (2000), “*Structural reliability of concrete bridges including improved chloride-induced corrosion models*”, Structural Safety, V.22, pp. 313-333.
- Yanaka, M, Ghasemi, S. H., Nowak, A. (2016), “*Reliability-based and life-cycle cost-oriented design recommendations for prestressed concrete bridge girders*”, Structural Concrete, V.17, pp. 836-847.

Analysis of the concrete-steel interface in specimens exposed to the weather and immersed in natural sea water

M. R. Sosa¹, T. Pérez^{1*}, V. M. J. Moo-Yam¹, E. Chávez², J.T. Pérez-Quiroz³

*Corresponding author: tezperez@uacam.mx

DOI: <http://dx.doi.org/10.21041/ra.v8i1.203>

Received: 27/06/2017 | Accepted: 21/12/2017 | Published: 31/01/2018

ABSTRACT

The electrochemical behavior in reinforced concrete structures with and without sodium chloride (NaCl) in the mixing water in a marine / tropical environment was evaluated. The monitoring consisted of measuring the corrosion potential (E_{corr}), the advance of carbonation front (x_{CO_2}) and a photographic record of the concrete / steel interface at different stages of the period of time of exposure. In the exposure to the weather, the addition of NaCl to the mixing water favored the advance of carbonation. The presence of chlorides was a determining factor at the beginning and development of the corrosion process in both exposures to the weather and immersion.

Keywords: reinforced concrete; carbonation; corrosion potential; concrete-steel interface, chloride ion.

Cite as: M. R. Sosa, T. Pérez, V. M. J. Moo-Yam, E. Chávez, J. T. Pérez-Quiroz (2018), "Analysis of the concrete-steel interface in specimens exposed to the weather and immersed in natural sea water", Revista ALCONPAT, 8 (1), pp. 16 – 29, DOI: <http://dx.doi.org/10.21041/ra.v8i1.203>

¹Centro de Investigación en Corrosión de la Universidad Autónoma de Campeche, Av. Heroes de Nacozari No. 480, Campus 6 de Investigaciones, C.P. 24070, San Francisco de Campeche, Campeche, México.

²Secretaría de la Defensa Nacional, Dir. Gral. Ings., U.D.E.F.A., E.M. I. Calz. Mex.-Tac. s/n, Del. Miguel Hidalgo, D. F., México.

³Instituto Mexicano del Transporte, área Materiales Alternativos Km 12 + 000 carretera Estatal no. 431 El Colorado – Galindo S/N, Sanfandila, Pedro Escobedo. Queretaro, México; C.P. 76703

Legal Information

Revista ALCONPAT is a quarterly publication of the Latinamerican Association of quality control, pathology and recovery of construction- International, A. C., Km. 6, antigua carretera a Progreso, Mérida, Yucatán, C.P. 97310, Tel.5219997385893, alconpat.int@gmail.com, Website: www.alconpat.org

Editor: Dr. Pedro Castro Borges. Reservation of rights to exclusive use No.04-2013-011717330300-203, eISSN 2007-6835, both awarded by the National Institute of Copyright. Responsible for the latest update on this number, ALCONPAT Informatics Unit, Ing. Elizabeth Sabido Maldonado, Km. 6, antigua carretera a Progreso, Mérida, Yucatán, C.P. 97310.

The views expressed by the authors do not necessarily reflect the views of the publisher.

The total or partial reproduction of the contents and images of the publication without prior permission from ALCONPAT International A.C. is not allowed.

Any discussion, including authors reply, will be published on the third number of 2018 if received before closing the second number of 2018.

Análisis de la interfaz concreto-acero de especímenes expuestos a la intemperie y sumergidos en agua de mar natural

RESUMEN

Se evaluó el comportamiento electroquímico en estructuras de concreto armado sin y con adición de cloruro de sodio (NaCl) en el agua de amasado en un ambiente marino/tropical. El monitoreo consistió en medir el potencial de corrosión (E_{corr}), avance del frente de carbonatación (xCO_2) y registro fotográfico de la interfase concreto/acero en diferentes etapas del periodo de exposición. En la exposición a la intemperie se observó que la adición de iones cloruro favoreció el avance de la carbonatación. La presencia de iones cloruro es determinante en el inicio y desarrollo del proceso de corrosión, tanto en exposición a la intemperie como en inmersión.

Palabras clave: concreto reforzado; carbonatación; potencial de corrosión; interfase concreto-acero, ión cloruro.

Análise da interface concreto-aço em corpos de prova expostos à intempérie e imersos em água do mar natural

RESUMO

O comportamento eletroquímico em estruturas de concreto armado sem e com adição de cloreto de sódio na água de amassar, em um ambiente marinho/tropical é avaliado. O monitoramento consistiu em medir o potencial de corrosão (E_{corr}), o avanço da frente de carbonatação (xCO_2) e o registro fotográfico da interface concreto/aço em diferentes estágios do período de exposição. Na exposição aos elementos, observou-se que a adição de íons cloreto favoreceu o avanço da carbonatação. A presença de cloreto ions é determinante no início e desenvolvimento do processo de corrosão, tanto na exposição à intemperie quanto na imersão.

Palavras-chave: Concreto armado, carbonatação, potencial de corrosão, interface de concreto de aço, cloreto ions.

1. INTRODUCTION

The durability of the infrastructure constructed using reinforced concrete depends directly on the quality of materials and design, considering the service to be provided and the impact of the particular environment in which it will be located. When properly prepared and cast, it provides adequate protection to the steel that may be embedded in the concrete and last several years without showing any visible signs of deterioration. However, the corrosion of reinforcing steel occurs due to the destruction of the passivating film formed naturally on the surface. It is feasible for two main reasons: a sufficient amount of chlorides or other despassing ions (Rosas et al, 2014), or a decrease of alkalinity of the concrete when reacting with CO_2 present in the environment (Helene et al, 2009; Castro et al, 2000a; Papadakis et al, 1991a).

Currently, deterioration of concrete by environmental factors is a major problem observed in buildings (Papadakis et al, 1991b). In urban areas the carbonation process is the most common. On coastal regions the main aggressors are chlorides, sulfates and humidity (Merchers et al, 2009; Ye et al, 2012; Zirou et al, 2007). However, CO_2 is becoming increasingly present in deterioration of concrete at southeastern Mexico (Solis et al, 2005; Moreno et al, 2004; Castro-Borges et al, 2013; Castro et al, 2000b).

As for the city of San Francisco de Campeche, experimental site of this work, the process of entering the sea breeze is conditioned by the direction of the winds, in such a way that although it is a coastal zone, the deposit of salts on the surface of concrete structures is limited (Pérez, 2000). Although there is no industry on the area, it is important to determine the progress of carbonation in concrete structures as a criterion of durability in construction (Chavez-Ulloa et al, 2013; San Miguel et al, 2012).

One of the most commonly used parameters for estimating the condition of reinforcement embedded in concrete is the measurement of the half cell potential, also called corrosion potential (E_{corr}). Standards ASTM C876-09 and NMX-C-495-ONNCCE-2015 establish intervals of E_{corr} that indicate the status of the steel armor. With the values obtained, a diagnosis of the corrosion degree on reinforcement is possible as long as it is complemented with measurements of environmental variables, carbonation versus chloride, and ion intake profile, among others. Although there are indirect techniques to know the damage by corrosion, the best option, when possible, is to look directly at the steel surface and make a photographic record.

This paper presents the analysis of the effect of two exposure conditions, the content of sodium chloride and deterioration of reinforced concrete attacked in a marine/tropical environment, in the southeast of Mexico. The presence of chlorides in the samples exposed to the atmosphere (weather) are determinant in the interface condition reflected on the E_{corr} values, the advance of the carbonation front and oxidation of reinforcements. As for the samples exposed in immersion, the chloride ion is the main aggressor agent that affects the corrosion process of the reinforcement.

2. EXPERIMENTAL PROCEDURE

2.1. Specimens Elaboration

For the manufacture of reinforced concrete, the commercial brand Portland Type I commonly used in the region was used. The coarse and fine aggregates are usual in the area and produced by the limestone crushing of Campeche. Conventional commercial steel rods (ASTM A 615) of 0.95 cm in diameter were used. Sodium chloride (NaCl) added to the mixing water was an analytical reagent grade of a commercial brand. The mixing was done with drinking water from municipal supply.

Two series of 3 specimens of reinforced concrete were manufactured without and with 3.5% by weight of sodium chloride (NaCl) added in the mixing water, similar to the salt concentration of seawater (Genescá, 1994), with the same water/cement ratio, 0.66, according to dosages shown in Table 1 and dimensions shown in Figure 1. NaCl addition was with the objective to accelerate the corrosion process.

Table 1. Dosage of the reinforced concrete samples (NOM C-159-85).

Cement (kg/m ³)	Fine Aggregate (kg/m ³)	Coarse Aggregate (kg/m ³)	Water (kg/m ³)	NaCl (g/l)
312.5	750	687.5	206.25	35
312.5	750	687.5	206.25	0

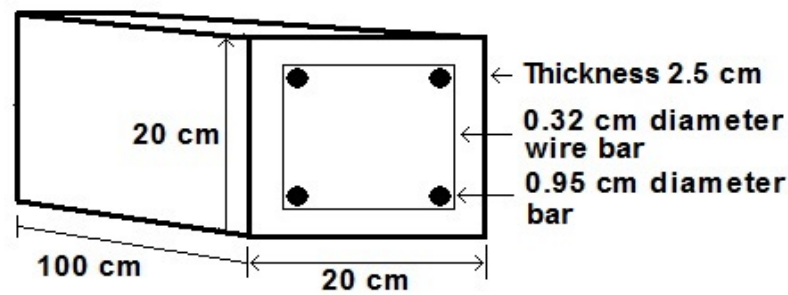


Figure 1. Specimen diagram.

The curing was carried out for 28 days (NOM C-159, ASTM C 192) and subsequently, the specimens were exposed to two different conditions: outdoors (ATM) and immersion in natural sea water (INM), in the southeast of Mexico (San Francisco de Campeche, Campeche, Mexico at 300 meters of the coastline). The structures exposed to the ATM were placed vertically on a concrete base 30 cm above the ground. The specimens exposed in INM were placed in small pools and the natural seawater was changed monthly.

2.2. Measurement of Corrosion Potential

The corrosion potential measurement was made according to the ASTM C876 standard. Figure 2a shows the way in which the corrosion potential in the structures exposed to the ATM was measured, taken from five points of the specimens at different heights of the concrete surface, using a saturated copper/copper-sulphate reference electrode, ($\text{Cu}/\text{CuSO}_{4\text{sat}}$). The measurement of the corrosion potential in the specimens exposed in INM was made using a silver-saturated silver chloride reference electrode ($\text{Ag}/\text{AgCl}_{\text{sat}}$) immersed in the seawater on one side of the sample, see Figure 2b.

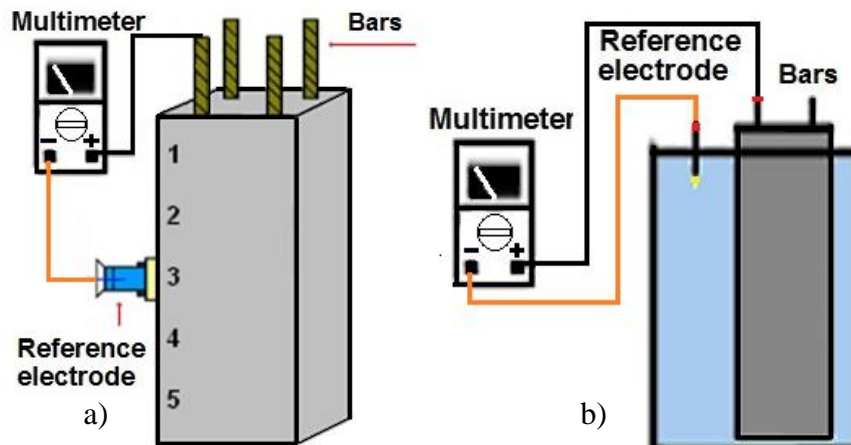


Figure 2. Diagram of the corrosion potential measurements: a) to ATM; b) to INM.

Table 2 presents the proposed criteria to analyze the corrosion potentials of reinforcing steel (E_{corr}) embedded in concrete. The analysis of corrosion potentials will be focused on the saturated silver-silver chloride reference electrode ($\text{Ag}/\text{AgCl}_{\text{sat}}$); therefore, the conversion of corrosion potentials obtained with the saturated copper-copper sulfate reference electrode is equal to +50 mV (Berkeley, 1990; Chess, 1998).

Table 2. Criterion used to measure the corrosion potential of the reinforcing steel in concrete [ASTM C876-09, Troconis de Rincón et al, 1997].

Ecorr vs Cu/CuSO₄(sat) (mV)	Ecorr vs Ag/AgCl(sat) (mV)	Corrosion Probability (%)
Greater than -200	Greater than -150	10% (Passive zone)
Between -200 and -350	Between -150 and -300	50% (Uncertain zone)
Less than -350	Less than -300	90% (Active zone)

2.3. Measurement of the Carbonation Front

For this test three cores of each series were extracted by using a core extractor, see Figure 3a [ASTM C42/C42M]. This procedure was performed in 4 periods of six months each (6, 12, 18, 24). The cores were removed in the middle part and parallel to the reinforcing steel, see Figure 3a.

The carbonation front was measured using acid-base indicators. Phenolphthalein is the commonly used indicator and its range of color change is between pH 8.2 and 9.8 varying its hue from colorless to reddish violet. Thymolphthalein is another indicator used because its range shift is between pH 9.3 and 10.5 with blue hue to colorless [Troconis Rincón et al, 1997; Standard UNE-112-011]. In this way it is possible to observe the pH change of the concrete paste and determine the advance of the carbonation front.

The acid-base indicators were applied up to 1 cm below the level of the reinforcing steel in equal parts, see Figure 3b. A photographic record of the advance of carbonation measured by a rule was taken. Concrete of good quality has a characteristic color of the indicator used and a carbonated concrete has no color. It is due to the decrease of pH resulted from the reaction of carbon dioxide (CO₂) with the alkaline components of concrete.

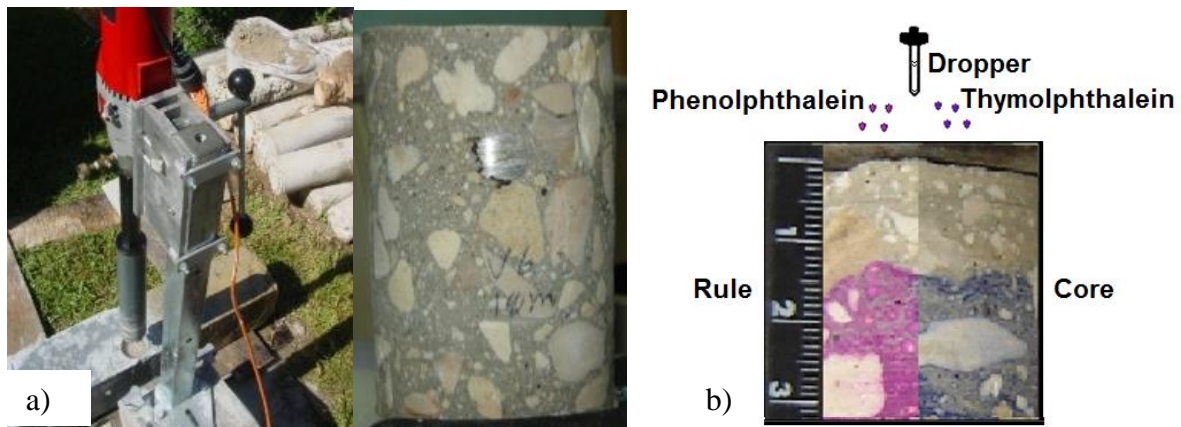


Figure 3. Carbonation front: a) Core extraction and b) Application of acid-base indicator.

The results present the average advance of the carbonation front of the cores extracted to determine visually and graphically the damage that the exposure medium generated in the concrete and consequently the probability that corrosion of the reinforcing steel could occur.

3. RESULTS

3.1. Carbonation Front

Figures 4 and 5 show the photographic record of the carbonation velocity in the cores of concrete obtained from specimens made without (0%) and with 3.5% by weight of sodium chloride (NaCl) added in the mixing water during two years of exposure to ATM and INM, respectively.

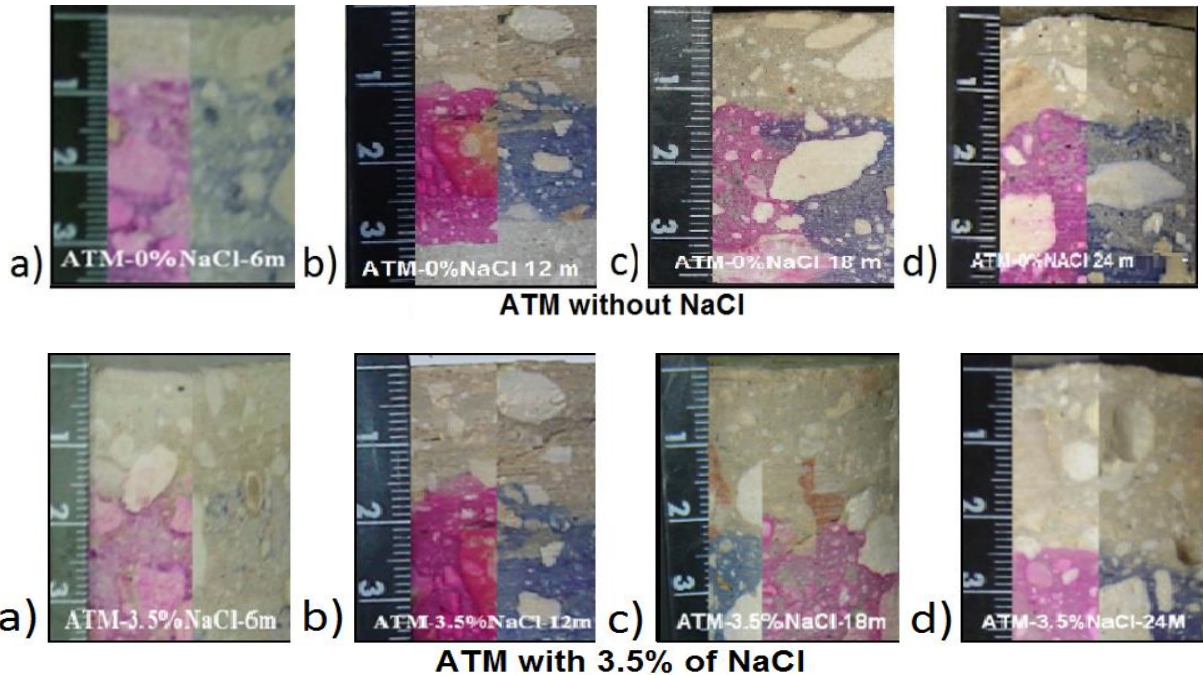


Figure 4. Carbonation front: a) 6, b) 12, c) 18 and d) 24 months, respectively, in concrete cores exposed to ATM.

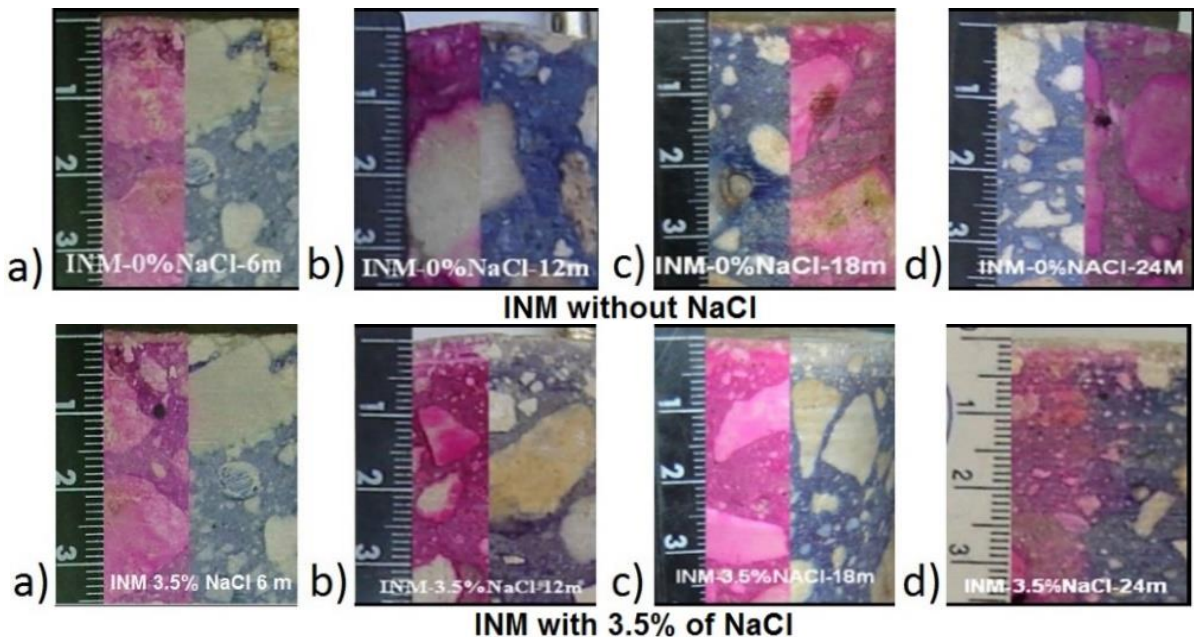


Figure 5. Carbonation front: a) 6, b) 12, c) 18 and d) 24 months, respectively, in concrete cores exposed to INM.

The photographic record of the structures exposed to the ATM, in Figure 4, shows that those made without additional NaCl present an average progress of 8 mm in depth after 6 months of exposure and a depth of 15 mm after 24 months. The most noticeable effect is on the structures containing additional NaCl in the mixing water that presents a greater advance of carbonation, reaching a depth of 15 mm on average in the first 6 months and 25 mm that on average at 24 months, reaching the level of the concrete cover established for reinforcing steel.

In the case of the structures exposed to INM, Figure 5, an insignificant advance of carbonation is observed on both manufacture conditions manufacture of reinforced concrete, reaching on average approximately 1 mm deep during the 24 months that the study lasted. The results were as expected, due to the low solubility of CO₂ in seawater, when the structures were immersed in seawater.

According to the results of the carbonation front, there was only a significant effect in the structures exposed to ATM related to the content of NaCl added in the mixing water that influenced the advance of carbonation in concrete. Table 3 records the three samples average results. As expected, the reaction between CO₂ and the alkaline components of the concrete is favored when the ambient concrete is between 50% and 80% of water content in the pores of concrete, which are the optimum conditions for carbonation (Pérez, T. et al, 2006; Corvo, F. et al., 2008). Each experimental condition shows closeness of *k* values during the period of exposure. It has been reported that the wind pattern in Campeche, due to its geographic position, is predominant from land to sea (Gutiérrez and Winant, 1996) and for this reason it is an atypical tropical marine environment (Pérez, T., 2000).

Table 3. Carbonation front of structures exposed to the weather ATM.

Time (year)	Increase in carbonation (mm)		Constant <i>k</i> (mm/year ^{1/2})	
	Without Cl-	With Cl-	Without Cl-	With Cl-
0.5	8	15	11.3	21.2
1.0	10	17	10.0	17.0
1.5	12	21	9.7	17.1
2.0	15	25	10.6	17.6
Average			10.4	18.2

The major advance of carbonation on structures with addition of NaCl, is related to the fact that the pores of the concrete remained partially saturated for a longer time under conditions that favored the entry of CO₂. Consequently, the reaction with the components of concrete increased; thus, accelerating the advance of carbonation (Trocónis de Rincón et al, 1997). This proposal is consistent due to the relative humidity (RH) that prevails in the region; approximately 70% annual average, and mainly due to the hygroscopic property of NaCl that favors the preservation of internal humidity. Together they favored the conditions to accelerate the carbonation progress, as was observed in the structures exposed to the ATM with additional NaCl in the mixing water (Pérez et al, 2010).

The advance of carbonation in the structures without additional NaCl, even though at two years did not reach the level of steel, its constant on average of 10.4 mm/year^{1/2} is significant because these values are more similar to those reported in urban environments [Moreno, et al., 2016]. The novelty of these results in a marine/tropical environment is related to a greater amount of pores due to the water/cement ratio of 0.66 used to manufacture them. Under such conditions the advance of carbonation will depend on the relative humidity of the medium and the necessary time it remains inside the concrete for the reaction of CO₂ with the alkaline components of the concrete to take place. It is proposed that the hygroscopic characteristics of NaCl favor the

retention of water in the pores of concrete, maintaining the humidity conditions propitious for the carbonation of concrete.

3.2. Corrosion potential (E_{corr})

Figure 6 shows the average E_{corr} results of reinforcing steel in concrete structures made without (0%) and with 3.5% by weight of sodium chloride (NaCl) added in the mixing water during 2 years of exposure to the ATM and INM.

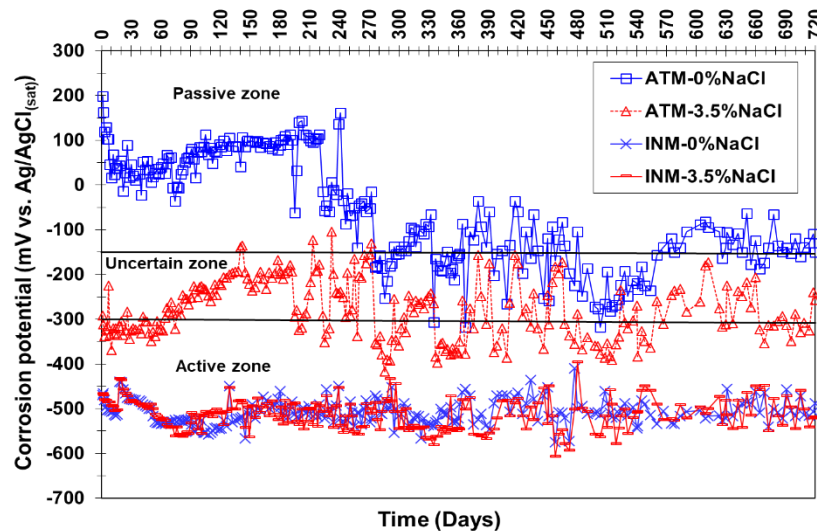


Figure 6. Corrosion potential of the reinforcing vs time.

Atmospheric exposure.

The corrosion potentials of the structures prepared without additional NaCl exposed to the ATM (ATM-0% NaCl), according to the criterion of Table 2, showed a passive behavior until day 270; later the potentials became more negative with variations between the passive and uncertain zone. Such behavior that prevailed until the end of the experiment. In the case of those samples made with additional NaCl exposed to the same condition (ATM-3.5% NaCl), the reinforcing steel started with a high probability of corrosion of the steel (active zone) during the first 40 days, reducing its activity and remaining within the uncertain zone approximately until day 200 and later presenting a variable behavior until the end of the study, between the active and uncertain zones. The E_{corr} instability is due to variations in meteorological conditions such as temperature and relative humidity, as well as the rainy season.

In samples of reinforced concrete exposed to the ATM the effect of carbonation was ruled out, although the series with additional NaCl, did reach the steel level after 24 months. It is notable that the effect is mainly attributed to the action of chlorides, which modify the conditions of the concrete-reinforcing steel interplay causing a polarization which displaces the E_{corr} measures to more negative values. Otherwise, when the presence of corrosive agents is discarded, whether it is an attack by CO_2 , chlorides or both, as in the series without the addition of the activity, it is not attributed to the onset of corrosion but to the partial saturation of water in the pores of the concrete. Due to the characteristic conditions of the region when being in a tropical environment, where the relative humidity prevailing on average is 65% - 80% (Pérez et al, 2010). In addition, the fact that the carbonation reaction requires water to take place, partially influenced the progress of carbonation in the concrete of each series. Another aspect to be considered is the chemical characteristic of the concrete that surrounds the reinforcing steel, which at the beginning of the study is the first resistance against the agents that cause steel corrosion. As it is

observed, the samples without NaCl addition are passive and those manufactured with additional NaCl have potentials with a high probability of corrosion.

Immersion exposure.

Regarding the structures exposed to INM, both series, without and with 3.5% NaCl (INM-0% NaCl and INM-3.5% NaCl), remained within the range between -400 and -500 mV vs electrode Ag/AgCl that corresponds to a behavior of high probability of corrosion of reinforcement steel (active zone), during the 720 days of exposure that lasted the experiment. These values belong to the area of active corrosion that indicates a high probability of corrosion in the reinforcing steel. This behavior is due to the polarization induced by the lack of oxygen in the concrete-rod interface that produces the displacement of E_{corr} to more negative values [Ávila, et al., 1994]. This condition predominates over the presence of chloride in the water used for the mixture. In the case of the series exposed to INM, the attack by carbonation is practically null, leaving as the main cause of corrosion the chlorides present in seawater and the addition in the mixing water. In this sense, both series presented the same electrochemical behavior with a high probability of corrosion. Under such conditions, it is also necessary to take into account that steel under immersion is exposed to a medium poor in oxygen which makes the potentials more negative similar to those reported.

3.3. Photographic record

Figures 7 and 8 show the photographic record of the visual inspection of the concrete-reinforcing steel interface in concrete specimens made without (0%) and with 3.5% by weight of NaCl added in the mixing water, for 2 years of exposure to ATM and INM.

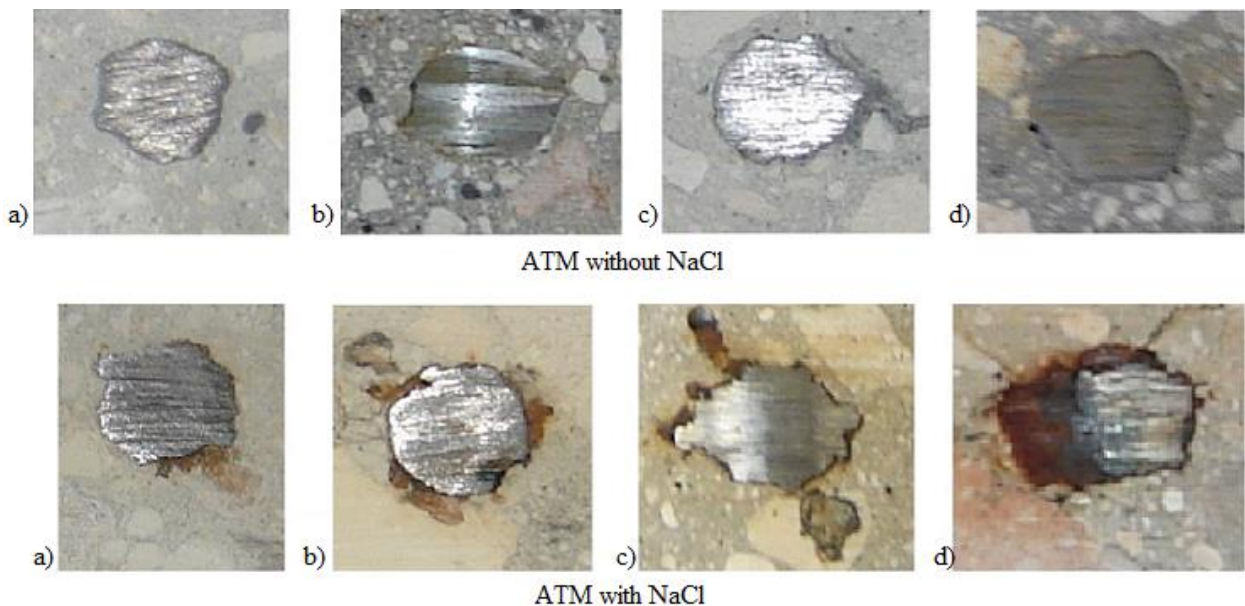


Figure 7. Photographic record of the concrete-reinforcing steel interface: a) 6, b) 12, c) 18 and d) 24 months, respectively, in structures exposed to ATM.

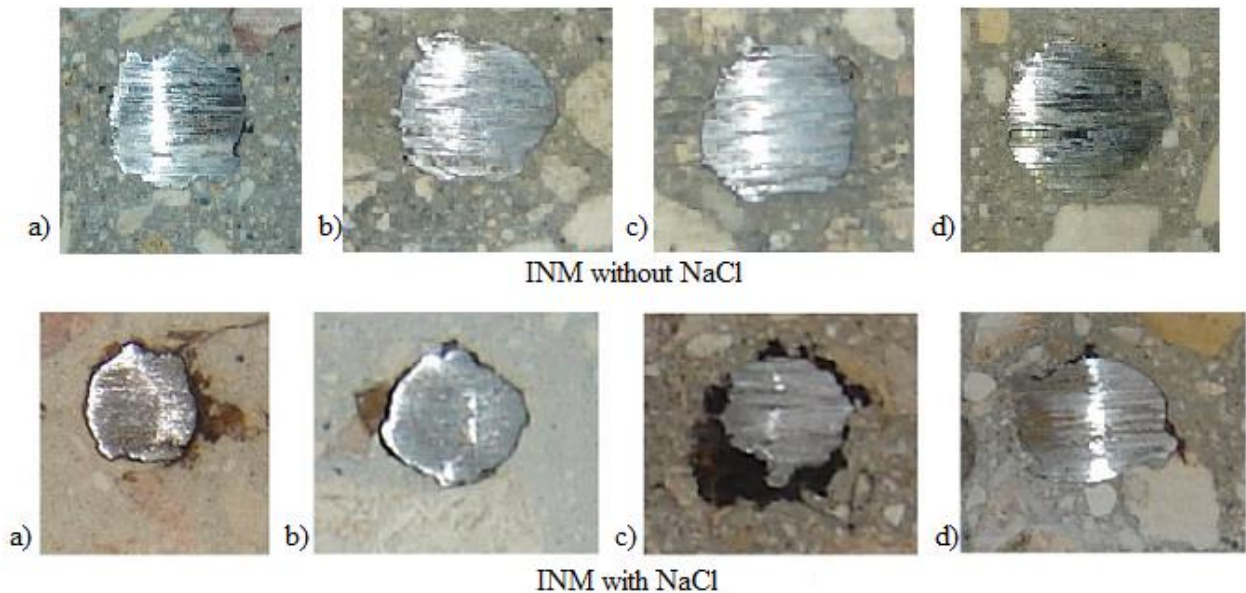


Figure 8. Photographic record of the concrete-reinforcing steel interface: a) 6, b) 12, c) 18 and d) 24 months, respectively, in structures exposed to INM.

Atmospheric Exposure.

The structures manufactured without additional NaCl exposed to the ATM, Figure 7, do not show corrosion products on the concrete-reinforcing steel interface on any of the four periods. When comparing these results with the structures with 3.5% of additional NaCl, corrosion products are observed on the concrete-reinforcing steel interface after the first 6 months and similarly within the three subsequent periods until the end of the 24-month experiment.

The absence of corrosion products in the structures without additional NaCl, exposed to the ATM, agrees with the electrochemical behavior of steel passivity reported in the corrosion potentials during the first 270 days. However, it subsequently passes to uncertain potentials of corrosion, behavior possibly related to the variation of environmental parameters. When the action of CO_2 is ruled out as well as the presence of chlorides at the level of the rod, the uncertain potentials are attributed to variations in environmental conditions, since no corrosion products were observed during the 2 years that the study lasted. Therefore, this behavior is attributed to the relative humidity, rainfall and temperature prevailing in the southeast of Mexico, which favors and gives the conditions to take the steel to potentials at uncertain values [Pérez et al, 2010].

The presence of corrosion products in the samples elaborated with additional NaCl, exposed to the ATM, is attributed mainly to the chlorides present since the beginning of the study, when the effect of carbonation was ruled out, since this reached the level of the rod until 2 years after the study started. These results agree with the corrosion potentials, however, with the photographic record it is not feasible to know precisely the corrosion start time. The E_{corr} that indicates a high probability of corrosion during the first 90 days evidence the attack of chloride ions to the steel. In this sense we must take into account that the newly manufactured concrete has the chemical property that protects the steel against corrosion. However, under exposure conditions, steel managed to reduce its activity, remaining within corrosion potentials of the uncertain zone, up to 210 days. Therefore, the corrosion activity decreases, with less negative E_{corr} values within the uncertain zone. The competition of passivation-depassivation reactions in the interface is the evidence (Pérez, 2000). In this case, an effect similar to that reported from the samples without additional NaCl was observed, approximately at 210 days of exposure, where the competition between the attack by the chlorides and the chemical protection of the concrete try to maintain the passive layer on the steel. This is attributed to the fact that corrosion potentials fluctuate

between the uncertain zone and the active zone, maintaining this behavior until the end of the study. In this sense, under the presented conditions the uncertain values obtained are related to the attack of chlorides to break the passive film and continue the corrosion of the steel.

Immersion exposure.

On those exposed to INM, Figure 8, the structures without additional NaCl do not show significant corrosion product formation on the concrete-reinforcing steel interface in the four periods; while in the structures with 3.5% NaCl added in the mixing water, oxidation is detected from six months after the start of the experiment. However, corrosion is not complete on the interface, since not all the area presents corrosion products. It is proposed that the damage to the film be limited due to the lack of oxygen when immersed in seawater. So, the chloride ion is the cause of corrosion.

In the samples prepared with additional NaCl exposed to INM, the presence of oxides in the concrete-reinforcing steel interface during the four stages of the photographic record coincides with the results of corrosion potentials with high probability of corrosion obtained in the 2 years of study. This is mainly attributed to the chlorides added to the mixing water since the the manufacture of concrete structures, when CO₂ was ruled out.

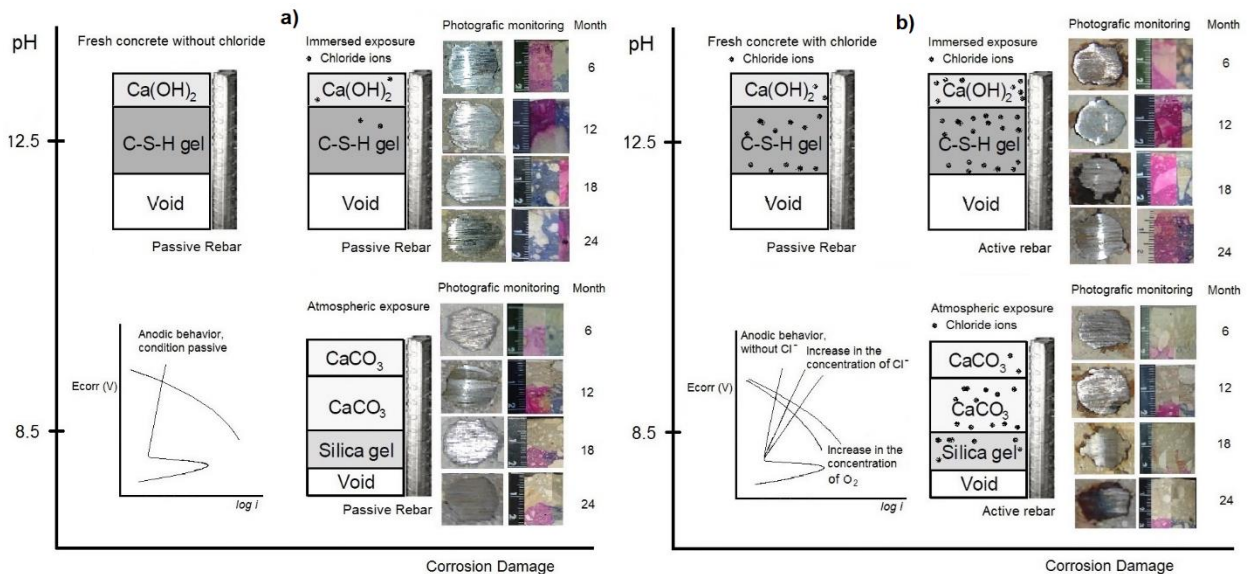


Figure 9: Summary of the damage progress in the reinforced concrete in the exposure conditions a) without chlorides and b) with chlorides, analyzed.

The presence of the aggressive agent is the triggering factor for corrosion in reinforcing steel when the conditions are favorable, as in this case and the one observed in the samples with additional NaCl exposed to the ATM. The opposite was observed on the samples without additional NaCl exposed to the ATM and INM where the action of CO₂ and chlorides at the rod level were discarded, leaving only the environmental conditions characteristic of the Southeast Mexico and the sea water as the only influences of the electrochemical behavior. In this sense, it is important to determine the presence of the corrosive agent in order to understand and interpret the corrosion potentials, as observed in the samples prepared without and with additional NaCl. Knowing the presence of the corrosive agent and also the significant presence of water is important and necessary element to carry out the chemical reactions of degradation of concrete and consequently the corrosion of reinforcing steel.

In general, the E_{corr} measures agree with the photographic record after 6 months. Potentials alone do not provide information on when steel corrosion could have started significantly, as was

observed on samples exposed to ATM with 3.5% NaCl. Corrosion is only inevitable when chlorides are already present at the level of reinforcing steel.

Figure 9 exemplifies the damage found on the specimens. On those exposed to ATM, carbonation leads to a decreasing pH of the material, although not enough to activate the steel. The same process is observed on prepared without and with NaCl. Meanwhile, the existing chloride ions reach the critical point to initiate the corrosion outbreak, but only on samples prepared with NaCl. On the specimens immersed in seawater, the trigger was the chloride ion, as observed for the existence of oxides since the first exposure period of samples prepared with NaCl. Those not prepared with NaCl did not develop corrosion at the concrete-steel interface.

4. CONCLUSIONS

Carbonation was not a factor for the development of corrosion in samples of reinforced concrete exposed to atmospheric conditions or in immersion. Only the samples prepared with additional NaCl in the mixing water, exposed to the ATM, reached a depth of 25 mm at the level of the rod 2 years after the study started. As for samples without additional NaCl, the advance of carbonation was lower, with an average depth of 15 mm at the end of the study.

The addition of NaCl in the mixing water and the characteristic environment in southeastern Mexico favored the advance of carbonation on samples exposed to the weather, reaching the steel level in two years of study; dissimilar to the structures without additional NaCl. This is due to the hygroscopic properties of NaCl, which together with the relative humidity prevailing in the tropical marine environment, maintain a longer moisture in the pores of the concrete which is conducive to carbonation reactions with the alkaline components of the concrete.

In the samples without additional NaCl, exposed to ATM and INM, no corrosion products were observed on the concrete and steel interface, which evidences that chloride ions are the determining factor to depass the interface.

In the case of samples with additional NaCl, corrosion was observed at the concrete-steel interface, which is in accordance with the corrosion potentials for both environmental conditions. This behavior was mainly attributed to the chlorides already present when the samples were prepared on the steel reinforcement interface of concrete. Therefore, chlorides were the main agent to initiate and develop the corrosion process which was evident for the presence of corrosion products on the concrete-rod interface. The same process was observed on both series of samples made with NaCl in the mixing water.

The visual inspection of the concrete-reinforcing steel interface was decisive to confirm the ranges of values of the steel corrosion potentials according to the variables analyzed.

The results obtained confirm that the corrosion potentials can lead to wrong inferences when the pores are saturated with water. Therefore, if the corrosive agent has reached the level of the rod, it offers greater certainty to determine the probability of corrosion in the reinforcing steel, as observed when comparing the samples prepared without and with additional of NaCl exposed to ATM and INM. This is related to the type of exposure that led potentials to more negative values due to the limited access of oxygen by water saturation, in the pores of the concrete, and not by the corrosion of the steel, as confirmed by the photographic record.

5. ACKNOWLEDGMENTS

The authors thank CONACYT projects CB-2008-01101891 and CB-2002-C01-40484 for partial support.

6. REFERENCES

- ASTM International (2002), “ASTM C192/C192M-02 Standard Practice for Making and Curing Concrete Test Specimens in the Laboratory”. Retrieved from https://doi.org/10.1520/C0192_C0192M-02.
- ASTM International (2009), “ASTM C876-09 Standard Test Method for Corrosion Potentials of Uncoated Reinforcing Steel in Concrete”. Retrieved from, <https://doi.org/10.1520/C0876-09>.
- ASTM International (2012), “ASTM C42/C42M-12 Standard Test Method for Obtaining and Testing Drilled Cores and Sawed Beams of Concrete”. Retrieved from https://doi.org/10.1520/C0042_C0042M-12.
- Berkeley, K. G., Pathmanaban, S. (1990), “Cathodic protection of reinforcement steel in concrete”, Ed. Butterworths, United Kingdom, ISBN 0-408-03270-1.
- Castro, P., Moreno, E. I. and Genescá, J. (2000a), “Influence of marine micro-climates on carbonation of reinforced concrete buildings”. Cement and Concrete Research V. 30, pp. 1565-1571, [http://dx.doi.org/10.1016/S0008-8846\(00\)00344-6](http://dx.doi.org/10.1016/S0008-8846(00)00344-6).
- Castro, P., Sanjuan, M. A. and Genesca, J. (2000b), “Carbonation of concretes in the Mexican Gulf”, Building and Environment., V. 35, pp. 145-149, [https://doi.org/10.1016/S0360-1323\(99\)00009-8](https://doi.org/10.1016/S0360-1323(99)00009-8)
- Castro-Borges, P., Veleza, L., Balancán-Zapata, M., Mendoza-Rangel, J. M., Juárez-Ruiz, L. A. (2013), “Effect of environmental changes on chemical and electrochemical parameters in reinforced concrete. the case of a tropical marine atmosphere”, International Journal of Electrochemical Science, V. 8, Issue 5, pp. 6204-6211.
- Chávez-Ulloa, E., Pérez-López, T., Reyes Trujeque, J., Corvo, Pérez, F. (2013), “Deterioro de elementos de concreto en medio ambiente marino tropical y cámara de carbonatación acelerada”, Rev. Téc. Ing. Univ. Zulia, V. 36, pp 104-113.
- Chess, P., Gronvold and Karnov, (1998), “Cathodic protection of steel in concrete”, E&FN Spon, United Kingdom, ISBN 0-419-23010-6.
- Corvo, F., Pérez, T., Martin, Y., Reyes, J., Dzib, L. R., González-Sánchez, J., Castañeda, A. (2008), “Time of wetness in tropical climate: Considerations on the estimation of TOW according to ISO 9223 standard”, Corrosion Science, V. 50, pp. 206–219.
- Genescá, J. (1994). *Más allá de la Herrumbre III: Corrosión y medio ambiente*. 1ra Edición. Fondo de Cultura Económica. México, D.F.
- Gutiérrez, G. and Winant, C. D. (1996) “Seasonal patterns of winds stress and wind stress curl over the Gulf of Mexico”. Journal of Geophysical Research, Vol. 101, No. 8, pp. 127.
- Helene, P., Castro-Borges, P. (2009), “A novel method to predict concrete carbonation”, Concr. Cem. Investig. Desarro. V. 1, No. 1, pp. 25-35.
- Melchers, R. E., Li, C. Q. (2009), “Reinforcement corrosion initiation and activation times in concrete structures exposed to severe marine environments”, Cement and Concrete Research, V. 39, issue 11, 1068, <http://dx.doi.org/10.1016/j.cemconres.2009.07.003>.
- Moreno, E. I., Domínguez Lara, G. G., Cob Sarabia, E. J., Duarte Gómez, F. (2004), “Efecto de la relación agua/cemento en la velocidad de carbonatación del concreto utilizando una cámara de aceleración Ingeniería”, Ingeniería, V. 8, No. 2, pp. 117-130.
- NMX-C-495-ONNCCE-2015 (2015), “Industria de la construcción – Durabilidad de estructuras de concreto reforzado – Medición de potenciales de corrosión del acero de refuerzo sin revestir, embebido en concreto – Especificaciones y método de ensayo”
- NOM C-159-85 (1985), “Concreto Elaboración y Curado en Laboratorio de Especímenes”.
- Papadakis, V. G., Vayenas, C. G., Fardis M. N. (1991a), “Fundamental modeling and experimental investigation of concrete carbonation”. ACI Materials Journal, V. 88, No. 4, pp. 363-373.

- Papadakis, V. G., Vayenas, C. G., Fardis M. N. (1991b), “*Physical and chemical characteristics affecting the durability of concrete*”, ACI Materials Journal., V. 88, No. 2, pp. 186-196.
- Pérez, T., Castro, P., Genescá, J. (2006), “*Influence of meteorological parameters over the chloride ingress to concrete exposed to marine environment*”. II Congreso Nacional ALCONPAT México 2006, 8 y 9 de Noviembre de 2006, Tampico, Tamaulipas, México ISBN 968 – 9031 -14 – 7.
- Pérez, T. (2000), “*Kinetics study of the concrete steel embedded reinforcement subject to different exposure conditions at marine environment*”, PhD thesis, UNAM, México.
- Pérez, T., Sosa, M. R., Dzib, L. R., Reyes, J., Camacho, R., Troconis-Rincon, O. y Torres-Acosta, A. (2010), “*Reinforced concrete beams deterioration in tropical marine environment: DURACON-Campeche*”. Concrete Under Severe conditions – Castro Borges et al (eds), Editorial Taylor & Francis Grup, London, pp. 413-420, ISBN: 978-0-415-59316-B.
- Rosas, O., Maya-Visuet, E., Castaneda, O. (2014), “*Effect of chloride ions on the electrochemical performance of LDX 2003 alloy in concrete and simulated concrete-pore solutions*”, J. Appl. Electrochem., V. 44, issue 5, pp. 631-646, DOI: <http://dx.doi.org/10.1007/s10800-014-0668-0>.
- San Miguel, G. F., Tamez, P. V., Alvarado, M. R., Alcorta, R. G., Garza, R. M., Farias, J. P. (2012), “*Deterioro por corrosión de elementos de concreto armado de un edificio industrial*”. Revista ALCONPAT, V. 2, No., 3, pp. 195 – 210. DOI: <http://dx.doi.org/10.21041/ra.v2i3.38>.
- Solís Carcaño, R. G., Moreno, E. I., Castro Borges, P. (2005), “*Durabilidad en la estructura de concreto de vivienda en zona costera. Ingeniería*”, Ingeniería, V. 9, pp. 13-18.
- Trocónis de Rincón, O. (1997), *Manual for inspecting, evaluating and diagnosing corrosion in reinforced concrete structures*. DURAR Network Members. CYTED. ISBN 980-296-541-3, Maracaibo, Venezuela. 1997/1998/2001 (1st ed. 2nd ed. and 3rd ed. in Spanish), 2000 (1st ed. in English).
- Trocónis de Rincón, O., Sánchez, M., Millano, V., Fernández, R., de Partidas, E. A., Andrade, C., Martínez, M., Castellote, M., Barboza, F., Irassar, J. C., Montenegro, R., Vera, A. M., Carvajal, R. M., de Gutiérrez, I., Maldonado, J., Guerrero, C., Saborio-Leiva, E., Villalobos, A. C., Tres-Calvo, G., Torres-Acosta, A., Pérez-Quiroz, J., Martínez-Madrid, M., Almeraya-Calderón, F., Castro-Borges, P., Moreno, E. I., Pérez-López, T., Salta, M., de Melo, A. P., Rodríguez, G., Pedrón, M., Derrégibus, M. (2007) “*Effect of the marine environment on reinforced concrete durability in Iberoamerican countries: DURACON project/CYTED*”, Corrosion Science, V. 49, Issue 7, pp. 2832-2843.
- UNE-112-011 (1994), *Corrosión en armaduras. Determinación de la profundidad de carbonatación en hormigones endurecidos y puestos en servicio.*, Madrid, Ed. AENOR.
- Ye, H., Jin, N., Jin, X. and Fu, C. (2012), “*Model of chloride penetration into cracked concrete subject to drying-wetting cycles*”, Construction and Building Materials, V. 36, pp. 259-269.
- Zitrou, E., Nikolaou, J., Tsakiridis, P. E. and Papadimitriou, G. D. (2007), “*Atmospheric corrosion of steel reinforcing bars produced by various manufacturing processes*”, Construction and Building Materials, V. 21, Issue 6, 1161-1169, <http://dx.doi.org/10.1016/j.conbuildmat.2006.06.004>.

On the influence of sugarcane bagasse ashes as a partial replacement of cement in compressive strength of mortars

R. A. Berenguer^{1*}, F. A. Nogueira Silva², S. Marden Torres³, E. C. Barreto Monteiro^{2,4}, P. Helene⁵, A. A. de Melo Neto¹

*Corresponding author: templarios_pm@hotmail.com

DOI: <http://dx.doi.org/10.21041/ra.v8i1.187>

Received: 24/02/2017 | Accepted: 21/12/2017 | Published: 30/01/2018

ABSTRACT

This paper presents an experimental program objectifying at investigating the potential of the use of sugarcane bagasse ash as a partial replacement of cement in the production of mortars. Sugarcane bagasse ashes from two origins were studied - one from sugarcane industry directly and other from pizzerias that uses this material replacing the wood in their ovens. The methodology followed the characterization of the material, where it was carried out through laboratory tests using X-ray diffraction (XRD) and X-ray fluorescence (WDXRF) and initial tests for the ideal quantification of cement substitution by residues. Results obtained indicated that both residues exhibited pozzolanic features presenting about 60% of amorphous material in their composition and compressive strength tests at different ages showed satisfactory results. Concluding that residues played an important role in increasing short and long term compressive strengths.

Keywords: sugarcane bagasse ashes; compressive strength of mortars; replacement of cement.

Cite as: R. A. Berenguer, F. A. Nogueira Silva, S. Marden Torres, E. C. Barreto Monteiro, P. Helene, A. A. de Melo Neto (2018), "On the influence of sugarcane bagasse ashes as a partial replacement of cement in compressive strength of mortars", Revista ALCONPAT, 8 (1), pp. 30 – 37, DOI: <http://dx.doi.org/10.21041/ra.v8i1.187>

¹ Departamento de Engenharia Civil-Estruturas e Materiais, Universidade Federal de Pernambuco, Recife-PE, Brasil.

² Departamento de Engenharia Civil, Universidade Católica de Pernambuco, Recife-PE, Brasil

³ Departamento de Engenharia Civil, Universidade Federal da Paraíba, João Pessoa-PB, Brasil

⁴ Departamento de Engenharia Civil, Universidade de Pernambuco, Recife-PE, Brasil

⁵ Ph.D.-Engenharia, Departamento de Engenharia Civil, Rua Visconde em Ouro Negro, São Paulo, Brasil

Legal Information

Revista ALCONPAT is a quarterly publication of the Latinamerican Association of quality control, pathology and recovery of construction- International, A. C., Km. 6, antigua carretera a Progreso, Mérida, Yucatán, C.P. 97310, Tel.5219997385893, alconpat.int@gmail.com, Website: www.alconpat.org

Editor: Dr. Pedro Castro Borges. Reservation of rights to exclusive use No.04-2013-011717330300-203, eISSN 2007-6835, both awarded by the National Institute of Copyright. Responsible for the latest update on this number, ALCONPAT Informatics Unit, Ing. Elizabeth Sabido Maldonado, Km. 6, antigua carretera a Progreso, Mérida, Yucatán, C.P. 97310.

The views expressed by the authors do not necessarily reflect the views of the publisher.

The total or partial reproduction of the contents and images of the publication without prior permission from ALCONPAT International A.C. is not allowed.

Any discussion, including authors reply, will be published on the third number of 2018 if received before closing the second number of 2018.

A influência das cinzas de bagaço de cana-de-açúcar como substituição parcial do cimento na resistência à compressão de argamassa

ABSTRACT

O artigo apresenta um programa experimental, objetivando investigar o potencial do uso das cinzas de bagaço de cana-de-açúcar como uma substituição parcial do cimento na produção de argamassas. As cinzas do bagaço de cana-de-açúcar de duas origens foram estudadas: uma oriunda diretamente da indústria de cana-de-açúcar e outra de pizzarias que utilizam este material em substituição a madeira em seus fornos. A metodologia seguiu com a caracterização do material, onde foi realizado através de testes de laboratório utilizando a difração de raios X (XRD) e a fluorescência de raios X (WDXRF) e testes iniciais para a quantificação ideal de substituição do cimento pelos resíduos. Os resultados obtidos indicaram que ambos os resíduos exibiram características pozolanas apresentando cerca de 60% de material amorfo na sua composição e testes de resistência compressiva em diferentes idades mostraram resultados satisfatórios. Concluindo que os resíduos desempenharam um papel importante no incremento das resistências à compressão a curto e de longo prazo.

Palavras-chave: cinza de bagaço de cana-de-açúcar; compressão de argamassa; substituição de cimento.

La influencia de las cenizas de bagazo de caña de azúcar como reemplazo parcial del cemento en la resistencia a la compresión de los morteros

RESUMEN

El artículo presenta un programa experimental, con el objetivo de investigar el potencial del uso de las cenizas de orujo de caña de azúcar como una sustitución parcial del cemento en la producción de morteros. Las cenizas del bagazo de caña de azúcar de dos orígenes fueron estudiadas: una oriunda directamente de la industria de caña de azúcar y otra de pizzerías que utilizan este material en sustitución de la madera en sus hornos. La metodología siguió con la caracterización del material, donde fue realizado a través de pruebas de laboratorio utilizando la difracción de rayos X (XRD) y la fluorescencia de rayos X (WDXRF) y pruebas iniciales para la cuantificación ideal de sustitución del cemento por los residuos. Los resultados obtenidos indicaron que ambos residuos exhibieron características de pozolanicidad presentando cerca del 60% de material amorfo en su composición y pruebas de resistencia compresiva en diferentes edades mostraron resultados satisfactorios. Concluyendo que los residuos desempeñaron un papel importante en el incremento de las resistencias a la compresión a corto y largo plazo.

Palabras clave: cenizas de bagazo de caña de azúcar; resistencia a la compresión de morteros; reemplazo de cemento.

1. INTRODUCCIÓN

Brazil is the most producer of sugarcane in the world and this commodity plays an important role in the country economy, especially in its northeastern region. This industrial sector is responsible for generating about 3.6 million direct and indirect jobs, besides being economically significant for the country in national and international trade relations, which account for 2.4% of gross domestic product (ALBINO et al, 2015).

These numbers shows the importance of the sector for the country economy and enhances the need for further research to enable rational use of the generated residue.

The most attractive waste from sugarcane industry is its bagasse, which can be used in several manners. One of these ways is the electric energy co-generation, a process that involves burning the bagasse at high temperatures that produces a significant amount of waste often referred as sugarcane bagasse ash. This type of ash is also generated in pizzerias that uses this material as a replacement of wood in their ovens. Recent researches indicates that the major chemical component of such ashes is the SiO_2 that exhibits great potential to be used as a mineral addition in concrete or mortars as pozzolanic aims.

The use of pozzolanic materials as a partial replacement of cement in mortar and concrete presents several advantages and the most important one is related with the reduction of CO_2 emissions because their obtention demands less energy than those involved in the clinker process. Furthermore, researches regarding the production of mortar and concrete using sugarcane bagasse ashes residues as supplementary cementitious materials (SCM) has already proved to be an efficient procedure with no loss of compressive strengths of tested specimens.

In this context, the paper discusses about the possibilities of using sugarcane bagasse ash (SCBA) from pizzeria as a partial cement replacement of Portland cement to produce mortars used in several applications in building industry.

2. EXPERIMENTAL PROGRAM

2.1 Materials

High initial strength Portland cement (Brazilian standard CPV ARI - similar to type III of ASTM), with a specific mass of 3.17 g/cm^3 and specific surface of $8924 \text{ cm}^2/\text{g}$ was used according to NBR NM 16372 (2015) and ASTM C231 / C231M - 17^a (2003).

Two types of sugarcane bagasse were used: one from a sugarcane industry (SCGA-Ind) and other from a pizzeria that uses this material in replacement of wood in its oven (SCGA-Piz). The ash temperatures of the sugarcane bagasse are $400 \text{ }^\circ\text{C}$ for the ash collected in the pizzeria and $500 \text{ }^\circ\text{C}$ collected in the industry, respectively. According to Ribeiro (2012) and Cordeiro (2009), the best burning sugarcane bagasse burning temperature is the burning at $600 \text{ }^\circ\text{C}$, under controlled burning. It is worth mentioning that the ashes collected remained in natura, without any type of thermal treatment.

The SCBA-Ind was collected from a sugar and alcohol producer located in the state of Pernambuco in the northeast of Brazil and the SCBA-Piz was collected in a pizzeria in metropolitan region of Recife capital of the state of Pernambuco that uses pressed ashes blocks in replacement of wood in its ovens. Samples of ashes used in the research were dried by means of sieving process for 20 minutes at a speed of 70 rpm to obtain a fraction passing through the sieve opening 0.075 mm .

Both pulverized ashes specific mass and specific surface are: 2.37 g/cm^3 and $6539 \text{ cm}^2/\text{g}$ for SCGA-Ind and 2.72 g/cm^3 and $6550 \text{ cm}^2/\text{g}$ for SCGA-Piz according NBR to NM 23 (2001) and ASTM D1298 - 12b (2017).

Tests used to assess the pozzolanic activity showed potential for both type of SCBA studied to be applied as pozzolanic admixture. The values obtained were also found by Nunes (2009), Cordeiro (2009) and Frias (2007). The chemical composition of bagasse ashes and Portland Cement used is presented in Table 1 and their and the crystallography in the diffractogram are shown in Figure 1 and Figure 2. These characteristic values with peaks at angles of 26.5° degrees SiO_2 were described by Ribeiro (2014). Both type of ashes are mainly composed by amorphous material according (BERENQUER, R.A; SILVA F.A.N. et.al. 2016).

Table 1. Chemical composition of studied ashes

Chemical element	Portland Cement	SCBA-Piz	SCBA-Ind
SiO ₂	18.30 %	63.61 %	84.86%
CaO	63.40%	7.18%	2.96%
MgO	0.62%	6.85%	2.54%
Fe ₂ O ₃	3.31%	6.63%	3.83%
SO ₃	3.32%	4.43%	0.38%
K ₂ O	0.78%	4.03%	1.38%
Al ₂ O ₃	4,01%	2.51%	1.91%
Cl	0.12%	1.81%	-
Na ₂ O	0.24%	1.04%	0.47%
P ₂ O ₅	0.38%	0.87%	0.38%
TiO ₂	0.21%	0.62%	0.75%
ZrO ₂	-	0.14%	0.12%
MnO	0.08%	0.12%	0.19%
Cr ₂ O ₃	0.02%	0.06%	0.05%
SrO	0.32%	0.05%	0.03%
ZnO	0.01%	0.04%	0.03%
Rb ₂ O	-	0.02%	0.015%

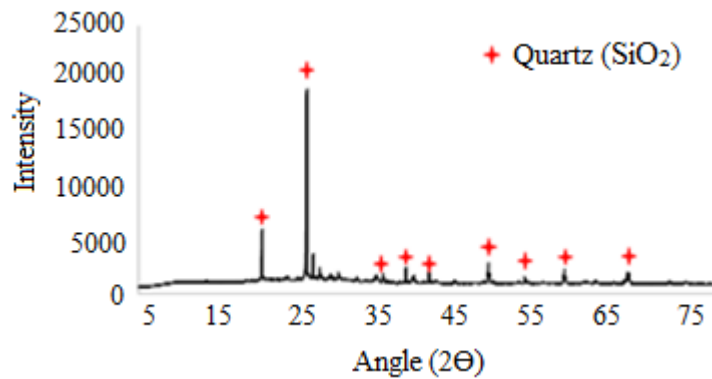


Figure 1. SCBA-Piz - XRD results. Font: Author (2016).

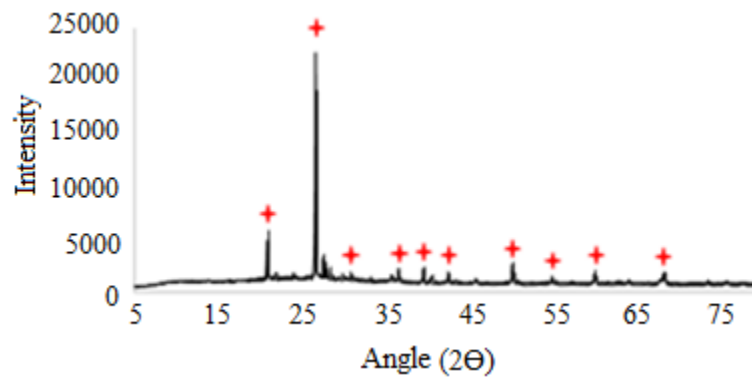


Figure 2. SCBA-Ind - XRD results. Font: Author (2016).

2.2 Mix designs

To find out the optimum amount of replacement of cement by both studied ashes six mixtures were produced: reference (REF), SCBA from pizzeria (SCBA-Piz-5%, SCBA-Piz-10%, SCBA-Piz-15%, SCBA-Piz-20%, SCBA-Piz-25% and SCBA-Piz-30%) and SCBA from sugarcane industry (SCBA-Ind-5%, SCBA-Ind-10%, SCBA-Ind-15%, SCBA-Ind-20%, SCBA-Ind-25% and SCBA-Ind-30%).

For each amount of substitution, six specimen were prepared to evaluate their compressive strengths after 28 days. Table 2 summarizes data of mortar mixtures used.

Table 2. Mortar mixtures used

SCBA (%)	Cement (kg)	Sand (kg)	Water (ml)	SCBA (g)
0	624,00	1.872	300	-
5	592,80	1.872	300	31,2
10	561,60	1.872	300	62,4
15	530,40	1.872	300	93,6
20	499,20	1.872	300	124,80
25	468,00	1.872	300	156,00
30	436,80	1.872	300	187,20

3. RESULTS AND DISCUSSION

Table 3 and Table 4 present results of compressive strengths performed in mortar-cylindrical specimens with dimensions of 50 mm in diameter and 100 mm in length in accordance to NBR 5739 (2007) and ASTM E9-89 00 (2000).

Table 3. Compressive strengths – SCBA from pizzeria

ID	REF	SCBA-Piz (5%)	SCBA-Piz (10%)	SCBA-Piz (15%)	SCBA-Piz (20%)	SCBA-Piz (25%)	SCBA-Piz (30%)
1	20,3	23,0	18,4	29,7	14,7	22,0	14,2
2	30,7	27,7	19,2	29,9	23,2	23,2	19,6
3	31,3	22,4	20,6	31,2	24,7	23,5	22,7
4	31,6	32,0	21,8	31,4	26,4	24,7	23,5
5	32,2	34,1	22,1	33,2	27,2	27,8	24,0
6	32,4	35,5	30,1	35,4	31,7	28,8	25,4
Average	29,8	29,1	22,0	31,8	24,7	25,0	21,6
SD (MPa)	4,7	5,6	4,2	2,2	5,7	2,7	4,1
COV (%)	15,7	19,3	19,1	6,8	23,0	10,9	19,0

Table 4. Compressive strengths – SCBA from sugarcane industry

ID	REF	SCBA-Ind (5%)	SCBA-Ind (10%)	SCBA-Ind (15%)	SCBA-Ind (20%)	SCBA-Ind (25%)	SCBA-Ind (30%)
1	20,3	14,8	24,9	34,8	26,9	25,7	22,5
2	30,7	28,8	25,4	35,1	28,6	26,0	23,0
3	31,3	29,3	29,1	35,5	29,0	26,8	23,5
4	31,6	36,6	37,0	35,8	29,7	26,9	24,7
5	32,2	38,4	37,5	36,1	30,5	27,1	24,9
6	32,4	39,5	38,9	36,3	30,7	27,4	25,3
Average	29,8	31,2	32,1	35,6	29,2	26,7	24,0
SD (MPa)	4,7	9,2	6,4	0,6	1,4	0,7	1,1
COV (%)	15,7	29,6	19,9	1,6	4,8	2,5	4,8

Finally, taken into account data from Table 3 and Table 4, the sugarcane bagasse ash from industry showed a better behavior with a very low coefficient of variation – 1.6%. More than 15% replacement caused a decreasing in compressive strengths of the mortars studied.

After choosing the optimum amount of replacement of cement by sugarcane bagasse ashes, new test specimens were produced in order to investigate compressive strengths at ages of 28, 63 and 91 days. Reference mortar mixture was designed to exhibit an average compressive strength of 40 MPa at 28 days.

Average compressive strengths and dispersion measurements are presented in Table 5.

Table 5. Average compressive strengths result and dispersion measurements

Mixture	Age (days)	Average compressive strengths (MPa)	Standard Deviation (MPa)	Coefficient of variation (%)
Reference	28	40,110	1,402	3,496
	63	41,699	1,919	4,603
	91	43,829	1,716	3,914
SCBA-Piz-15%	28	40,126	1,804	4,496
	63	42,678	1,820	4,265
	91	44,128	0,612	1,405
SCBA-Ind-15%	28	39,686	0,853	2,150
	63	41,179	1,446	3,511
	91	43,201	0,869	2,012

The statistical parameters and coefficients of variation obtained confirm that there is a consistent increase in the average strength with age for all mixtures studied. The coefficients of variations were all below 5% in all cases and this fact highlight the excellent control procedures of the preparation, molding and testing of specimens.

Results obtained showed that mortars made with replacement of cement mass by ashes from pizzeria and from sugarcane industry exhibited a good performance in terms of average compressive in all ages studied. This is specially important when one consider that mortar mixes made with ashes had a cement content lesser than those made using only cement as an agglomerating agent. This means that both ashes studied played a role as binder and as pozzolanic material. In fact, the increase in compressive strength at 91 days was approximately

8% for the mortars made with sugarcane bagasse ashes while for the mortar without replacement the increase was only 5%, at the same age.

These results encourage the use of sugarcane bagasse ashes as cement replacement in several applications in civil engineering field with the added advantage of producing two important and beneficial side effects: (a) reduction of environmental impact of the disposal of this agroindustrial waste in nature and (b) decrease in cement consumption with consequent significant reduction of CO₂ emissions per ton of cementitious materials.

In order to assess tensile strengths of the mortar studied, splitting tensile tests were performed at the same ages of the compressive tests and the results are summarized in Table 6.

Table 6. Average tensile strengths results and dispersion measurements

Mixture	Age (days)	Average tensile strengths (MPa)	Standard Deviation (MPa)	Coefficient of variation (%)
Reference	28	4,460	0,885	19,85
	63	4,082	0,103	2,52
	91	4,400	0,228	5,18
SCBA-Piz-15%	28	4,346	0,342	7,86
	63	4,034	0,083	2,06
	91	4,421	0,126	3,86
SCBA-Ind-15%	28	4,409	0,281	6,38
	63	4,067	0,154	3,80
	91	4,500	0,282	6,50

As it can be seen, tensile strengths of mortar made with sugarcane bagasse ashes exhibited almost the same values obtained for the reference mortar for all ages. This means that the use of such ashes cause no undesirable effect on tensile strengths of mortars.

4. CONCLUSION

Based on the procedures and equipment adopted in this research to assess compressive and tensile strengths of mortar, it was verified that the replacement of a content of 15% of cement mass by SCBA from pizzeria and sugarcane industry generated a binder an pozzolanic effect on mortars. The increase in compressive strength at 91 days was approximately 8% for the mortars made with sugarcane bagasse ashes while for the mortar without replacement the increase was only 5%, at the same age.

No undesirable effect in tensile strengths of the mortars made with sugarcane bagasse ashes was observed.

Furthermore, 30% of SCBA had performed as a pessimum content in this study for all strengths determinations.

The chemical composition of the ashes associated with its large surface specific and high degree of amorphousness explain this behavior.

Obtained results encourage the use of sugarcane bagasse ashes as cement replacement in several applications in civil engineering field with the added advantage of producing two important and beneficial side effects: (a) reduction of environmental impact of the disposal of this agroindustrial waste in nature and (b) decrease in cement consumption with consequent significant reduction of CO₂ emissions per ton of cementitious materials.

5. REFERENCES

- Albino, J. C., Creste, S., Figueira, A. (2015), *Mapeamento genético da cana-de-açúcar. Biotecnologia Ciência e Desenvolvimento*, 36: 82 – 91.
- Associação Brasileira de Normas Técnicas (2007), *NBR 5739: Cimento Portland - Determinação da resistência à compressão – Método de ensaio*. Rio de Janeiro.
- Associação Brasileira de Normas Técnicas (2001), *NM 23 - Cimento portland e outros materiais em pó - Determinação da massa específica*. Rio de Janeiro.
- Associação Brasileira de Normas Técnicas (2015), *NBR 16372 - Cimento Portland e outros materiais em pó - Determinação da finura pelo método de permeabilidade ao ar (método de Blaine)*. Rio de Janeiro.
- ASTM International (2000), *ASTM E9-89a 2000 Standard Test Methods of Compression Testing of Metallic Materials at Room Temperature* (Withdrawn 2009). <https://doi.org/10.1520/E0009-89AR00>
- ASTM International (2003), *ASTM C231/C231M-17a Standard Test Method for Air Content of Freshly Mixed Concrete by the Pressure Method*. https://doi.org/10.1520/C0231_C0231M-17A
- ASTM International (2017), *ASTM D1298-12b (2017) Standard Test Method for Density, Relative Density, or API Gravity of Crude Petroleum and Liquid Petroleum Products by Hydrometer Method*. <https://doi.org/10.1520/D1298-12BR17>
- Berenguer, R. A., Nogueira Silva, F. A., Barreto Monteiro, E. C., Silva Lins, C., Lima, A. (2016), “*Effect of Sugarcane Bagasse Ash as Partial Replacement of Cement on Mortar Mechanical Properties*”. *The Electronic Journal of Geotechnical Engineering*, v. 21, pp. 4577-4586.
- Cordeiro, G. C., Fo Toledo, R. D. and Fairbairn, E. M. R. (2009), *Characterization of sugar cane bagasse ash for use as pozzolan in cementitious materials*. *Química Nova*; 32 (1), pp: 82-86. <http://dx.doi.org/10.1590/S0100-40422009000100016>
- Cordeiro, G. C., Fo Toledo, R. D. and Fairbairn, E. M. R. (2009), *Effect of calcination temperature on the pozzolanic activity of sugar cane bagasse ash*. *Construction and Building Materials*. 23 (10), pp: 3301-3303. <http://dx.doi.org/10.1016/j.conbuildmat.2009.02.013>
- Frías, M., Villar-Cocina, E. and Valencia-Morales, E. (2007), *Characterisation of sugar cane straw waste as pozzolanic material for construction: calcining temperature and kinetic parameters*. *Waste Management*. 27 (4), pp: 533-538. PMID:16714102. <http://dx.doi.org/10.1016/j.wasman.2006.02.017>
- Nunes, I. H. S., Vanderlei, R. D., Secchi, M. and Abe, M. A. P. (2009), *Estudo das características físicas e químicas do bagaço de cana-de-açúcar para uso na construção*. *Revista Tecnológica*. (17), pp: 39-48.
- Ribeiro, D. V., Morelli, M. R. (2014), “*Effect of Calcination Temperature on the Pozzolanic Activity of Brazilian Sugar Cane Bagasse Ash (SCBA)*”. *Materials Research (São Carlos. Impresso)*, v. 17, p. 974-981.
- Ribeiro, D. V., Labrincha, J. A. and Morelli, M. R. (2012), *Effect of calcined red mud addition on the hydration of portland cement*. *Materials Science Forum*. 727-728:1408-1411. <http://dx.doi.org/10.4028/www.scientific.net/MSF.727-728.1408>

Potential of thermographic analysis to evaluate pathological manifestations in façade cladding systems

O. T. Takeda¹, W. Mazer*¹

*Corresponding author: wmazer@utfpr.edu.br

DOI: <http://dx.doi.org/10.21041/ra.v8i1.181>

Received: 02/03/2017 | Accepted: 23/11/2017 | Published: 30/01/2018

ABSTRACT

The present article discusses the potential of thermographic analysis in the evaluation of pathological manifestations in building façades. Its use may assist the identification and diagnosis of pathologies by reducing time and cost of these activities. For the application of this technique, the thermal sensor was calibrated, and the tests were performed in two distinct periods of solar incidence. The obtained results from this study demonstrate that the application of the thermographic analysis enables the identification and measurement of hidden pathological manifestations in façade cladding systems, including hard to reach sites, complementing the results of visual inspections and reducing its subjectivity.

Keywords: durability; façade; thermographic analysis; nondestructive testing; pathological manifestations.

Cite as: O. T. Takeda, W. Mazer (2018), “*Potential of thermographic analysis to evaluate pathological manifestations in façade cladding systems*”, Revista ALCONPAT, 8 (1), pp. 38 – 50, DOI: <http://dx.doi.org/10.21041/ra.v8i1.181>

¹Universidad Tecnológica Federal de Paraná, Universidad en Curitiba, Brasil.

Legal Information

Revista ALCONPAT is a quarterly publication of the Latinamerican Association of quality control, pathology and recovery of construction- International, A. C., Km. 6, antigua carretera a Progreso, Mérida, Yucatán, C.P. 97310, Tel.5219997385893, alconpat.int@gmail.com, Website: www.alconpat.org

Editor: Dr. Pedro Castro Borges. Reservation of rights to exclusive use No.04-2013-011717330300-203, eISSN 2007-6835, both awarded by the National Institute of Copyright. Responsible for the latest update on this number, ALCONPAT Informatics Unit, Ing. Elizabeth Sabido Maldonado, Km. 6, antigua carretera a Progreso, Mérida, Yucatán, C.P. 97310.

The views expressed by the authors do not necessarily reflect the views of the publisher.

The total or partial reproduction of the contents and images of the publication without prior permission from ALCONPAT International A.C. is not allowed.

Any discussion, including authors reply, will be published on the third number of 2018 if received before closing the second number of 2018.

Potencial da análise termográfica para avaliar manifestações patológicas em sistemas de revestimentos de fachadas.

RESUMO

O presente artigo discute o potencial da análise termográfica na avaliação de manifestações patológicas em fachadas de edifícios. Seu uso pode ajudar na identificação e no diagnóstico, reduzindo tempo e custos destas atividades. Para colocar em prática esta técnica, foi realizada a calibração do sensor térmico e os ensaios foram realizados em dois períodos diferentes de luz solar. Os resultados obtidos demonstraram que a aplicação da análise termográfica permite a identificação e medir a extensão de manifestações patológicas ocultas em sistemas de revestimento de fachadas, incluindo locais de difícil acesso, complementando os resultados das inspeções visuais e diminuindo a sua subjetividade.

Palavras chave: durabilidade; fachadas, termografia, ensaios não destrutivos, manifestações patológicas.

Potencial del análisis termográfico para evaluar manifestaciones patológicas en sistemas de revestimiento de fachadas

RESUMEN

El presente artículo discute el potencial del análisis termográfico en la evaluación de las manifestaciones patológicas en las fachadas de edificios. Su uso puede ayudar en la identificación y diagnóstico, reduciendo tiempo y costos de estas actividades. Para poner en práctica esta técnica, se realizaron la calibración del sensor térmico y los ensayos en dos periodos diferentes de luz solar. Los resultados obtenidos demostraron que la aplicación del análisis termográfico permite la identificación y extensión de las manifestaciones patológicas ocultas en sistemas de revestimientos de fachadas, incluyendo sitios de acceso difícil, complementando los resultados de las inspecciones visuales y disminuyendo su subjetividad.

Palabras clave: durabilidad; fachadas, termografía, ensayos no destructivos, manifestaciones patológicas.

1. INTRODUCTION

The building sector is one of the economic foundations of the country and it has evolved as much in constructive techniques as it has in building material development. However, the pathological manifestations in constructions continue to occur, possibly originating in the project phases, from execution or from usage and operation (Santos, 2013).

The absence of detailed projects or failures in its conception and compatibility, the wrong choosing of constructive systems and/or execution techniques, errors during material definition and specification, in quality and technological control, and environmental factors from the construction site region, during execution as well as usage and operation, may cause direct and indirect problems to constructions and owners, users or not of the properties (Santos, 2013).

According to Carvalho Jr. *et. al.*, (1999) in the case of façades, the cladding pathological manifestations compromise the image of engineering and architecture in the country, being an aggression to population perspective, to construction integrity and injuring the concepts of habitability. In addition to the natural depreciation of the property due to visual aspects, the

cladding basis, without the appropriate final finishing, becomes vulnerable to water and gas infiltrations, therefore leading to severe building deterioration of aesthetic or structural order. Due to severity, potential risk of accidents and material damage and its implications, the investigation of pathological manifestations in façades may involve the investigation of pathologies as well as of constructive processes used, assessing quality, safety and performance criteria through document analysis, visual inspections and site and laboratory tests required to give foundation to technical reports (Gomide, 2006).

In this regard, the investigation technique of the present article was based on nondestructive testing (NDT) through thermographic analysis that enables the identification of thermal anomalies in façade cladding systems, linking them to the analysis of typology and found damage extension, demonstrating the technique potentialities for both identifying and mapping the preexisting pathological manifestations.

2. LITERATURE REVIEW

2.1 Investigation of pathological manifestations

The systematization of investigation practices and the gathering of pathological manifestation information in building façades has been studied for a long time and by many authors (Mazer *et al*, 2016; Romero *et al*, 2011; Japiassú *et al*, 2014; Galletto, Andreello, 2013).

According to Gomide (2006), the façade inspections begin with in loco visual investigations of the damaged areas physical conditions. Such exams provide fundamental technical information to the inspection and assist in determining the problem cause and indicating its solution. In addition, the author states that such data collections are complicated due to approximated viewing difficulties of all the façade areas, recommending the utilization of additional technical procedures in the inspection.

In this type of situation, it becomes necessary to take advantage of other resources that may allow a meticulous visualization required for the data collection, whether they are direct or indirect. The mapping with tests consists on direct data collection with annotation in the blueprints of the damaged areas through the observation, by percussion, when descending along the façade, in a Bosun's chair or suspended scaffold. The indirect resource usually used in this type of investigation consists in photographically mapping the façade (Gomide, 2006). Another usable indirect resource is the façade thermographic mapping analysis.

2.2 Thermography principles

Thermography is a nondestructive and noninvasive inspection technique that has its base on the detection of infrared radiation naturally emitted by the bodies with intensity proportional to its temperature. This technique enables the identification of regions, or points, where the temperature is altered in relation to a preestablished pattern. It is based on the measurement of electromagnetic radiation emitted by a body in a temperature above absolute zero (Bauer, 2013).

The technique may be classified in active and passive according to the thermal excitation used. For the passive thermography, a natural temperature differential between the sample and the current environment is necessary, that is, no artificial thermal stimulation is used. For the active thermography, an external stimulus is imperative to induce the thermal contrasts between the sample and the environment (Maldague, 2001; Bauer, 2013).

The infrared radiation cannot be detected by the human eye; therefore, the infrared camera has the function of acquiring and processing data, presenting images that describe the temperature variations in the target objects (FLIR, 2012).

The radioactive properties of objects generally are described in relation to a perfect black-body, that is, a perfect emitter/absorber of radiant energy. In the real world, there are no perfect

emitter/absorber objects; however, it is possible to find objects with properties that are really close to those characteristics (FLIR, 2012).

Considering that the energy emitted by a perfect black-body is denoted by W_{bb} and that the energy emitted by a regular object in the same temperature is denoted by W_{obj} , the relation between these two values describes the object emissivity ε , as indicated in (1).

$$\varepsilon = \frac{W_{obj}}{W_{bb}} \quad (1)$$

Therefore, the emissivity is a value that varies from 0 to 1 and the better are the radiant object properties, the higher its emissivity is.

An object that has the same emissivity in all the wave-lengths is called a grey-body. The emission energy (W) of these bodies is determined by the Stefan-Boltzmann Law, presented in (2):

$$W = \varepsilon\sigma T^4 \quad (2)$$

Where ε is the object emissivity, σ is the Stefan-Boltzmann constant and T is the temperature. Besides the object radiation in analysis, the camera lenses receive radiations from the surrounding environment that are reflected in the object surface. These two radiation components are attenuated by the atmosphere that also absorbs and emits in its own way part of the radiation (FLIR, 2012). Given the previous premises, the total received radiation (W_{tot}) by the camera may be written as follows in (3):

$$W_{tot} = \varepsilon\tau W_{obj} + (1 - \varepsilon)\tau W_{amb} + (1 - \tau)W_{atm} \quad (3)$$

Where ε is the object emissivity, τ is the transmission through the atmosphere, W_{amb} is the effective energy from the surrounding object environment (or the energy reflected by the environment) and W_{atm} is the energy present in the atmosphere between the object and the camera.

2.3 Thermographic techniques in the façade investigation

The growing utilization of the infrared thermography in civil construction is intrinsically related to the fact that it is a nondestructive test, presenting itself as a great diagnostic tool (Soares, 2014).

With the infrared thermography it is only possible to detect anomalies associated to measurable modifications of the thermal characteristics, such as heat flow and resulting temperatures, and pathological manifestations with limited depths, in other words, close to surface (Pavón, 2015).

Laboratory studies demonstrate that adherence failures or mortar absence behind the ceramic claddings are easily identifiable through thermography, presenting superior superficial temperatures during the positive heat flow period than in the surrounding area, and inferior superficial temperatures during the negative heat flow period (Bauer *et al*, 2015).

In a study by Edis *et al.* (2014), it was demonstrated that it is also possible to identify areas with the presence of confined moisture under the ceramic claddings. This situation is configured by the identification of anomalies in superficial temperatures of the suspected areas in ceramic claddings during the positive heat flow, characteristics of detachment problems or of areas with presence of moisture.

For the case of façades coated with mortar and painting/texture, it is possible to identify other types of pathological manifestation such as fissures and moisture. Fissures are frequently associated with the presence of moisture, and the extension of affected areas is easily identifiable during the day, because water evaporation causes a reduction in superficial temperature within these regions. Similarly, the presence of moisture in masonry walls and concrete structures due to capillarity is also easily identifiable during the positive heat flow period (Pavon, 2015).

Menezes *et al.* (2015) performed inspection campaigns of several anomalies using visual inspections, thermography, percussion tests, karsten tube and hygrometer tests in order to formulate a field methodology for investigating the pathological manifestations in claddings. As a result of the study, it was verified that the visual inspections together with qualitative thermography were sufficient in the fast identification of most of the found anomalies, especially for allowing the inspection of places with difficult access.

In civil construction, a temperature variation from 1°C to 2°C is usually an indicative or a suspicion of problem existence. Over 4°C it is possible to affirm the existence of abnormality in the body (Maldague e Marinetti, 1996; Cortizo *et al.*, 2008).

For Bauer (2013), the main influences in the results of quantitative thermographic inspections are in the material emissivity, which is function of the superficial temperature and of the observation angle; in the surface reflectivity, function of the direct incident radiation and of the radiation of close objects; and in the atmospheric mitigation, function of the meteorological conditions.

3. METHODOLOGICAL PROCEDURES

First, an exploratory study was conducted on the façades of blocks B and C at Campus Curitiba, Ecoville headquarters of UTFPR for the purpose of investigating the anomalies occurrence and the existent types of pathological manifestations through qualitative visual and thermographic inspections to define the study areas.

Secondly, the characterization of the study areas was carried out and the calibration parameters of the calibration camera were defined, consisting in the determination of material emissivity, ambient temperature, humidity and distance between the thermal imager and the analyzed images during the confirmatory study.

Finally, the obtained thermograms were analyzed and compared in the exploratory study as well as in the confirmatory campaign with the intention of verifying if the found thermal anomalies may be linked to the existing pathological manifestations in the studied areas.

3.1 Infrared camera specification

A FLIR infrared camera (thermal imager), model E60, was used during the inspections. The camera personalized calibration parameters consist on emissivity, ambient temperature, reflected temperature, air relative humidity and distance to the object.

The equipment technical main specifications are presented in Board 1:

Board 1. Technical specifications of the Infrared Camera FLIR E60.

Model	FLIR E60
IR Resolution	320 x 240 pixels
Digital Camera Resolution	3.1 MP
Thermal Sensitivity	< 0.05 °C
Precision	+/- 2 °C or +/- 2% of reading
Temperature range	(-20.00 °C a 650.00 °C)
Spectral range	7.5 a 13µm
Field of vision (FOV)	25°
Focus	Manual
Uncooled microbolometer	LWIR (Long Wave InfraRed)
Colorful Display	3.5" (320 x 240)
Frame Rate	60Hz
Mobile measuring points	3
File format (Thermogram)	Radiometric JPG

Fonte: FLIR – Infrared Camera Manual, model E60 (2015).

3.2 Exploratory study and definition of study areas

The exploratory study consisted in the visual and thermographic inspection of the blocks B and C façades of the Ecoville headquarters of the Federal Technological University of Parana – UTFPR. The choice study areas was made during the morning period through visual inspections of the existing anomalies in the façades, and also qualitative thermographic inspections to identify the temperature gradients in different regions of a same material, setting the device using the standard emissivity parameter of concrete ($\epsilon=0.95$) and the parameters of ambient temperature (20°C) and air relative humidity (70%). During inspection, the climate conditions were stable, without the presence of rain, partially cloudy and without the occurrence of wind.

The façade cladding systems found in the exploratory study consisted of external concrete brick masonry with white paint (IJ Block); external concrete brick masonry, mortar plaster and light gray acrylic texture (Blocks A, B and C); and ceramic cladding applied over mortar plaster (Blocks B and C).

Bellow, boards will be presented together with pictures and thermograms obtained in the exploratory study followed by a brief description of the interferences, found thermal anomalies and possibly associated pathological manifestations.

In Figure 1 is presented the study area 1, defined in the Block C façade, along with its region thermogram.

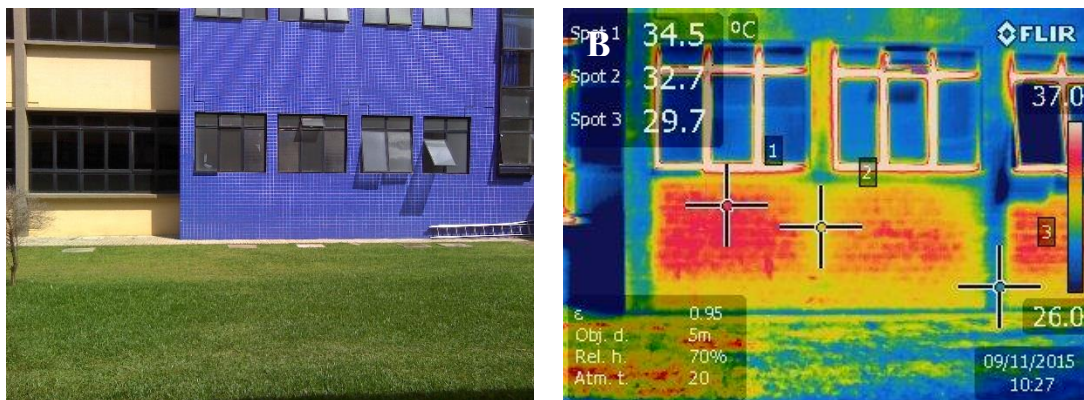


Figure 1. A) Block C façade constituting the study area
B) Thermogram of study area 1.

Points with damaged grout joints between the ceramic tiles around the window framing region were identified in the visual exam of study area 1 presented in Figure 1A.

Additionally, the percussion test detected hollow sounds in wall parts and window framing regions. Figure 1B shows a thermogram where it is possible to identify thermal anomalies in part of the façade executed with ceramic tiles during the positive heat flow in region with direct exposure to solar irradiation during the morning period.

The visual inspection performed in study area 2, presented in Figure A, verified the existence of fissures in the cladding. Additionally, the percussion test detected hollow sounds along the entire fissure region and below the fissure.

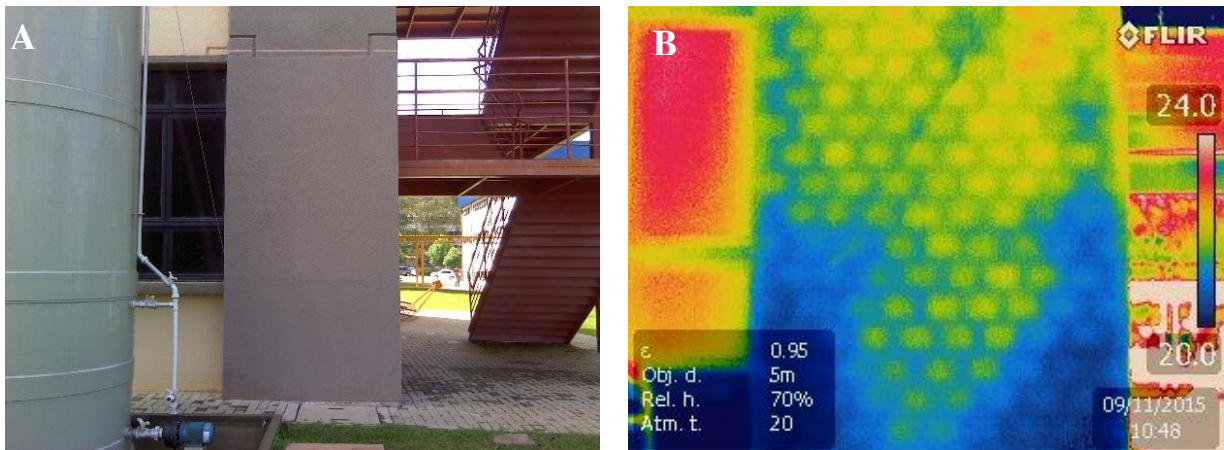


Figure 2. A) Part of Block C façade consisted of light gray acrylic texture over mortar plaster. B) Thermogram of study area 2.

In the thermogram presented in Figure 2B it is possible to identify a thermal anomaly in part of the façade during a positive heat flow period in region with no direct exposure to solar irradiation during the morning period. The characteristic anomaly from the presence of moisture identified by the thermogram, together with the presence of a fissure in the cladding and the coating detachment, infers the presence of moisture in the inferior region, between the mortar plaster and the concrete brick masonry.

In study area 3, shown in Figure 3A, it is possible to observe block B lateral façade executed with light gray acrylic texture over mortar plaster applied in a concrete brick masonry during the positive heat flow period in a region with no direct exposure to solar irradiation during the morning period.

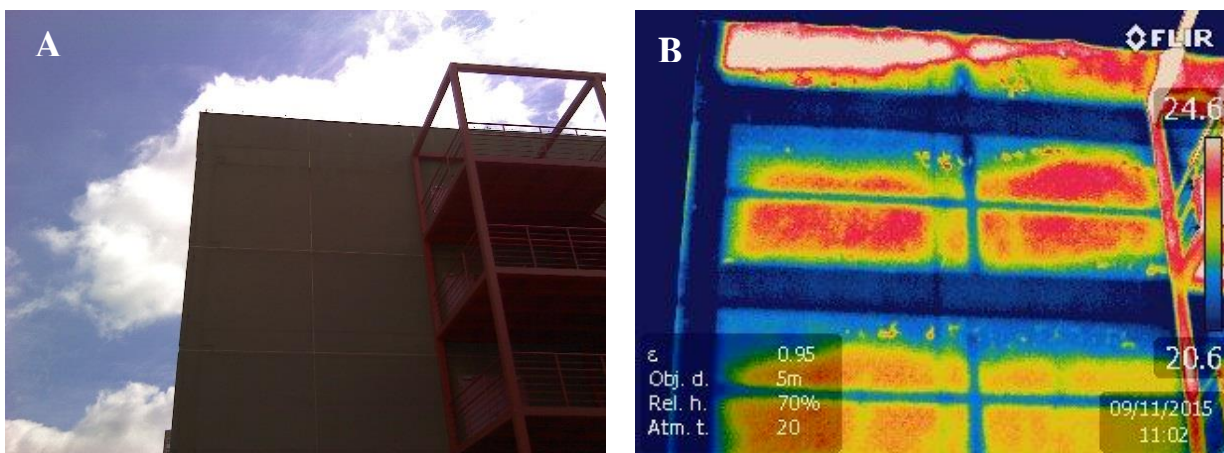


Figure 3. A) Block B lateral façade. B) Thermogram of study area 3.

In the thermogram presented in Figure 3B it is possible to observe a thermal anomaly in the interface region between the concrete brick masonry and the structural beam above, which is a characteristic of moisture presence. Likewise, it is possible to identify the structural elements, concrete tie beams that hold the concrete brick masonry walls and the more elevated temperature in the roof parapet wall region exposed to solar irradiation.

3.3 Determination of the thermal imager calibration parameters

Once the study areas were defined, field tests were carried out to determine the emissivity of the materials found. The tests consisted in determining the emissivity of the façade materials by comparing their surface temperatures with the temperatures of a material with known emissivity and in thermal stability with the analyzed surface.

For the material emissivity determination tests, pieces of black insulating tape adhered to the surface were used. The configuration parameters set for the thermal imager were:

- Measuring distance: 5m.
- Ambient temperature: 22 °C
- Air Relative Humidity: 88%
- Isolating tape Emissivity: 0.96.

The test consisted in measuring the surface temperature of the insulation tape, thermally stable with the surface indicated by point A, followed by the measurement of temperature in the material region to be analyzed, indicated by point B, modifying the emissivity parameter of the thermal imager until the temperature indicated at point B is equal to the temperature measurement indicated on the insulating tape surface. Figure 4 shows the calibration performed on the thermal imager for a ceramic cladding.

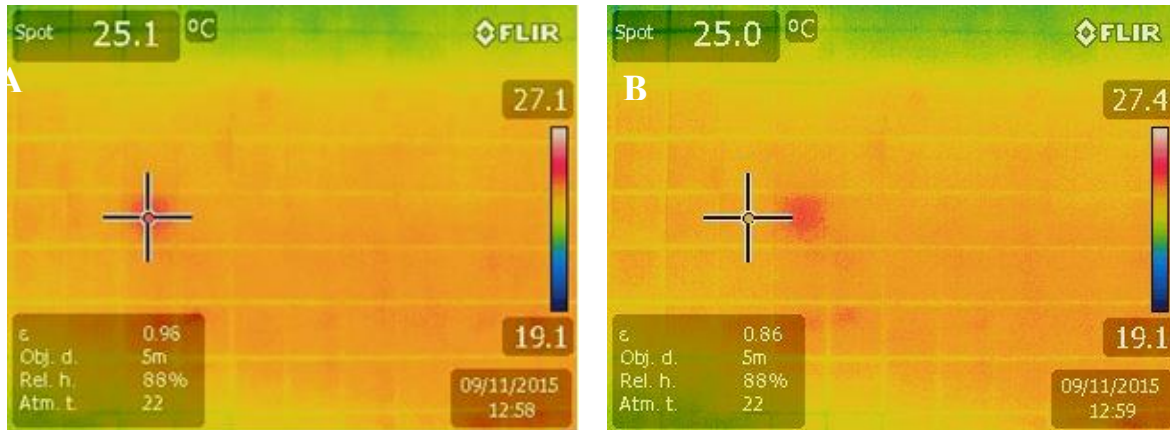


Figure 4. Ceramic cladding emissivity determination.

This procedure was performed for all claddings found in the study areas. The emissivity values found are presented in Table 1.

Table 1. Obtained values of the material emissivity of the study areas.

Surface	Emissivity
Gray acrylic texture	0.80
Red ceramic cladding	0.86
Blue ceramic cladding	0.86
White painting over concrete bricks	0.70

Fonte: Own authorship.

As the emissivity parameter used in the exploratory study was fixated, the thermographic inspection of this stage was qualitative, since the absolute temperature values of the surfaces did not reflect their real values. Nevertheless, the thermograms obtained in the exploratory study were entirely able to identify temperature gradients characteristic of the thermal anomalies in the inspected regions.

3.4 Confirmatory studies with the thermal imager

The confirmatory study sought to obtain complementary information on the heat flow dynamics of the study areas 1, 2 and 3 surfaces in order to confirm the preliminary suspicions about the potential pathological manifestations observed.

On the evening of the same day, the thermal imager was used in the study areas with a quantitative character, setting the equipment with the emissivity parameter obtained in Table 1 and the parameters of ambient temperature (22° C) and relative air humidity (88%).

Figure 5 shows the exploratory and confirmatory study thermograms of the study area 1.

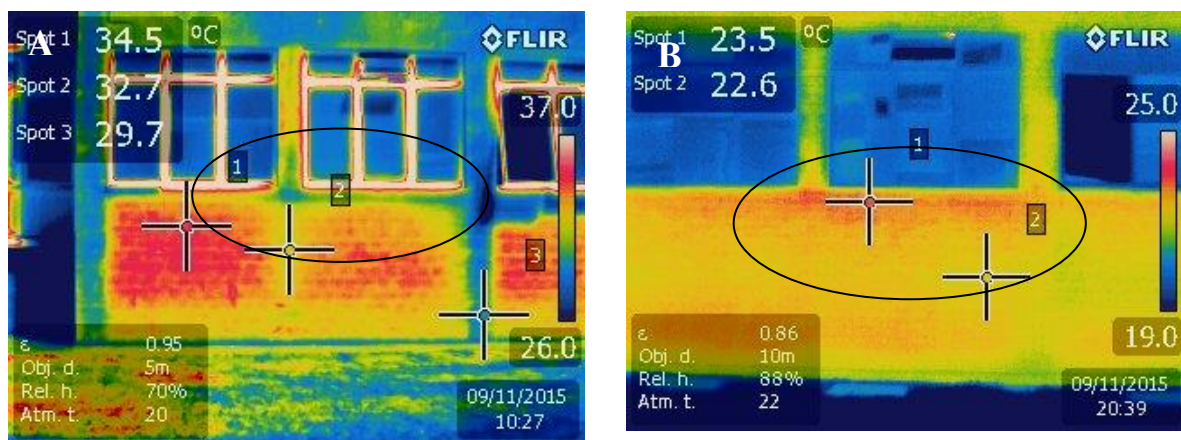


Figure 5. A) Exploratory study thermogram.
B) Confirmatory study thermogram.

In the confirmatory study of study area 1, presented in Figure 5B, it is possible to identify a thermal anomaly that may be associated to a possible detachment with presence of moisture below the ceramic cladding in the window framing region, since the presence of moisture in the region has the characteristic of maintaining higher temperatures in the thermograms during the negative heat flow period in comparison to the unaffected region. This hypothesis is reinforced by the identification of points with damaged grout between the ceramic tiles in the window region. It is also possible to observe in the exploratory study thermogram, shown in Figure 5A, that during the positive heat flow period the temperatures in the window framing regions are smaller due to water evaporation.

A fissure was observed in the cladding of study area 2, as presented by the thermograms shown in Figure 6.

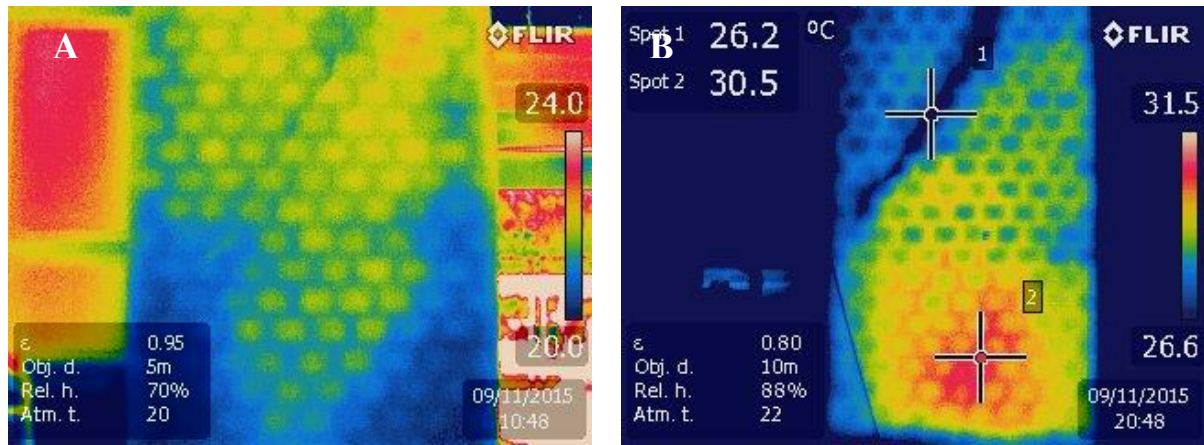


Figure 6. A) Exploratory study thermogram.
B) Confirmatory study thermogram.

In the exploratory study thermogram, shown in Figure 6A, it is possible to observe the existence of a thermal gradient in the lower part of the façade and a diagonal line, with temperatures lower than the central part of the façade. In the confirmatory study thermogram, illustrated in Figure 6B, it is possible to verify the existence of the diagonal fissure, marked by point 1, and the region with mortar plaster detachment together with moisture presence marked by point 2, with a higher temperature due to the ability water has of retaining heat during negative heat flow periods when compared to that of cladding materials.

The exploratory and confirmatory study thermograms of study area 3 are presented in Figure 7.

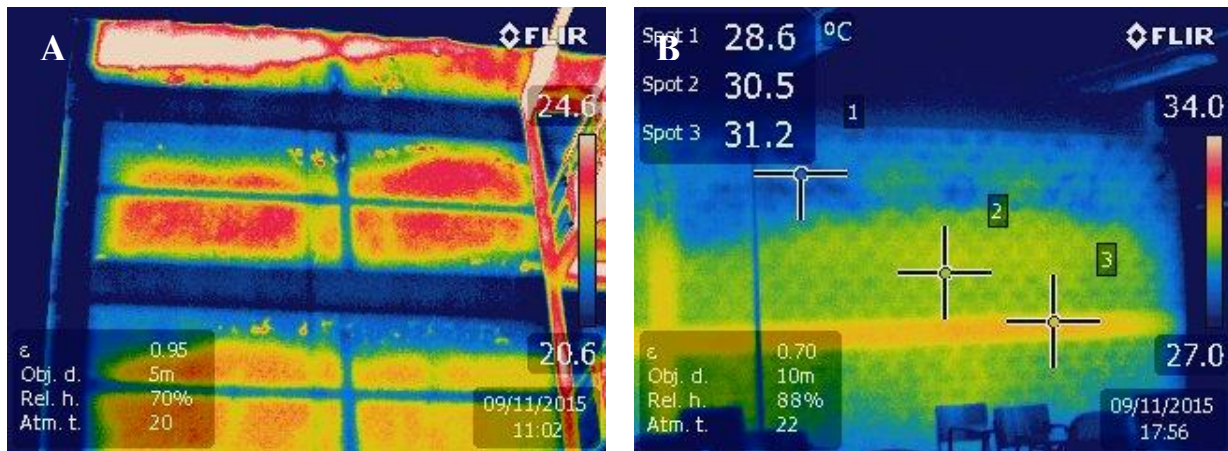


Figure 7. A) Exploratory study thermogram.
B) Confirmatory study thermogram.

In the exploratory study shown in Figure 7A, it is possible to observe the existing temperature variation, indicating lower temperatures in regions close to beams. In Figure 5B, obtained from the last floor interior, it is possible to observe a thermal anomaly in the region of the interface region between the concrete brick masonry and the structural beam above. The presence of moisture was evident in the interior of the building due to mold presence on walls in the humid region identified by the thermogram.

In addition, a visual inspection was carried out in the external region, due to the possibility of access by the fire scape ladder, from where it was verified the presence of a fissure in the entire extension of the interface region between the concrete brick masonry and the structural beam above in the affected region, thus allowing water infiltration into the building.

4. RESULTS AND DISCUSSION

The capacity of identifying thermal anomalies associated with pathological manifestations through thermography expedites the inspection process and allows the characterization of areas that should be subjected to more rigorous investigations, either by performing confirmatory thermographic studies or by using other field or laboratory tests.

Although it is relatively simple to use a thermal imager to obtain thermograms during the inspections, if the interferences and the environmental conditions in which the images were obtained are not taken into consideration, the analysis and interpretation of the thermograms can lead to mistaken conclusions. In order to avoid this, the theoretical background and the equipment usage experience to identify the thermal anomalies, characteristic from the investigated pathological manifestations, are fundamental to obtain the adequate basis for its interpretation and, consequently, to correctly associate its characteristics with the correspondent pathological manifestations.

Regarding the calibration parameters of the thermal imager, the emissivity values and other environmental parameters must be determined for each inspection situation when it is intended to obtain thermograms with precise temperature measurements of the analyzes surfaces, that is, in quantitative analyzes. For the identification of anomalies in a qualitative manner, these influence parameters do not impair the identification of temperature gradients on surfaces of the same material, a fact confirmed in the exploratory study.

However, the determination of the correct parameters must always be performed to support the analysis and interpretation of thermal anomalies for the diagnosis of pathological manifestations. The behavior dynamics of the surface heat flows and the deviations associated to certain pathological manifestations are also factors that require attention during the thermogram inspections and analysis. The determination of the best inspection and condition periods may assist obtaining thermograms that evidence the thermal anomalies that may be associated to pathological manifestations.

Regarding the determination of existing pathological manifestations severity and extent, thermography allows the identification of influence regions as well as the deleterious synergy of joint pathological manifestations. An example of this situation is the association of moisture presence and detachments in a same region, a condition that potentializes the evolution of both damages and, consequently, present an elevated damage potential to the performance and durability of cladding façade systems.

Considering the positive and negative heat flow observed in the morning and afternoon inspections, it was possible to determine the presence of moisture in 100% of the inspected regions, a fact confirmed by visual inspection. Likewise, in 60% of the cases it was possible to determine the existence of cladding detachment, being the ceramic cladding detachment easier to detect. The existence of fissures could only be detected when there was moisture inside the fissure, observed in 20% of the analyzed cases.

Some operational limitations were identified during the inspections. The thermogram resolution (320x240 pixels) is relatively low, making it difficult to identify the thermal anomalies with adequate accuracy and leading an impossibility of interpretation when the analyzed regions are at great distances. Another potential limiting factor in obtaining the thermograms is the possible result variation due to the observation angle between the camera and study region. In field studies this situation can be bypassed by increasing the observation distances to avoid capturing images at angles greater than 45°, according to the equipment manual.

5. CONCLUSIONS

Based on the obtained results during inspections, it was possible to characterize the pathological manifestations based on thermographic and visual inspections, complemented with visual inspection and percussion tests in places of possible access.

Percussion tests and confirmatory inspections during the negative heat flow period confirmed the cladding detachment in the suspected regions identified by thermography in the exploratory study. Both techniques confirmed the efficiency of infrared thermography in the identification of façade cladding detachments.

The thermogram interpretation based on the thermal anomalies and heat flow characteristics associated to each one of the pathological manifestations enabled the identification of their real extension.

The obtained results in this study confirmed the feasibility of thermography as a nondestructive test applicable to the cladding façade inspections with great usage potential and in monitoring the evolution of pathological manifestations with great advantages regarding the agility of inspections and reliability of results when compared with the usual techniques of façade inspection, reducing the subjectivity of exclusively photographic inspections, eliminating the works at height safety risk and enabling the predictive and preventive maintenance of façade cladding systems.

6. REFERENCES

- Bauer, E. (2013) “*Condicionantes das medições termográficas para avaliação de temperatura em fachadas.*”, X Simpósio Brasileiro de Tecnologia das Argamassas, Fortaleza:CE (Brasil).
- Bauer, E., Freitas, V. P., Mustelier, N., Barreira, E., Freitas, S. (2015), “*Infrared Thermography – Evaluation of the results reproducibility.*”, Structural Survey, v. 33, n. 1, p. 20-35.
- Carvalho, Jr., A. N., Silva, A. P., Neto, F. M. (1999), “*Perícias em patologias de revestimentos de fachadas. Congresso brasileiro de engenharia de avaliações e perícias.*”, X COBREAP. Porto Alegre:RS (Brasil).
- Cortizo, E. C., Barbosa, M. P., Souza, L. A. C. (2008), “*Estado da arte da termografia*”, Fórum Patrimônio, Ambiente Construído e Patrimônio Sustentável, v. 2, n.2, p 158 – 193, mai/ago. Belo Horizonte:MG (Brasil).
- Edis, E., Flores-Colen, I., Brito, J. (2014), “*Passive thermographic detection of moisture problems in façades with adhered ceramic cladding.*”, Construction and Building Materials, V. 51, pp 187-197. DOI: <https://doi.org/10.1016/j.conbuildmat.2013.10.085>
- FLIR (2012), “*The Ultimate Infrared Handbook for R&D Professionals*”, FLIR-Forward Looking Infrared.
- Galletto, A., Andrello, J. M. (2013), “*Patologias em fachadas com revestimentos cerâmicos.*”, IX Congresso Internacional sobre Patologia y Recuperación de Estructuras, CINPAR, Joao Pessoa:PB (Brasil).
- Gomide, T. L. F. (2006), “*Pericias de ingeniería em fachadas de edificaciones*”, IBAPE-SP, Sao Paulo: SP (Brasil).
- Japiassú, J., Carasek, H., Cascudo, O., Velosa, A. L. (2014), “*Caracterización da interface azulejo/argamassa de fachadas históricas*”, Revista ALCONPAT, V. 4, No. 1, pp. 55-76. DOI: <http://dx.doi.org/10.21041/ra.v4i1.61>
- Maldague, X. (2001) “*Infrared and Thermal testing: Nondestructive testing handbook.*”, (Columbus, OH, Patrick O. Moore, 3th ed.).
- Maldague, X., Marinetti, S. (1996), “*Pulse phase infrared thermography.*”, Journal Applied Physics, New York, v. 79, p. 2694-2698. DOI: <https://doi.org/10.1063/1.362662>

- Mazer, W., Silva, L. M. R., Lucas, E., Santos, F. C. M. (2016), “*Avaliação de manifestações patológicas em edifícios em função da orientação geográfica.*”, Revista ALCONPAT, Volumen 6, Número 2, mayo – agosto 2016, Páginas 145 – 156. DOI: <http://dx.doi.org/10.21041/ra.v6i2.135>
- Menezes, A., Gomes, M. G., Flores-Colen, I. (2015), “*In-situ assessment of physical performance and degradation analysis os rendering walls.*”, Construction and Building Materials. DOI: <https://doi.org/10.1016/j.conbuildmat.2014.11.039>
- Pavón, E. (2015), “*Termografia de infrarojo na identificação e avaliação de manifestações patológicas em edifícios.*”, Concreto & Construções, IBRACON, V. 79, p. 93-98.
- Romero, N., Dupuy, C., Quiñones, J. (2011), “*Influencia de la contaminación atmosférica em la fachada de rascacielos, caso Torre Colpatria*”, Revista ALCONPAT, V. 1, No. 3, pp. 228-235. DOI: <http://dx.doi.org/10.21041/ra.v1i3.17>
- Santos, S. S. (2013), “*Patologia das Construções.*”, Instituto de Pós-Graduação e Graduação - IPOG, Revista On Line IPOG Especialize, Curitiba:PR (Brasil).
- Soares, T. C. R. (2014), “*Termografia na avaliação do desempenho higrotérmico de edifícios – análise de sensibilidade.*”, Tese de Mestrado em Engenharia de Construção e Reabilitação, Instituto Politécnico de Viseu, Santa Maria (Portugal).

Adaptation of a damage map to historical buildings with pathological problems: Case study at the Church of Carmo in Olinda, Pernambuco

E. A. Rocha^{1*}, J. V. S. Macedo¹, P. Correia¹, E. C. B. Monteiro²

*Corresponding author: eu_des@hotmail.com

DOI: <http://dx.doi.org/10.21041/ra.v8i1.198>

Received: 24/02/2017 | Accepted: 21/12/2017 | Published: 31/01/2018

ABSTRACT

This article presents the elaboration and implementation of a damage map in a 16th century building with the aim of promoting the preservation of this historical-cultural heritage. The study adopts the elaboration of the damage map from the damage identification sheets developed during the inspections, configuring itself as an important tool to register problems and guide the prophylaxis services. The complexity of the analysis of historical buildings is emphasized, since it is essential to know the techniques and materials used in these constructions. It is concluded that the use of the indicated stages, in the elaboration of the map of damages, provides subsidies that facilitate the analysis of the symptomatology and the correct diagnosis, guaranteeing a more reliable treatment.

Keywords: construction pathology; damage map; diagnosis; church; patrimony.

Cite as: E. A. Rocha, J. V. S. Macedo, P. Correia, E. C. B. Monteiro (2018), “*Adaptation of a damage map to historical buildings with pathological problems: Case study at the Church of Carmo in Olinda, Pernambuco.*”, Revista ALCONPAT, 8 (1), pp. 51 – 63, DOI: <http://dx.doi.org/10.21041/ra.v8i1.198>

¹Universidade de Pernambuco, Recife, Brasil.

²Universidade de Pernambuco, Recife, Brasil e Universidade Católica de Pernambuco, Recife, Brasil.

Legal Information

Revista ALCONPAT is a quarterly publication of the Latinamerican Association of quality control, pathology and recovery of construction- International, A. C., Km. 6, antigua carretera a Progreso, Mérida, Yucatán, C.P. 97310, Tel.5219997385893, alconpat.int@gmail.com, Website: www.alconpat.org

Editor: Dr. Pedro Castro Borges. Reservation of rights to exclusive use No.04-2013-011717330300-203, eISSN 2007-6835, both awarded by the National Institute of Copyright. Responsible for the latest update on this number, ALCONPAT Informatics Unit, Ing. Elizabeth Sabido Maldonado, Km. 6, antigua carretera a Progreso, Mérida, Yucatán, C.P. 97310.

The views expressed by the authors do not necessarily reflect the views of the publisher.

The total or partial reproduction of the contents and images of the publication without prior permission from ALCONPAT International A.C. is not allowed.

Any discussion, including authors reply, will be published on the third number of 2018 if received before closing the second number of 2018.

Adaptação de mapa de danos para edifícios históricos com problemas patológicos: Estudo de Caso da Igreja do Carmo em Olinda PE

RESUMO

O artigo apresenta a elaboração de mapa de danos buscando implantá-lo em um edifício do Séc. XVI objetivando incentivar a preservação deste patrimônio histórico-cultural. A pesquisa adota a elaboração de mapa de danos a partir das Fichas de Identificação dos Danos desenvolvidas nas inspeções realizadas, configurando o mapa de danos como ferramenta fundamental para registrar problemas, norteados serviços de profilaxia. Enfatiza também a complexidade na análise das edificações históricas, pois torna-se indispensável conhecer as técnicas construtivas e materiais utilizados nestas edificações. Conclui, finalmente, que a utilização das etapas indicadas, na elaboração de mapa de danos, fornece subsídios que facilitam a análise da sintomatologia e do correto diagnóstico das patologias encontradas, garantindo uma proposta mais confiável para o tratamento das anomalias.

Palavras-chave: patologia das construções; mapa de danos; diagnóstico; igreja; patrimônio.

Adaptación de mapa de daños a edificios históricos con problemas patológicos: Estudio del caso de la Iglesia del Carmo en Olinda PE.

RESUMEN

Este artículo presenta la elaboración e implementación de un mapa de daños en un edificio del siglo XVI con el objetivo de fomentar la preservación de este patrimonio histórico-cultural. El estudio adopta la elaboración del mapa de daños a partir de las fichas de identificación de daños desarrolladas durante las inspecciones, configurándose como una herramienta importante para registrar problemas y guiar los servicios de profilaxis. Se enfatiza la complejidad del análisis de edificios históricos, puesto que es indispensable conocer las técnicas y materiales utilizados en estas construcciones. Se concluye que el uso de las etapas indicadas, en la elaboración del mapa de daños, proporciona subsidios que facilitan el análisis de la sintomatología y el correcto diagnóstico, garantizando un tratamiento más confiable.

Palabras clave: patología de las construcciones; mapa de daños; diagnóstico; iglesia; patrimonio.

1. INTRODUCTION

Generally, structural degradation processes are directly related to the exposure of buildings to physical, chemical, and biological agents present in the environment and in the building materials themselves. In other words, the structure is subject to the action of endogenous mechanisms, which cause deterioration of the structure from elements present in the chemical and mineralogical constitution of building materials; or to exogenous mechanisms, which correspond to (i) the action of man and the climate on the structure, (ii) the presence of pathological microorganisms, and (iii) the urban-architectural spatial transformation of the surrounding area. In this sense, it is extremely important that the diagnosis of the anomalies present in a building be correctly based on critical and investigative analyses of the origins of the problems found, in order to propose the most effective treatments and recover the useful life of the damaged material.

In this respect, it is necessary that surveys of the pathological manifestations and documents elaborated from these surveys be objective and clear to eliminate any doubts that may arise regarding their interpretation.

One of these documents, originating from surveys and building inspections, is the damage map, a fundamental tool for investigating a building's conservation state, especially when the inspected structure is a property with historical preservation interest, where interventions carried out and materials used in the past are highly important in the diagnostic phase.

However, despite such importance, and with few exceptions (studies that suggest regulation proposals, such as Negri and Russo (2008), Tinoco (2009), Costa and Baisch (2015), and the methodology indicated by the National Institute of Historical and Artistic Heritage - IPHAN), there is still no standardization indicating or determining the best procedure to be followed, which can make it difficult for restorers and pathologists to interpret damages that are present in the structures surveyed.

In view of the above, this article is the result of a Master's research project in progress and presents the processes of drawing a damage map based on the methodologies adopted by IPHAN, seeking to implement them in a real case study on the façades of the Carmo Church in the municipality of Olinda, PE.

The selection of this building first took into account its location, as it is part of the historic site of the city of Olinda, which holds the title of World Cultural Heritage Site, awarded by the United Nations Educational, Scientific and Cultural Organization (UNESCO) in 1982. Then, the date of its construction was considered, which corresponds to the middle of 1588, thus making it the oldest church of the Carmelite order in Brazil, and finally, the fact that the building has been fixed and restored recently, in July, 2012. Despite this recent restoration, there are some observable pathological manifestations to be found in its façades.

2. DEVELOPMENT

2.1 Characterization of the building under study

2.1.1 Brief history of the building

The construction of the Carmo Church began after the arrival of the Carmelite priests in Brazil in 1580. The plans at the time also included the construction of an adjacent convent that was begun in 1583, according to Mendes et al. (2011). According to Santos-Filho and Cunha (2008), this construction represents the oldest temple of the Carmelite Order built in Brazil.

Construction work on both the convent and the church lasted for many years, mainly due to the Dutch invasion in 1630, when the church together with the convent were looted and burned, leaving little of the originally planned structure. It held the largest church bell in the city, which was removed and transformed into armaments by the Dutch troops.

According to Oliveira and Ribeiro (2015), after the fall of Dutch rule, the reconstruction projects were resumed, but with difficulties in the second half of the seventeenth century, due to internal disagreements in the Carmelite Order. By the beginning of the eighteenth century, the crowns of the bell towers were completed, with the design of the pediment and windowsills being modernized to the aesthetic standards of the Pernambuco baroque period. The work developed between the middle of the eighteenth century until its end included internal ornamentation of the high altar and the central nave.

In 1907, the Franciscan convent, which can be observed in Figure 1, was demolished by order of the Olinda prefecture, as it had structural problems that constituted a serious threat to the population and to the Carmo Church itself (Gusmão Filho, 2001). At present, remains of the vestibule of the lobby and of the former convent's foundation can be seen (see Figure 2).

Around the year 2000, the Carmo Church underwent several interventions, undergoing restoration and stabilization of the slopes on which the building is supported, including the need to rebuild the slopes and reinforce the foundations and the east bell tower, which had become compromised (see Figure 3). The restoration and recovery services lasted about 10 years before

the Church was returned to the population. However, only 4 years following the restoration work, some anomalies in the façades can be observed.



Figure 1. Old Carmo Church with convent.
Source: Cultural Foundation of the City of Recife (FCCR)



Figure 2. Current Carmo Church: vestiges of the Carmelite convent.
Source: Authors.



Figure 3. Structural damage to the Carmo Church in the year 2000. Source: Public Collection of Olinda.



Figure 4. Current damages to the Carmo Church. Source: Authors.

2.1.2 Architectural and constructive characteristics

The Carmo Church is one of the most beautiful representations of Brazilian colonial religious architecture, an important historical asset that should be preserved. The building was federally registration by IPHAN on October 5, 1938 and plays an important role in tourism to the Historic Site of Olinda, which was granted the title of Cultural Heritage of Humanity by UNESCO in 1982.

The church has a pediment and façade in the baroque style, with some renaissance traits. The choir windows and the niche between them exhibit beautiful stonework (OLIVEIRA; RIBEIRO, 2015).

The ornamentation in the interior of the building, originally very simple with only the altarpieces of the high altar and side chapels standing out, gradually began to occupy the walls of the nave, as the baroque style arrived at the colony. According to Gusmão Filho (2001), its interior is imposing and treated with great wisdom, where a soft light, filtered through few openings, molds and defines the emptiness of the architecture, producing a mystical atmosphere.

With regard to its construction, it can be inferred that the Carmo Church adopted the typical constructive typologies of the Brazilian colonial period, inherited from the Portuguese and native

Indians. In this case, the stone or structural walls were fitted with thick stones for the base and support of the structures and the internal walls were built with bricks or adobe.

Figure 5 below shows the floor plan of the ground floor of the building. The projection of the ruins of the former convent of the Third Order of Carmo can be seen. It is also possible to note the extreme thickness of the main walls that support the loads of the bell towers and the roof.

The stone used in the construction of this building was limestone (although there are marble carvings in ornaments near the main altar), as Rieck and Souza (2007) attest. Limestone is a sedimentary rock having low resistance and high porosity, and was used throughout all the works of masonry present in the façades of the Carmo Church.

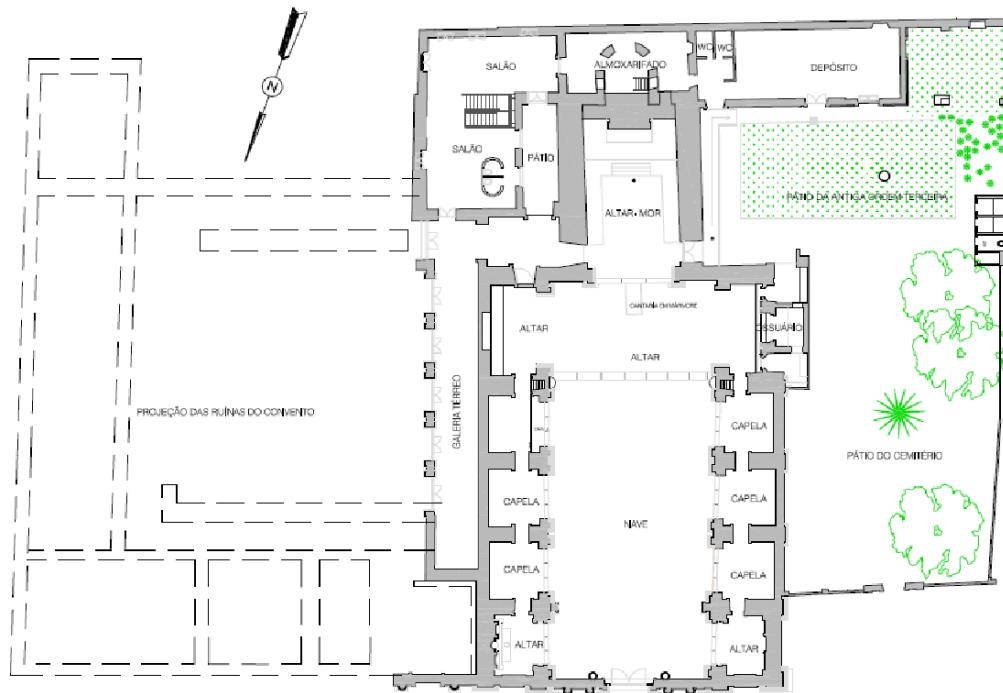


Figure 5. Floor plan of the ground floor of Our Lady of Carmo Church. Source: IPHAN (adapted).

2.2 Examining the damage

The process of mapping the anomalies for the damage map was divided into three stages: identification of the pathological problems, marking these anomalies on the façade blueprints, and photographing the pathological manifestations.

During the first stage, identification of the pathological problems, a tactical-visual inspection was carried out on the lower sections and a visual inspection on the upper sections, using equipment to reach the upper sections of the four façades of the Carmo Church. The second stage was carried out with the aid of printed elevations of the façades, on which the anomalies identified in the first stage were marked with distinct colors, taking care to mark lesions at the exact places in which they were found. In the third step, the anomalies were registered photographically in order to identify precisely the type of pathological problem found as well as the correct location of each.

Finally, in order to record the damages found and by associate them with analysis and diagnostic possibilities, the Damage Identification Form (DIF) was elaborated. This document is important because it allows the pathological manifestations to be registered and promotes their respective diagnoses, organizing the findings of the surveys to permit comparisons to be made.

The damage identification sheet proposed in this article lists the damages found in the façade elements, initially separating them into (i) damage to the walls (focuses mainly on anomalies in

the plaster), (ii) damages to the masonry, and (iii) damage occurring in the frames. For each anomaly, a symbol is presented, so that it can be replicated on the other façades studied, creating a representative pattern for the pathological manifestations.

It is worth noting that the inspection method adopted for the investigation of anomalies found is classified by Tinoco (2009) as an indirect method that, through non-destructive actions, searches for analyses and interpretation of the data in historical documents, in order to provide a base for hypotheses and conclusions regarding the diagnosis of the damage.

It should also be noted that the investigations carried out were restricted to the façades of the building only, meaning that the roof and interior of the church were not surveyed for the preparation of this article.

The investigations carried out affirm that the most commonly observed pathological problems in the façades of the Carmo Church were: dirt, vegetation, cracks, and humidity, with recurrences of black crust also being found in the east, west, and north façades. During the inspections, pieces of reinforced concrete with highly corroded steel reinforcement were also found, as well as a rotted wooden door in the north facade. In the following figures, the identification cards for the principal pathological manifestations are presented succinctly.



Figure 6. Damage identification form for the north façade of the Carmo Church. Source: Authors.

The DIF is organized to present, in addition to the list of damages found, some relevant photographs of the anomalies and the date on which the surveys were carried out, in order to establish a relationship between the state of degradation of the building and the time when it was inspected, as shown in Figure 6. The period in which the building was surveyed is important, in light of the possibility of the evolution of damage, as pathological manifestations tend to develop when the environment in which the building is located is conducive.

Figure 7 shows the identification form for the east façade, where it was observed that the pathological problems most frequently found were wet stains, dirt, cracks in the plaster, vegetation, and corrosion of reinforcements.

EAST FACADE		DAMAGES TO WALLS (MASONRY)		COURRENCY AND SIMBOLOGY
			1.GROUT'S DISPLACEMENT	X
			2.GROUT'S DISPLACEMENT WITH EXPOSED MASONRY	
			3.FIRE ACTION'S STAINS	
			4. MOISTURE STAINS	X
			5. BIODEGRADATION (FUNGI AND ALGAE)	
			6.VEGETATION	X
			7. DIRT ACUMULATION (DIRTINESS)	X
			8.EFFLORESCENCE (SALINIZATION)	
			9.SURFACE FISSURES (NON-ESTRUCTURAL)	X
			10.ESTRUCTURAL FISSURES (SHELVES AND TRINKS)	
			11.INTERVENTION WITH CEMENT/MORTAR	X
			12. VANDALISM (GRAFFITI)	X
			13. STEEL REINFORCEMENT'S CORROSION	X
			STONEMWORK'S DAMAGES	
			1. ALVEOLIZATION	
			2. GRANULAR DISAGGREGATION	
			3. PITTING	
			4. SECTION LOSS/LACQUES	
			5. ESFOLIATION	
			6. DARK CRUST	
			SQUADRON'S DAMAGES	
			1. TERMITE'S ATACKS	
			2. MOLD	
			3. WOOD DEGRADATION	X

Figure 7. Damage identification form for the east façade of the Carmo Church. Source: Authors.

The use of reinforced concrete, demonstrated by the presence of reinforcement corrosion, indicates an intervention in the structure with the use of construction technologies that did not exist at the time of the original construction of the church. Therefore, the treatment of this pathological manifestation should be done as soon as possible, and in a way that does not interfere with safety, while preserving the architectural features of the façade.

It is important to note that the east façade of the building has a higher incidence of saline mist. The Carmo Church is located in a coastal area, so structures made with reinforced concrete are subject to the degenerative action of chlorides and the cycles of wetting and drying produced by the rains.

In this sense, the correction of the corroded points found during the east façade inspection must be performed as quickly as possible, in order to avoid the loss of steel sections, the breaking of steps, or the displacement of larger areas.



Figure 8. Damage identification form for the south façade of the Carmo Church. Source: Authors.

On the southern façade, damp spots with accumulations of dirt were also observed, including ascending moisture stains along the entire length of the façade (see Figure 8).

Some alterations to the initial design of the building were also verified, including former doorways that have been sealed and windows that have been reduced in size. No information was found about these interventions, making it difficult to identify the material that was used to seal these elements.

It is believed that the material used was probably something with high porosity and high permeability, since moisture spots can be observed in the areas where these changes were made.

Another point identified was the appearance of a vertical crack with a gap ranging from 0.5 to 2 mm near the deposit wall (south façade). Because the Carmo Church has a history of structural problems resulting from settling, having undergone foundation reinforcement in 2001, treatment of this problem will require monitoring of the fissure in order to identify its origin.

Figure 9 shows the damage identification form for the west façade. The anomalies found were similar to the other façades; however, this façade had more damage to its masonry structures, which presented granular disintegration, pitting, and section losses (gaps).

The DIF for the west façade (Figure 9) also showed that the water penetration process capillarity action in the soil was intensified by the construction of a metallic ramp that causes water to splash onto the façade when it rains. This explains the development of mold and slime at this location.















WEST FACADE		DAMAGES TO WALLS (MASONRY)		OCURRENCE AND SIMBOLGY
		1.GROUT'S DISPLACEMENT	X	
		2.GROUT'S DISPLACEMENT WITH EXPOSED MASONRY		
		3.FIRE ACTION'S STAINS		
		4. MOISTURE STAINS	X	
		5. BIODEGRADATION (FUNGI AND ALGAE)		
		6.VEGETATION	X	
		7. DIRT ACUMULATION (DIRTINESS)	X	
		8.EFFLORESCENCE (SALINIZATION)		
		9.SURFACE FISSURES (NON-ESTRUCTURAL)	X	
		10.ESTRUCTURAL FISSURES (SHELVES AND TRINKS)		
		11.INTERVENTION WITH CEMENT/MORTAR		
		12. VANDALISM (GRAFFITI)		
		13. STEEL REINFORCEMENTS CORROSION		
		STONEMASONRY'S DAMAGES		
		1. ALVEOLIZATION		
		2. GRANULAR DISAGGREGATION	X	
		3. PITTING	X	
		4. SECTION LOSS/LACQUES	X	
		5. ESFOLIATION		
		6. DARK CRUST		
		SQUADRON'S DAMAGES		
		1. TERMITE'S ATTACKS		
		2. MOLD		
		3. WOOD DEGRADATION		

Figure 9. Damage identification form for the west façade of the Carmo Church. Source: Authors.

2.3 Elaboration of the Damage Map

Tinoco (2009) defines a damage map as graphic-photographic, synoptic representation, where all manifestations of deterioration of the building are rigorously and meticulously illustrated and detailed, in order to synthesize the results of the investigation of structural and functional alterations in the materials, techniques, systems, and building components.

The author also warns that the term “damage map” not be confused with damage mapping, since the first corresponds to the document or set of documents that illustrate the state of conservation of the building on a specific date. Damage mapping, on the other hand, refers to a phase of surveys where investigations are conducted and data is produced in order to draw up the damage map.

Therefore, to prepare the damage map, it is necessary to collect information about the building to better understand the pathological problems that can be found during the damage mapping phase. The constructive methods, history of interventions, and understanding of the area where the building is located are fundamental factors for the analysis of pathological manifestations.

Using the damage identification forms for each façade analyzed (with each damage found identified by a symbol), the photographic records, and the notes on the historical data and construction materials of the building, the damage map can be prepared.

Figures 10, 11, 12, and 13 below show the damage maps produced for the north, east, south, and west façades, respectively, of the Carmo Church.



Figure 10. Damage Map of the North Façade of the Carmo Church. Source: Authors.

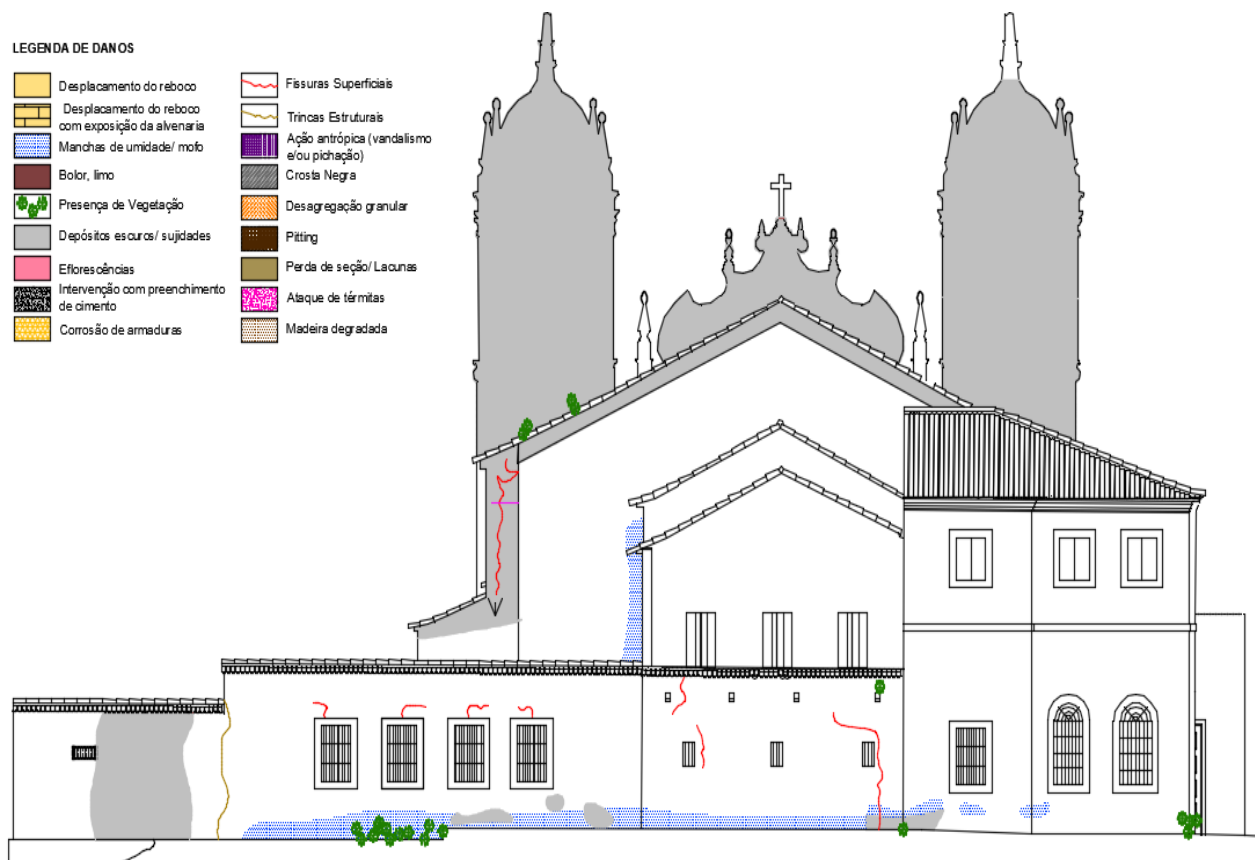


Figure 11. Damage Map of the South Façade of the Carmo Church. Source: Authors.

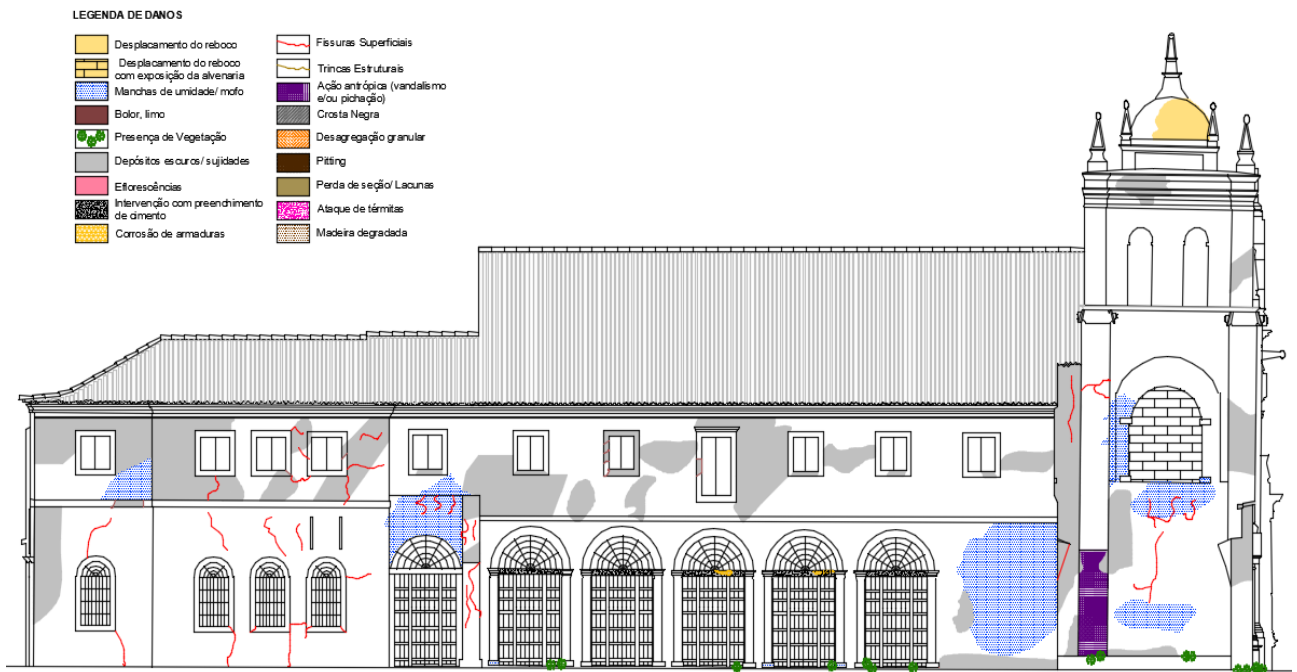


Figure 12. Damage Map of the East Façade of the Carmo Church. Source: Authors.

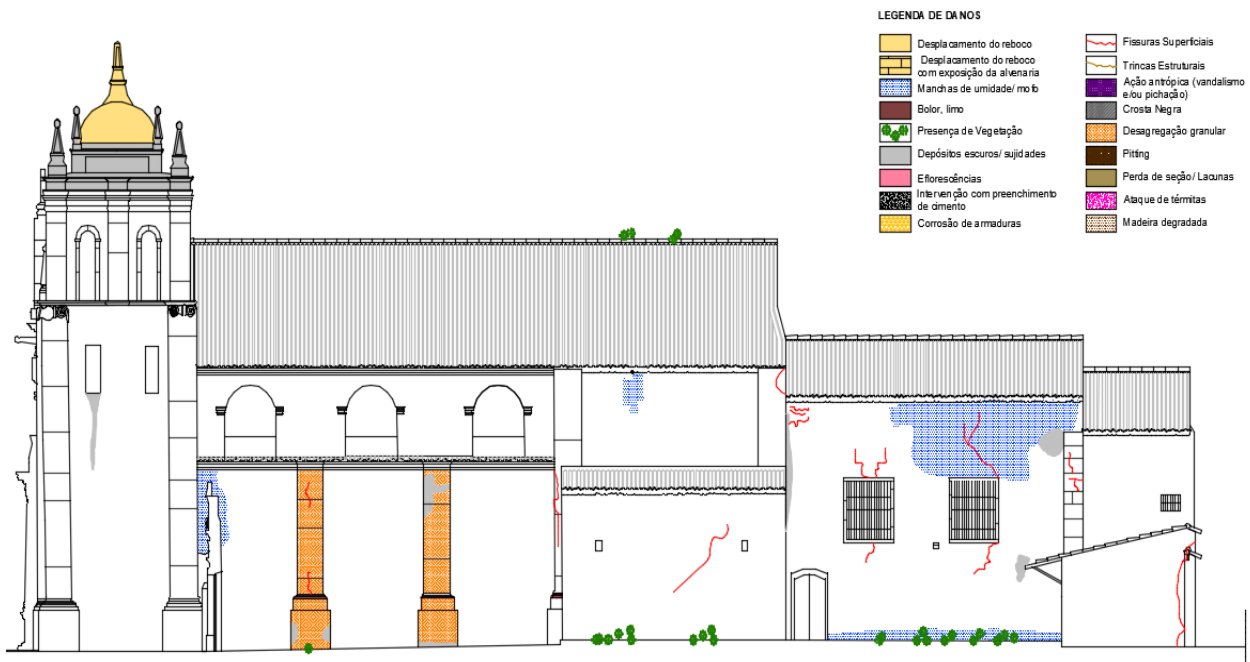


Figure 13. Damage Map of the West Façade of the Carmo Church. Source: Authors.

It should be noted that the damage map shown in Figure 10 was based on the information obtained by the DIF shown in Figure 6. Figure 11, in turn, considered the observations presented in the DIF of Figure 8. Figure 12 was based on information from the DIF in Figure 7 and the damage map of Figure 13 was drawn from the data contained in the DIF of Figure 9.

3. DISCUSSION

It is known that an analysis of the origin of pathological manifestations is crucial so that the intervention performed to correct the problem found will adequately restore the structure and guarantee that the same anomaly will not recur, thereby increasing the useful life of the structure. For example, corrosion was found in an area of the east façade of the Carmo Church where an intervention had been performed using reinforced concrete. Later, the analysis that the area is near the sea demonstrates the importance taking into account the environment in which a building is located, especially because saline mist can aggravate the effect of the corrosion.

Thus, the analysis of the conditions for the development of the anomaly is essential in diagnosing the nature of the problem. Questions such as "why did that anomaly appear at this location?" should be asked so that an understanding of the origin of the pathological manifestations can be generated.

In this sense, the elaboration of Damage Identification Forms (DIF) contributes actively to the analysis of the pathological problems, while at the same time constituting a fundamental tool for building a documentary record of the visits made and anomalies found in the structure.

The DIF is a model that can be applied not only for historical buildings, but also for any concrete structures that develop pathological problems at an early stage, as long as they have structural elements (pillars, beams, slabs, etc.), sealing elements (masonry, partitions, panels), or any other constructive system that can be inspected.

This adaptability of the DIF is advantageous because it makes it possible to register and organize data collected during inspections that indicate the state of damage to the system at the exact moment of the inspection, enabling a quicker diagnosis and proposal of solutions.

After creating the DIF, damage maps are made in order to simplify the visualization of each pathological manifestation, showing in a practical way the location of the problems and their dimensions on each of the façades studied.

This helps to determine the best therapy procedure for the problems studied, as well as to identify the best attack plan for recovery and/or restoration of the asset under analysis.

The study also demonstrates the necessity and importance of correctly using materials appropriate to the environment in which they are inserted. In the studies carried out, specifically at the Carmo Church, it can be shown that most of the pathological manifestations discovered could have been avoided with the adoption of less porous and permeable materials.

Despite this perception, it is also important to remember that these constructions from the colonial period were often rudimentary and subject to the degrading action of man and the environment, the transformations of the urban atmosphere and, principally, the deterioration provoked by the action of time itself.

Another observation of this study was the difficulty of dealing with property having special preservation interests, considering that the laws and regulations necessary for historical preservation can interfere significantly in the maintenance of the building when associated with an inefficient management and with restoration techniques that are inappropriate for the conservation of the property.

4. FINAL CONSIDERATIONS

The importance of the damage map and the damage identification form are reiterated as essential tools for the diagnosis and therapy of historic buildings as they represent documented records of the state of construction degradation.

It should also be pointed out that this methodology of inspection and registration of pathological problems can be used both in the preservation of historical assets and in the conservation of

newly constructed buildings, as long as the constructive elements considered in the DIFs are altered so as to represent the structures that were surveyed and analyzed.

5. ACKNOWLEDGEMENTS

The authors would like to thank the Polytechnic School of the University of Pernambuco and CAPES (Coordination for the Improvement of Graduate Personnel) for the research funding, as well as to the Public Collection of Olinda, SEPAC (Secretariat of Heritage and Culture of Olinda), and IPHAN (Institute of National Historical and Artistic Heritage) for allowing and making available the data and information presented in the history of the church under study.

6. REFERENCES

- Costa, L.G.G., Baisch, L.F. (2015). “*Cronidas: proposta de padronização de representação em mapas de danos*”. In: A Conservação do Patrimônio no Brasil Teoria e Prática: 1º Seminário da Rede Conservação_BR. Olinda: Centro de Estudos da Conservação Integrada.
- Gusmão Filho, J. de A. (2001). “*A cidade histórica de Olinda: problemas e soluções de engenharia*”. Recife: Editora Universitária da Universidade Federal de Pernambuco. 193p.
- Mendes, F., Veríssimo, F., Bittar, W. (2011). “*Arquitetura no Brasil: de Cabral a Dom João VI*”. Rio de Janeiro, Brasil: Imperial Novo Milênio. 232 p.
- Negri, A., Russo, J. (2008). “*Degrado dei material lapidei: Proposta di simbologia gráfica*”. In: CARBONARA, Giovanni (ed.): Trattato di restauro architettonico. Secondo Aggiornamento. Grandi temi di Restauro, Utet: Torino.
- Oliveira, M.A.R. de, Ribeiro, E.S. (2015). “*Barroco e Rococó nas Igrejas de Recife e Olinda*”. Brasília, DF: Instituto do Patrimônio Histórico e Artístico Nacional (IPHAN). V. 2, 225p.
- Rieck, F.E., Souza, J.C.de (2007). “*Condições de conservação e patologias dos bens pétreos de monumentos históricos da zona da mata pernambucana*”. In: III Congresso Brasileiro de Rochas Ornamentais, Natal, Rio Grande do Norte, Brasil. Nov, 2007. 108-118 p.
- Santos-Filho, P., Cunha, F.C.da (2008). “*Um dia em Olinda*”. Olinda, Brasil: Aerpa Editora. 164p.
- Tinoco, J.E.L. (2009). “*Mapa de danos recomendações básicas. CECI: Centro de Estudos Avançados da Conservação Integrada*”. Olinda, Brasil.

Load check on anchored curtains located in geotechnical hazard areas in the city of Rio de Janeiro

A. X. Machado*¹, L. C. Mendes¹

*Corresponding author: alexandrem2007@gmail.com

DOI: <http://dx.doi.org/10.21041/ra.v8i1.200>

Received: 21/06/2017 | Accepted: 07/12/2017 | Published: 31/01/2018

ABSTRACT

This article aims to investigate the load behavior on the tie rods of anchored curtain walls built to eliminate geological-geotechnical hazards on hillsides in the city of Rio de Janeiro. Taking into account increases in overload due to the growth in construction uphill of these structures and the end of their service lives, a simulation was conducted using the Plaxis computational system to estimate the loads on the tie rods of 20 anchored curtains after 50 years. Those results were compared with results obtained from residual load verification tests. The comparison shows that although the theoretical simulations indicate increases in loads over 50 years due to the additional overloads, the tie rods tend to lose load, even with increased overloads in the anchored curtains.

Keywords: anchored curtain; overload; durability.

Cite as: A. X. Machado, L. C. Mendes (2018), “Load check on anchored curtains located in geotechnical hazard areas in the city of Rio de Janeiro”, Revista ALCONPAT, 8 (1), pp. 64 – 78, DOI: <http://dx.doi.org/10.21041/ra.v8i1.200>

¹ Universidade Federal Fluminense, Brasil.

Legal Information

Revista ALCONPAT is a quarterly publication of the Latinamerican Association of quality control, pathology and recovery of construction- International, A. C., Km. 6, antigua carretera a Progreso, Mérida, Yucatán, C.P. 97310, Tel.5219997385893, alconpat.int@gmail.com, Website: www.alconpat.org

Editor: Dr. Pedro Castro Borges. Reservation of rights to exclusive use No.04-2013-011717330300-203, eISSN 2007-6835, both awarded by the National Institute of Copyright. Responsible for the latest update on this number, ALCONPAT Informatics Unit, Ing. Elizabeth Sabido Maldonado, Km. 6, antigua carretera a Progreso, Mérida, Yucatán, C.P. 97310.

The views expressed by the authors do not necessarily reflect the views of the publisher.

The total or partial reproduction of the contents and images of the publication without prior permission from ALCONPAT International A.C. is not allowed.

Any discussion, including authors reply, will be published on the third number of 2018 if received before closing the second number of 2018.

Verificação de carga em cortinas ancoradas localizadas em áreas de risco geotécnico na cidade do Rio de Janeiro

RESUMO

Este artigo tem como objetivo verificar o comportamento da carga em tirantes de cortinas ancoradas executadas para eliminação de risco geológico-geotécnico em encostas da cidade do Rio de Janeiro. Considerando o aumento de sobrecarga devido ao crescimento de construções a montante destas estruturas e o término de sua vida útil, realizou-se uma simulação através do sistema computacional Plaxis para estimar a carga em tirantes de 20 cortinas ancoradas após 50 anos executadas e comparou-se com os resultados obtidos por meio de ensaios de verificação residual de carga. Os resultados mostram que, apesar da simulação teórica indicar aumento de carga em 50 anos devido a sobrecarga adicional, os tirantes tendem a perder carga mesmo com acréscimo de sobrecarga nas cortinas ancoradas.

Palavras-chave: cortina ancorada; sobrecarga; durabilidade.

Verificación de carga en cortinas ancladas ubicadas en áreas de riesgo geotécnico en la ciudad de Río de Janeiro

RESUMEN

Este artículo tiene como objetivo la verificación y comportamiento de carga en tirantes de cortinas ancladas, ejecutadas para eliminar el riesgo geológico-geotécnico en cuevas de la ciudad de Río de Janeiro. Considerando el aumento de sobrecarga debido al crecimiento de construcciones aguas arriba de estas estructuras y el término de su vida útil, se realizó una simulación a través del sistema computacional Plaxis para estimar la carga en tirantes de 20 cortinas ancladas después de 50 años de ejecutadas y se comparó con los resultados obtenidos mediante ensayos de verificación residual de carga. Los resultados muestran que, a pesar de la simulación teórica que indica un aumento de carga en 50 años debido a una sobrecarga adicional, los tirantes tienden a perder carga incluso con un aumento de sobrecarga en las cortinas ancladas.

Palabras clave: cortina anclada; sobrecarga; durabilidad.

1. INTRODUCTION

The city of Rio de Janeiro, which is known for both the tragedies caused by landslides on its slopes and the terrain formed by the encounter of the ocean with the mountains, has built more than eleven thousand interventions on hillsides located at different sites in the municipality over the past 50 years. Approximately 20% of those constructions were executed on anchored curtains. This type of hillside containment structure stands out as the most important of those executed in the city over the years, both due to the type's structural design and its investment and maintenance costs. An anchored curtain is a reinforced concrete structure that has a specific geometry and is comprised of large vertical panels of slabs with reinforcements in the support region (tie rods) and structural steel elements that anchor it to the ground.

On the hillsides of the city of Rio de Janeiro, where most of these containment constructions are located, poor communities grow, and informal residential properties are constructed. Their main characteristic is the absence of adequate technical standards, often without surrounding urbanization and without important public services such as sanitary sewage and household waste collection.

Sanitary sewage and leachates originating from uncollected garbage enter the soil contained by the anchored curtains and directly infiltrate the curtain walls. In many cases, their presence can be perceived as they run down through the drains of the structure.

These reinforced concrete structures are subjected to aggressive attacks by agents in the sanitary sewage originating from informal buildings and leachates from uncollected garbage, both of which cause pathological manifestations that decrease the service lives of these structures.

It is necessary to know, evaluate, and classify the degree of aggressiveness of the environment and to know the concrete and geometry of the structure, thus establishing the correspondence between both, i.e., between the aggressiveness of the environment and the durability of the concrete structure (HELENE, 1983).

Due to the increasing problems of early degradation observed in the structures, new competitive needs, and sustainability requirements in the civil construction sector, in the last two decades there has been a worldwide tendency to focus on design aspects related to durability and the extension of the service life of reinforced and prestressed concrete structures (CLIFTON, 1993).

As prescribed in European Concrete Standard EN 206-1 2007, the design service life for current structures is at least 50 years, which is applicable to reinforced concrete structures with anchored curtains. This indicator is useful to ensure minimum performance levels.

In view of the approaching end of the minimum design service life of approximately 25% of the anchored curtain walls executed on the hillsides of the city, a survey program for those structures was established. A large presence of pathological manifestations was found, indicating that the service lives of the anchored curtains are less than the minimum of 50 years after their execution.

In addition, several of these structures present either losses or increases in work load on their tie rods, the values of which are often different from the loads incorporated at the times of the execution of the structures.

Changes in load through time indicate changes in the distribution of forces along the structural wall of the curtain, which result in increased cracking of the concrete surface and openings for the entry of aggressive agents present in the contained and contaminated soil.

Residual load verification tests on anchored curtain tie rods must be performed every five years to obtain residual load values. Although NBR 5629 2006 (Testing of tie rods anchored to the ground) specifies the procedures for verifying the performance of a tie rod using four tests (basic, qualification, reception and fluency), this test has the same nature as the previous tests, which is to place a load on the tie rod so that it presents a performance compatible with that determined by the design.

Residual load checking tests on tie rods are important for maintaining anchored curtain containment structures and is performed on 15% to 20% of tie rods. However, the distribution of this test, in addition to being random, may increase when the results of the initial tests demonstrate loss of load for tie rods in a certain region of the structures.

In addition to the practical tests used to evaluate the load behaviors of the tie rods over time, theoretical tests of the rods were carried out using the Plaxis computational tool, which allows simulations of increases in overload due to increases in residential and other buildings uphill from the anchored curtain occurring throughout the years. The loads on the tie rods in reinforced concrete structures of the hillside containment structures located in the city of Rio de Janeiro need to be evaluated. This is because increases in overload cause deformations and cracks in the concrete structures, which in turn serve as the main entrances for aggressive agents such as sulfuric acid from sewage uphill, which penetrate the structures through the contained ground.

The objective of this research, which is related to the study of pathological manifestations due to the cracking processes of structures, is to analyze whether increasing loads on the tie rods of the anchored curtain containment structures behave as predicted by computational simulations when taking into account increases in informal properties uphill of those structures.

2. ANCHORED CURTAIN HILLSIDE CONTAINMENT STRUCTURES IN THE CITY OF RIO DE JANEIRO

The city of Rio de Janeiro is known worldwide for its natural beauty, which is mainly characterized by its particular geomorphology, i.e., the mountain massifs that are covered by Atlantic forest vegetation and located near the ocean.

The main massif is known as the Tijuca massif and is located in regions of the southern and northern zones and downtown area of the city. The Tijuca massif has the highest occupational density. It has been occupied for more than 100 years by people living in informal constructions since the beginning of the first *favela* in Brazil, which was located on Providência Hill in the downtown area in 1897.

The name *favela* was first used because the first inhabitants of Providência Hill referred to the place as the "*favela* hill", which was a reference to a hill of the same name located in Canudos (a municipality in northeast Brazil) that was covered by a low shrub also called "*favela*". Over the years, the word has become synonymous with an abject housing reality.

The population, which was incapable of moving from the downtown area of the city and from the larger concentration of job offers, looked for other ways to stay in the region, which resulted in the beginning of the first *favelas* in the city. Urban development and the lack of mobility of the poor population make it essential for them to remain in the central regions, regardless of the housing conditions offered (ABREU, 1988).

High unemployment rates, informal growth, real estate speculation, a lack of housing policies for the low-income population and an unsatisfactory public transportation system are among the reasons for the growth of the *favelas* in the municipality of Rio de Janeiro.

Data released by the Brazilian Institute of Geography and Statistics (Instituto Brasileiro de Geografia e Estatística - IBGE) Census in 2010 reveal that 20% of the city's population currently lives in slums, which means that 1,393,314 people live in the 763 *favelas* in the municipality. Of those, approximately one million inhabitants live on slopes located in hazardous areas that present high probabilities of suffering mass movements (landslides, falls, rocks rolling down-slope, and debris flows) involving soil, rock, vegetation and garbage/rubble.

Landslides in the hills of the city of Rio de Janeiro are a cyclical phenomenon that lead to enormous economic and social damage that includes road blockages and the destruction of common types of houses, resulting in homelessness and in many cases loss of life.

Therefore, the prediction of landslides and other geotechnical accidents has been gaining increasing importance in the geomorphological and geotechnical literature on the city. Figure 1 shows landslide susceptibility maps for four communities in the city of Rio de Janeiro.

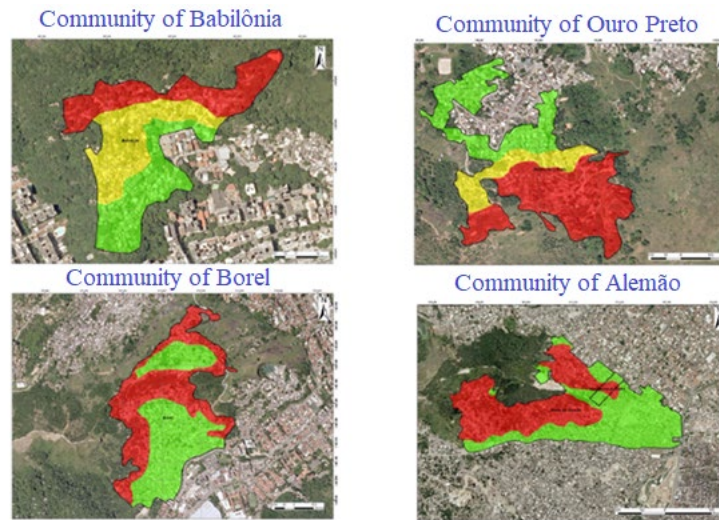


Figure 1. Landslide susceptibilities in hazardous areas. Rio de Janeiro, Brazil (GEO-RIO 2014)

Several concepts are used to address the landslide problem and its forms of investigation. Most proposed methodologies aim to define areas that are critical to landslides, that is, areas of greater susceptibility for the process to occur.

The term accident refers to an event that has already occurred and for which social and/or economic damage (losses and damages) has been recorded. Hazards, however, represent the possibility or probability of some damage to a population (people, physical structures, and production systems) or to a segment of a population. It is a potential condition under which an accident could occur. (AUGUSTO FILHO et al. 1990a). The implementation of hillside containment structures in poor communities is a response to public policies intended for hazard mitigation on hillsides, urbanization, and improvements in accessibility and mobility for residents. Figure 2 shows the front view of an anchored curtain built in the community of Barro Preto in the district of Méier, Rio de Janeiro.



Figure 1. An anchored curtain in a geotechnical hazard area (Author)

This geotechnical solution constitutes the most adequate technical solution for containing the high horizontal forces resulting from deep excavations with minimum displacements of soil mass and structures located in the vicinity.

The execution of anchored curtains, although old, is among the most modern containment methods. The method employs prestressed rods and anchors to support the terrain. Its primary advantage is its potential application without having to cut anything beyond that necessary. Using this geotechnical solution, it is possible to overcome any height and situation, but there are disadvantages, which include high implementation costs due to its time-consuming execution.

3. APPLYING THE PLAXIS COMPUTATIONAL TOOL TO THE CASE OF EXISTING CURTAINS

With the development of computers, finite-element numerical modeling has become a powerful and widely used tool for analyzing containment structures in geotechnical environments. This sophisticated tool improves the modeling of containment structures because it allows analyses of their construction sequences and behaviors through time, including the effects of additional overloads on the structures and tie rods anchored to the ground, which are the object of study of the present work. Numerical finite element analyses requiring software aids are widely used to solve structural engineering problems.

According to Lopes (1995), the finite element method (FEM) is the most commonly used numerical method employed in geotechnical civil engineering due to its ease in dealing with heterogeneous, nonlinear (nonlinear elasticity and plasticity) and time dependent (viscosity and densification) problems.

In stress-strain analyses involving soils, Safety Factors (SFs) can be obtained using soil resistance or workload parameters pertinent to the problem under study. SF therefore can be estimated using FEM simulations of service ruptures, which are characterized by soil plastification.

SFs are evaluated as functions of reductions in soil resistance parameters by dividing the actual parameters by their respective estimated values and by then employing those evaluations to calculate the degree to which soil resistance is mobilized. The values of c^* and ϕ^* are obtained using

$$C^* = \frac{c}{M}, \text{ and} \tag{1}$$

$$\tan \phi^* = \frac{\tan \phi}{M}, \tag{2}$$

where

c - Soil cohesion;

c^* - Cohesion reduced by the SF for use in the simulation;

ϕ – Soil friction angle;

ϕ^* - Soil friction angle as reduced by the SF for use in the simulation; and

M – Value for the reduction of the resistance parameters.

The SF ensures the global stability of the model for soils on the verge of rupturing, i.e., soil plastification. This will occur when SF is equal to M or when the system's workloads are divided by an estimated value, but in either case, the degree to which the resistance is mobilized is evaluated.

Finite element modeling involves the definition and manipulation of the geometry and specifications of the material and its properties, generation of the finite element mesh, and definition of the loads and displacements that will be applied to the component. A schematic representation is shown in Figure 3.

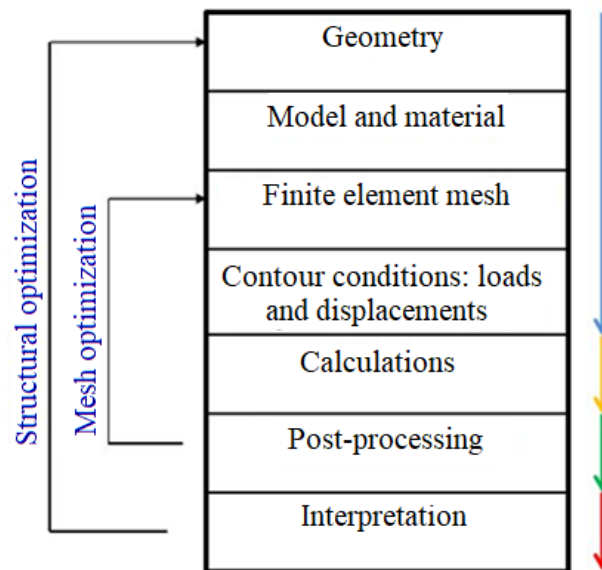


Figure 3. Schematic representation of the finite element analysis (Tschiptschin, 2011).

Four basic procedures are employed for solving geotechnical engineering problems using the finite element method: discretization of the continuous medium, selection of the displacement model, calculation of the stiffness matrix, and calculation of the unknown variables of the problem. In the first phase, the continuous medium or domain of the problem is divided into sub-domains called finite elements that are connected by a finite number of nodal points or, more simply, nodes.

The discretization of the continuous medium occurs when it is divided by imaginary lines and surfaces that result in a finite number of two-dimensional elements that, for this research, was verified to be sufficient for the analysis.

To select the displacement model, a set of polynomial functions is then used, i.e., functions composed of a polynomial that defines the displacement field as a function of the nodal displacements of each element.

The calculation of the stiffness matrix, an interpolation function, allows relating the value of the variable of the problem to be solved in the nodes of each element with its geometry and property, generating a system of equations in matrix form.

The reinforcing bars of a hillside containment structure must absorb the tensile and compressive stresses arising primarily in the vertical parameters of the anchored curtains, which are dimensioned to resist not only bending but also the punching shear in the region of the tie rods.

The calculation model is a two-dimensional geometric model with length and height dimensions. Auxiliary lines are used to simulate the excavation of the structure. The base supports are fixed, and the lateral supports are movable to allow for lateral displacements.

It is recommended, for the good development of the modeling of the curtain, that the conditions of plane state deformation be satisfied. In this case, the axial stiffness (AS) and the bending stiffness (BS) are determined by equations 3, 4 and 5, where E_{eq} is the modulus of elasticity, and t is the thickness of the curtain.

$$EBS = \frac{E_{eq} t^3}{12} \quad (3)$$

$$BS = E_{eq} t \quad (4)$$

$$EAS = E \quad (5)$$

In the curtain anchorage modeling, different elements are observed and divided into free and anchored sections. Between the free section and the ground, the mobilized shear stress is ignored, and spring elements are used to connect the curtain to the anchor bulb.

The anchored section generates three-dimensional stresses on the soil mass and presents \ less satisfactory modeling than that of the curtain because it approaches a plane state of deformation due to the use of two dimensions.

Because the modeling is two-dimensional, soil deformations occurring between the anchor lines perpendicular to the presented model are completely ignored. Care must be observed with issues such as data entry, specification of soil and material parameters, spacing of the tie rods, and the distribution of the forces applied to the tie rods in this measurement.

The anchorage-free section is modeled by an elastoplastic element denominated in Plaxis as the “node-to-node anchor element” because the pre-stress is applied to that element.

The anchoring bulb is modeled using one element per meter having only axial stiffness, which is denominated in Plaxis as a “geogrid”. These elements are only subjected to tensile stresses and are thus characterized by the axial stiffness AS.

According to BEIJINHA (2009), the behavior of the curtain can be realistically approximated to a plane strain state, and the anchors are not satisfactorily represented in Plaxis 2D because they generate a three-dimensional state of stresses in the mass of soil.

In the modeling carried out for the 20 anchored curtains, the soil behavior was investigated in relation to the shear strength, its plastification at the time of the execution of the structure, and its projection after 50 years of service life. In Figures 4 and 5, the anchored curtain does not present changes in the plastification points or shear strength of the soil at the structure’s service life of 50 years in the service life of the structure. This is due to the fact that the curtain has three rows of tie rods, which impart a smaller variation on the forces on the soil structure.

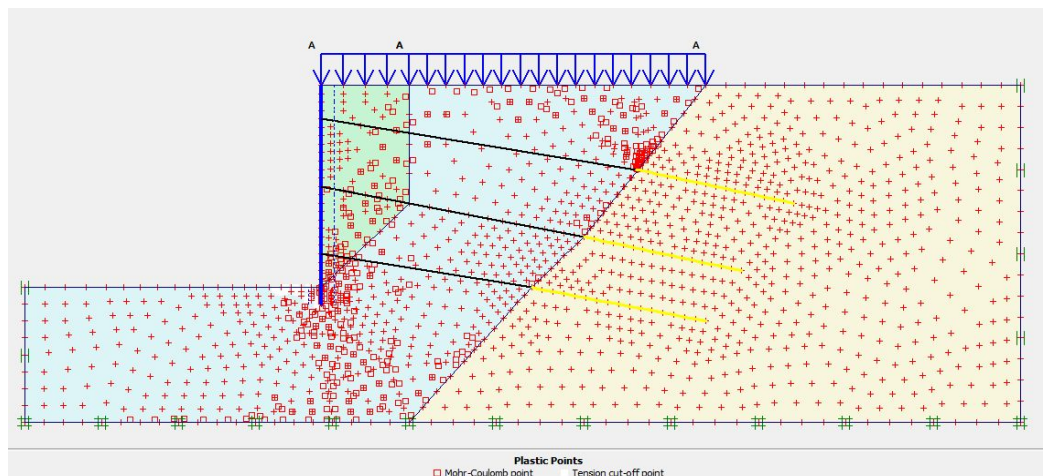


Figure 4. Initial plasticity of the soil (Plaxis).

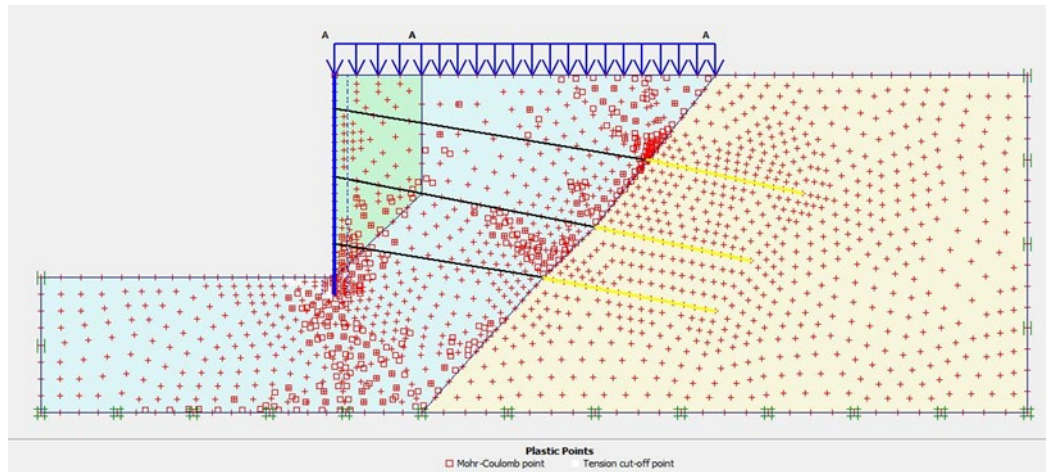


Figure 5. Soil plasticity after 50 years.

Soil strains or displacements (see Figure 6), which can occur between the anchor lines in the direction normal to the plane of the problem, are ignored in the two-dimensional situation. For that reason, the actual force applied on the rods is divided by the spacings between the rods in the normal direction.

The verification of the plastification points and the shear strength of the soil contained by the anchored curtain over time allows determining whether alterations in soil behavior occur under additional overloads and at the points near the curtain with greatest vulnerability, where the tendency for soil rupture exists.

With increasing overloads over time, a second plastification occurs in the lower part of the panel of the anchored curtain, with a small change in the plastification zones of the contained soil. It has been verified that there is no plastification of the soil in the upper section of the panel.

The region near the support of the curtain and the first row of tie rods, which coincides with the displacement that the curtain undergoes due to the increase in overload over time, and the second row of tie rods, which is a section near the transition between the free section and the anchored section of the tie rod, indicate a stress zone in the soils.

Although the FEM modeling employing the Plaxis 8.2 computational program considers some of the particular characteristics of the soil such as its dilating nature, the determination of the boundary between the plastification and elasticity zones of the soil can be considered as absent.

For analyzing soil behavior in geotechnical problems, one usually implicitly assumes that for regions with elastic behavior, the soil is analyzed using a linear-elastic model that would allow verification of the immediate settlements of a foundation, i.e., the stress distribution related to the strains in the soil.

For the plastified region of the soil, on the other hand, a rigid plastic model with resistance parameters such as cohesion and angle of friction of the soil, which are related to its stability and rupture, would be used. In other words, the amount of soil undergoing a flow process is evaluated.

Therefore, neither the elastic nor plastic behaviors of the soil change with increasing overload over time and although the boundary zone between the two soil behaviors cannot be determined, one concludes that it also does not undergo significant changes.

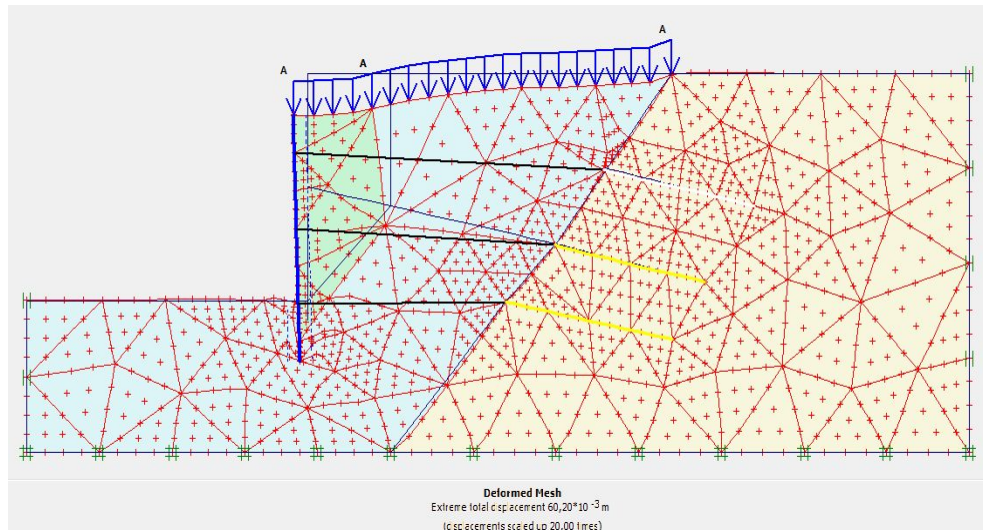


Figure 6. Displacement of the anchored curtain after 50 years (Plaxis).

These observations are important in order to know the point at which the added overload results in significant changes in the soil and how that may impact the reinforced concrete panel of the curtain.

The soil tends to settle over time, and the distributions of the grain particles and voids occupied by water are readjusted, which cause the material to consolidate and its resistance to increase.

4. COMPARISON OF THE THEORETICAL DATA WITH THE PRACTICAL DATA FROM THE LOAD VERIFICATION TESTS

Initially, the analysis of the structural behaviors of the 20 anchored curtains executed in the city of Rio de Janeiro was developed considering the effects of the overload stresses due to the additional forces at the end of the project service life, which was estimated to be 50 years, as established in standard EN 206-1 2007.

Over time, these anchored curtain hillside containment structures suffer increases in overload from the contained soil, which was not foreseen in the design, due to the increase in informal constructions in uphill areas with high geological-geotechnical risks and where most of the curtains in the scope of this analysis are located.

It is known that load change phenomena originally foreseen in the projects can compromise the structural performance and service life of the structure's design, primarily due to the multiple cracks that a structure with a flat and thin geometry such as an anchored curtain can present in comparison with other reinforced concrete structures such as pillars, beams and more robust slabs.

If they excessively develop over time, these cracks will allow the entry of aggressive agents from the sanitary sewage originating from the informal constructions uphill from the containment structures executed in poor communities, which will attack the reinforcement and concrete structure.

To perform the numerical simulation, the dimensions and rigidity of the curtain, vertical and horizontal spacings, length and load of the tie rods, characteristics of the ground where the bulb and foundation are anchored and other relevant characteristics were used as parameters according to the specification of the design of the hillside containment structures used by the Geotechnical Foundation Institute of Rio de Janeiro (*Fundação Instituto de Geotécnica - GEO-RIO*).

Therefore, to simplify the model and given the unavailability of survey reports for each executed curtain, the soil behavior was modeled using the Mohr-Coulomb model, which closely represents the behavior of soil in general.

The properties of the materials were input so that the model can be as close as possible to the actual situation for each of the studied cases.

Another important consideration in the case analysis is that it is hard to obtain information regarding the informal properties located uphill from the anchored curtains or their residents, either due to high resident turnover or the construction dynamics of the houses. Thus, an average construction pattern implying an overload of 40 kN/m^2 was established. Table 1 presents the geotechnical parameters used in the numerical modeling of the soil layers and earthwork for each anchored curtain.

Table 1. Geotechnical data for the contained ground (GEO-RIO 2010).

Parameter	Symbol	Unit	Backfilling	Layer 1	Layer 2
Model	-	-	Mohr Coulomb	Mohr Coulomb	Jointed Rock
Behavior	-	-	Drained	Drained	Drained
Section	-	-	Free	Free	Anchored
Dry specific weight	γ_d	kN/m^3	17	16	20
Natural specific weight	γ	kN/m^3	20	18	20
Horizontal permeability	K_h	m/day	1	1	1
Vertical permeability	K_v	m/day	1	1	1
Young's Modulus	E_{50}	k/Pa	1.300E+04	1.000E+04	1.139E+05

The material property parameters used for modeling the reinforced concrete curtain are shown in Table 2. They represent the parameters adopted by the GEO-RIO Foundation that are used in modeling specifications for the designs of the anchored curtains.

The homogenization of the material parameters was only possible because the structures, which were built over a span of decades, employed the same technical specifications and executive processes developed by the Design Department of the GEO-RIO Foundation. Therefore, the curtains were designed and constructed in different places on the hillsides of the city of Rio de Janeiro using the same procedures, with changes to their geometric characteristics only.

Table 2. Material properties of the anchored curtain.

Parameters	Symbol	Value	Unit
Behavior	-	Elastic	-
Normal strength	AS	2.10^5	kN
Plane spacing	L_s	2.00 to 3.50	m
Workload	CT	160 a 200	kN
Maximum force	F_{max}	1.10^{15}	kN

Table 3 presents the workload, plane spacing, and maximum force for the tie rods as adopted by GEO-RIO.

Table 3 – Workload for the tie rods of the anchored curtains (GEO-RIO 2010).

Parameter	Symbol	Value	Units
Behavior	-	Elastic	-
Axial stiffness	AS	12.10^6	kN/m
Bending stiffness	BS	0.12×10^6	kN m ² /m
Thickness	d	0.25	m
Weight	w	6	kN/m/m
Poisson coefficient	v	0.15	-

After the modeling was performed using the Plaxis 8.2 computer system for 20 curtains anchored with the same executive pattern but with different geometries, the modeling results were compared with the results obtained for the experimental load verification tests with the purpose of observing the loads on the tie rods after the increase in overload over 50 years.

For each anchored curtain, the residual load verification test was performed by randomly sampling up to 20% of the existing tie rods, but at least one rod per line was chosen.

In the last five years, the structural recovery program of the Construction Department of the GEO-RIO performed 229 Residual Load Verification Tests (RLVT) for 20 anchored curtains.

The execution of an RLVT is shown in Figure 7; the test was performed during the structural recovery of the hillside containment structure, which had already accumulated additional overloads over the 50 years since it was built.



Figure 7. Residual load verification testing underway.

The graph in Figure 8 shows (blue line) the maximum RLVT results for all of the 20 anchored curtains surveyed over a period of 5 years. To obtain conservative values for the residual loads, the maximum residual load in tons for each anchored curtain was considered.

The maximum value of residual load for the tie rods was 22 tons for the curtain located near the Linha Amarela expressway in the suburbs of Rio de Janeiro, and the lowest value of ZERO tons was obtained for the curtain on Mauriti Street in the burrow of Santa Tereza.

The simulated residual loads on the tie rods after 50 years for the same anchored curtains are shown in Figure 8 (blue line). The values of the residual load changed over time from a maximum value of 28 tons for two curtains located in Saint Tereza and in the Tuiuti community to a minimum value of 18 tons for a curtain located in the Coréia community.

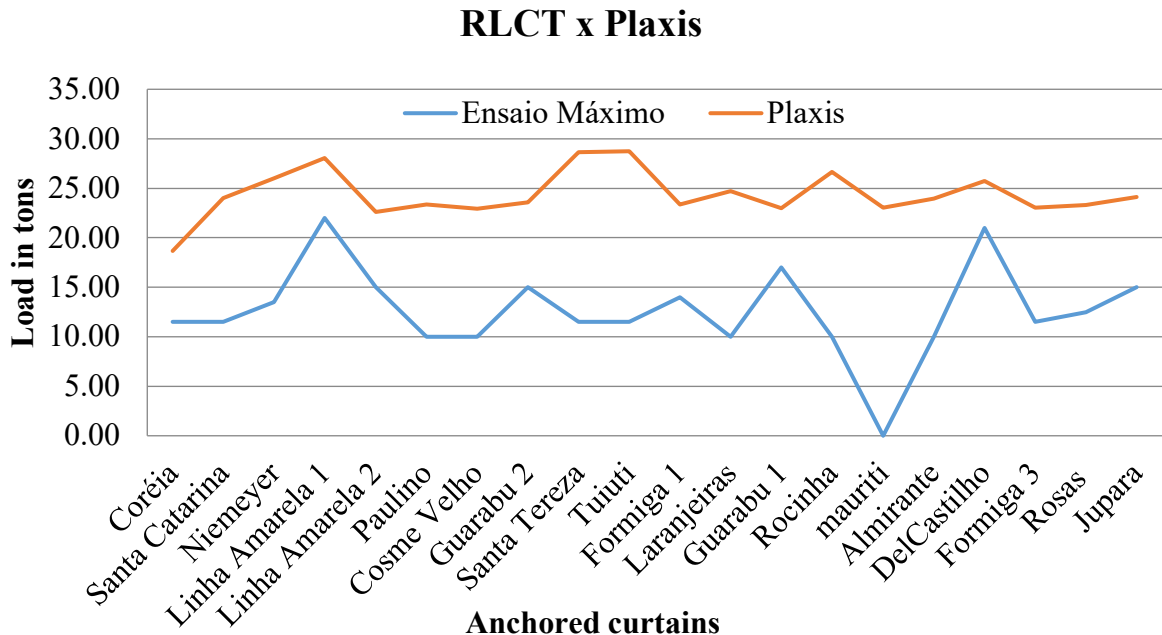


Figure 8. Graph of the RLVT and Plaxis results (Author).

It can be seen that the two lines that represent the tests simulated using the Plaxis computational system (blue line) and residual load verification test (red line) do not meet for any of the 20 anchored curtains surveyed over five years during this research.

5. CONCLUSIONS

Anchored curtain hillside containment structures are reinforced concrete structures that have estimated service lives of 50 years. They are basically composed of reinforced concrete panels with pile foundations that are anchored to the ground using prestressed steel tie rods and that support the vertical loads of the contained slopes.

The approximately 2,200 structures that have served as the primary solution for geological-geotechnical hazard mitigation in the city of Rio de Janeiro for 50 years since the creation of GEO-RIO require special maintenance attention and interventions to restore and extend their service lives. Considering the uncontrolled growth in informal real estate uphill and surrounding these containment structures, soil contamination by aggressive agents such as sulfuric acid, which is highly corrosive to steel reinforcements, occurs in addition to increased overloads.

After comparing the results of the practical tests and the theoretical tests developed using the Plaxis 8.2 2D computational tool (Figure 8), it was found that the results of the residual load verification tests did not show increases in load over time.

On the other hand, the theoretical tests, i.e., the theoretical load results from the computational model, presented results that were higher than those of the Residual Load Verification Test (RLVT) for the anchored tie rods, indicating that the Plaxis program was unable to perceive their load loss phenomenon over time.

The conclusion is that the Plaxis 8.2 2D computational tool does not consider in its analysis the prestress losses of the tie rods due to the relaxation phenomenon and consolidation of the contained ground over time if compared with the projected future residual loads to which the rods will be subjected after a service life of 50 years.

It is recommended that the developer of the Plaxis 2D geotechnical and structural computational tool review the modeling of anchored curtain structures while considering the temporal development of the loads on the tie rods anchored to the ground due to the increase in overload of the contained slope considered in the proposed model.

It is also concluded that the anchored curtains' reinforced concrete structures may present during their service lives increases in surface cracks in the concrete due to variations in residual load over time.

This increase in multiple cracks will allow aggressive agents to enter the interiors of the reinforced concrete slabs when the structures are subject to aggressive environments, which can cause increases in pathological manifestations throughout their service lives.

6. REFERENCES

- Abreu, M. (1988), "*Evolução Urbana do Rio de Janeiro*". IPLANRIO. Rio de Janeiro: Ed. Jorge Zahar, 1988.
- Amaral, C. P. (1996) "*Escorregamentos no Rio de Janeiro: inventário, condicionantes e redução do risco*". Tese de Doutorado, Eng. Civil, PUC-Rio.
- Andrade, T. (2005), "*Tópicos Sobre Durabilidade do Concreto*". In: ISAIA, Geraldo Cechella. (Ed) Concreto: Ensino, Pesquisa e Realizações. São Paulo: Editora Ibracon, V1. Cap. 25, p. 753-754, 761,762.
- Associação Brasileira de Normas Técnicas (2014), "*Projeto de Estruturas de Concreto – Procedimento, NBR – 6118*". ABNT, Rio de Janeiro.
- Associação Brasileira de Normas Técnicas (2006), "*Execução de tirantes ancorados no terreno – NBR 5629*". Rio de Janeiro.
- Augusto Filho, O., Cerri, L. E. S., Amenomori, C. J. (1990a), "*Riscos Geológicos: Aspectos Conceituais*". In: Simpósio Latino-Americano Sobre Risco Geológico Urbano, 1, São Paulo, 1990. Anais... São Paulo: ABGE, pp. 334-341.
- Bejinha, A. M. D. (2009), "*Estruturas de Contenção Acoradas Sujeitas a Ação Sísmica – Análise de Comportamento*". Instituto Superior Técnico – Universidade Técnica de Lisboa.
- Brinkgreve, R. B. J. (2002), "*Finite Element code for Soil and Rock Analyses – Plaxis – 2D user's manual*". Rotterdam, Netherlands, Balkema.
- Brinkgreve, R. B. J. (2017), "*Plaxis – 2D manuals*". Rotterdam, Netherlands, Balkema.
- Censo do IBGE: <https://censo2010.ibge.gov.br/materiais.html>
- Clifton, James R. (1993), "*Predicting the Service Life of Concrete*". ACI Materials Journal, v. 90, n. 6, p. 611-16.
- Durval, R. (1992), "*La Durabilité des armatures et du béton d'enrobage*". Paris: Presses de l'École Nationale des Ponts et Chaussées, p. 173-225
- European Committee for Standardization (CEN). "*Betão: Parte 1 – Especificação, desempenho, produção e conformidade*". EN 206-1, Portugal, 2007.
- Farah, F. 2003, "*Habitação e Encostas*". Coleção Habitar/Finep. São Paulo/SP.

- Figueiredo, Enio P., Helene, P. R. L. (1994), "*Assim caminha a corrosão*". Revista Técnica, v. 2, n. 10, p. 28-33, mai. /jun. 1994.
- Georio (2014), "*Manual Técnico de Encostas*". Volumes 1,2,3 e 4, 2ª edição, Rio de Janeiro.
- Helene, P. (1983), "*La Agresividad del Medio y la Durabilidad del Hormigón*". Asociación Argentina de Tecnología del Hormigón, p.25 – 35.
- More, J. Z. P. (2003), "*Análise numérica do comportamento de cortinas atirantadas em solos*". Dissertação (Mestrado em Engenharia Civil) PUC-RIO.120f
- Tschiptschin, A. P. (2011), "*Método de Elementos Finitos Aplicado à Seleção de Materiais*", USP.

Structural and functional conditions of bridges and viaducts on federal highways in Pernambuco

C. J. G. Silva^{*1}, E. Monteio¹, J. P. A. Vitório¹

*Corresponding author: claytonjgsilva@gmail.com

DOI: <http://dx.doi.org/10.21041/ra.v8i1.199>

Received: 15/06/2017 | Accepted: 09/11/2017 | Published: 31/01/2018

ABSTRACT

This paper discusses the structural and functional conditions of 332 bridges and viaducts on federal highways in Pernambuco, adopting as a methodology the database of the National Department of Infrastructure of Transportation (DNIT) and structural inspections on a selected sample. The information obtained was analyzed according to the criteria of DNIT Standard 010/2004 – PRO and ABNT Standard NBR 9452/2016. It is the first survey in Brazil with such a large quantity of structures utilizing two normative systems. Even with the limitations present in this type of study, the conclusions show that it is a significant contribution to the improvement of Brazilian highways bridges that, in general, suffer from the same problems that were found in the bridges analyzed.

Keywords: pathological manifestations; structures; inspection; bridges and viaducts.

Cite as: C. J. G. Silva, E. Monteio, J. P. A. Vitório (2018), “*Structural and functional conditions of bridges and viaducts on federal highways in Pernambuco*”, Revista ALCONPAT, 8 (1), pp. 79 – 93, DOI: <http://dx.doi.org/10.21041/ra.v8i1.199>

¹ Universidade de Pernambuco - UPE, Recife, Brasil.

² UNICAP - Universidade Católica de Pernambuco, Universidade de Pernambuco - UPE, Recife, Brasil.

Legal Information

Revista ALCONPAT is a quarterly publication of the Latinamerican Association of quality control, pathology and recovery of construction- International, A. C., Km. 6, antiga carretera a Progreso, Mérida, Yucatán, C.P. 97310, Tel.5219997385893, alconpat.int@gmail.com, Website: www.alconpat.org

Editor: Dr. Pedro Castro Borges. Reservation of rights to exclusive use No.04-2013-011717330300-203, eISSN 2007-6835, both awarded by the National Institute of Copyright. Responsible for the latest update on this number, ALCONPAT Informatics Unit, Ing. Elizabeth Sabido Maldonado, Km. 6, antiga carretera a Progreso, Mérida, Yucatán, C.P. 97310.

The views expressed by the authors do not necessarily reflect the views of the publisher.

The total or partial reproduction of the contents and images of the publication without prior permission from ALCONPAT International A.C. is not allowed.

Any discussion, including authors reply, will be published on the third number of 2018 if received before closing the second number of 2018.

Condições estruturais e funcionais de pontes e viadutos das rodovias federais de Pernambuco

RESUMO

Este artigo tem como objetivo discutir as condições estruturais e funcionais de 332 pontes e viadutos das rodovias federais de Pernambuco, adotando-se como metodologia a consulta ao banco de dados do Departamento Nacional de Infraestrutura de Transportes (DNIT) e inspeções nas obras que constituem a amostra estudada. As informações obtidas foram analisadas conforme os critérios da norma DNIT 010/2004 – PRO e da norma ABNT NBR 9452/2016. Trata-se da primeira pesquisa no Brasil com tal quantidade de obras utilizando dois sistemas normativos. Mesmo com as limitações inerentes a esse tipo de estudo, as conclusões mostram que ele significa uma contribuição para a melhoria das pontes rodoviárias brasileiras que, de modo geral, padecem dos mesmos problemas existentes nas pontes analisadas.

Palavras-chave: manifestações patológicas; estruturas; inspeção; pontes e viadutos.

Condiciones estructurales y funcionales de puentes y viaductos de las vías federales de Pernambuco

RESUMEN

El presente trabajo tiene como objetivo analizar las condiciones estructurales y funcionales de 332 puentes y viaductos de las autopistas Federales de Pernambuco, adoptando como metodología la base de datos del Departamento Nacional de Infraestructura del Transporte (DNIT) y las inspecciones estructurales que constituyen la muestra estudiada. La información obtenida se analizó según los criterios de la norma DNIT 010/2004 - PRO y la norma ABNT NBR 9452/2016. Siendo la primera investigación en Brasil con tal cantidad de estructuras usando dos sistemas normativos. Aunque con las limitaciones de este tipo de estudio, las conclusiones muestran que significa una contribución al mejoramiento de los puentes de carreteras brasileños que, en general, sufren los mismos problemas que existen en los puentes analizados.

Palabras clave: manifestaciones patológicas; estructuras; inspección; puentes y viaductos.

1. INTRODUCTION

In the 1970s, Brazil went through the so-called economic miracle (Cunha, 2011), which promoted the acceleration of the consolidation of large multinational companies, a concrete example being the automobile industry; and the financing of public works by international institutions, as was the case with the expansion of the Brazilian road network, including a large number of bridges and viaducts. This resulted in a significant increase in vehicle flow and cargo transportation.

However, the lack of policies and strategies aimed at public works maintenance over the past few decades has allowed a process of highway deterioration to take place, directly affecting the projects known as “Special Engineering Structures,” which present a variety pathological manifestations and structural damages. Some factors have also aggravated the current situation, such as the older Brazilian norms that were in force at the time the structures were designed and constructed, which did not predict the current load or traffic intensity on highways and in urban centers. The environmental aggressiveness at the locations where the bridges were built was also not taken into account, and this theme has been covered by several scholars who have done research on the subject, such as (Vitório, Barros, 2013) and (Milani, Kripka, Pravia, 2011).

The lack of public strategies for maintenance has also generated a large gap with regard to information on the actual state of Brazil's infrastructure projects, especially the Special Engineering Structures (SES), making it imperative to carry out inspections to obtaining the critical data regarding the safety conditions and functionality of these structures.

It was in this context that the structural conditions, functionality, and durability of bridges and viaducts of the principal federal highways of Pernambuco were analyzed. In light of the results obtained in this sample, the current panorama of SES that make up the Brazilian federal highways was outlined.

2. DEVELOPMENT OF THE STUDY

2.1 Methodology utilized

Most of the information contained in the present study was obtained from DNIT's Special Engineering Structures Management System (SGO) database, and from detailed analyses of several bridges and viaducts located on federal highways crossing the State of Pernambuco, whose denominations are shown in Table 1 below.

A survey was also carried out to identify the construction periods and the typical mobile loads of each structure. Failure to supply most of the original designs meant that much of this information was obtained by comparing the evolution of the bridge cross-sections of federal highways over time with the mobile loads that were used on bridges built in the respective periods, as shown in Figure 1.

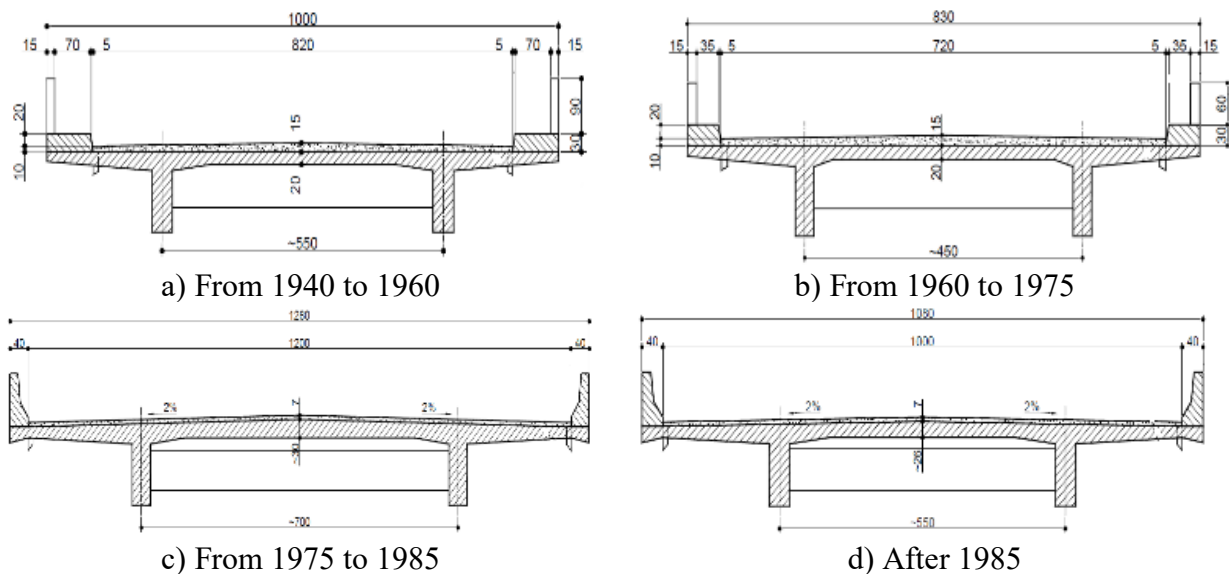


Figure 1. Evolution of the transverse cross-section of federal road bridges (Measurements in cm)

For the analyses of the structural and functional conditions, DNIT Standards 010/2004 - PRO were used, which specify the stability condition of the structure by assigning a technical grade that varies from 1 (critical structure) to 5 (structure without problems). The new version of NBR 9452 (ABNT, 2016) was also used, which introduced structural, functional, and durability parameters to guide the classification of bridge structures. The procedures foreseen in these two norms are usually adopted in Brazil to identify and diagnose the main anomalies in bridge structures, including pathological manifestations and the most frequent types of damage.

Finally, the results obtained in the research were interpreted and evaluated, in order to determine the structural and functional conditions of the SES studied and to propose solutions for the correction of existing problems, applying a more comprehensive view that can be applied not only to the bridges and viaducts of Pernambuco, but to other structure that make up the Brazilian road system as a whole.

2.2 Bridges analyzed by construction period, typical load, and construction system

Table 1 shows the federal highways within the jurisdiction of the State of Pernambuco, totaling 546 bridges and viaducts, and the amount inspected in this study, corresponding to 332 structures. This sample represents approximately 60% of all of the existing bridges in the state road network.

Table 1. Total amount and number of SES inspected, by highway

Highway	SES inspected	Total SES per highway
BR-101	115	117
BR-104	35	57
BR-110	24	33
BR-116	7	7
BR-232	64	80
BR-316	5	83
BR-407	30	31
BR-408	17	54
BR-423	30	30
BR-428	5	54
Total	332	546

The study also classified the Special Engineering Structures by period of construction (Table 2) and by the project model load, which is defined as the set of mobile loads to be applied to the structure in a position that produces the most unfavorable forces for each section and combination of loads calculated. As previously explained, the information was acquired from the SGO/DNIT and through the analysis of the evolution of the transversal cross-section of the structure, associated with the changes that occurred in the Brazilian standards specifying mobile load values over time for those projects where data from the construction time period was not available. The Special Engineering Structures for which this information could not be obtained were considered unidentified.

Table 2. Classification of Special Engineering Structures by period of construction

Period Constructed	Total
1940 to 1960	27
1960 to 1975	113
1975 to 1985	54
1985 to 2000	10
After 2000	83
Unidentified	45
Total	332

Regarding the project model load, Figure 2 shows that 50.60% of the structures were qualified with 360 kN loading. The mobile loads of 450 kN, currently used, represent 28.31% and those of 240 kN represent 7.83% of the total sample. There were also 13.25% of structures whose project model loads were not possible to identify.

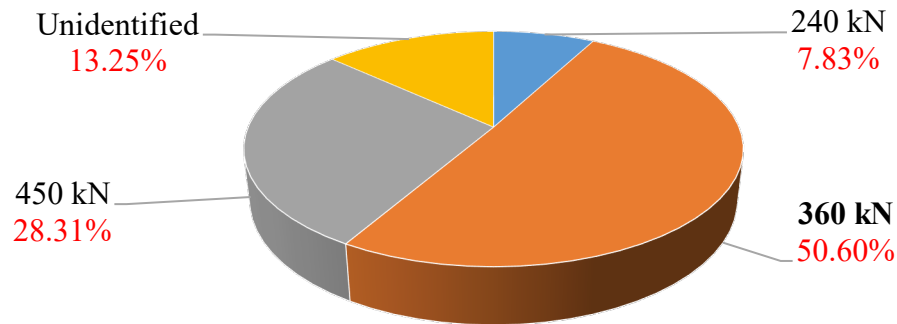


Figure 2. Project model load of bridges evaluated

Regarding the constructive system, it was verified that reinforced concrete poured on-site was predominant, used in 76.20% of the bridges and viaducts. The second most prominent system was prestressed concrete, adopted in 23.19% of the structures. Pre-cast reinforced concrete accounted for 0.60%. These data are shown in Figure 3.

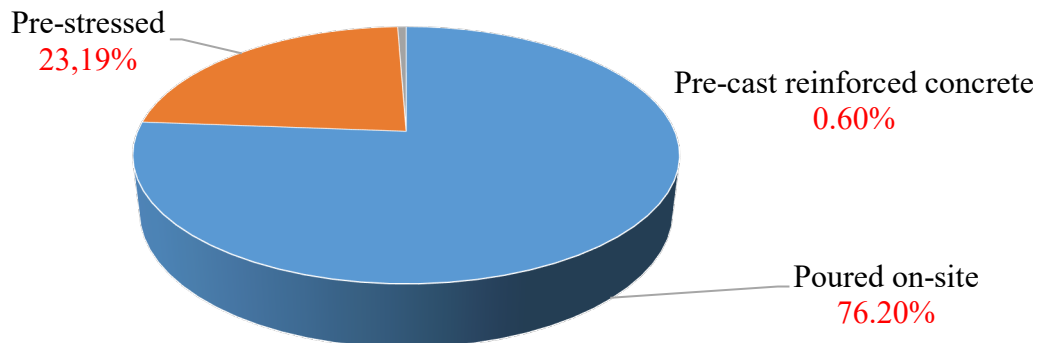


Figure 3. Constructive systems used on evaluated bridges

2.3 Pathological manifestations identified in the studied sample

In order to identify pathological manifestations, observations were made at each site during the inspections and the SGO survey reports were analyzed. The major pathological problems identified are illustrated in Figures 4 to 7.



Figure 4. Presence of efflorescence, displacement of concrete coating, and reddish-brown spots due to the corrosion of reinforcement



Figure 5. Exposed and rusty reinforcement on beams, some with broken strips



Figure 6. Erosion of the foundation and misalignment of the pillar in relation to the pipe



Figure 7. Metal bearing on a Gerber tooth with visible damage and infiltration

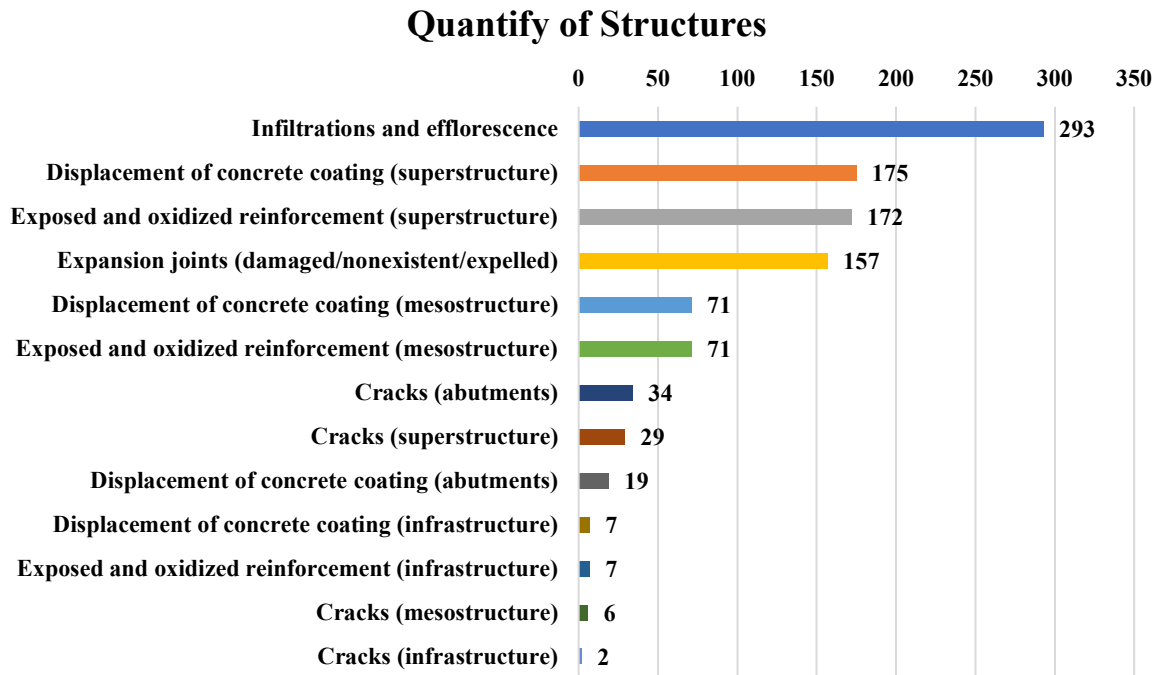


Figure 8. Occurrences of pathological manifestations in the analyzed structures

Figure 8 synthesizes the highest incidences of pathological manifestations for the evaluated set, showing the predominance of infiltrations and efflorescence, present in 293 SES. The following anomalies are also worth mentioning: displacement of the concrete (of the superstructure) in 175 structures, exposed and oxidized reinforcement (of the superstructure) in 172 structures, and damaged and/or nonexistent expansion joints in 157 SES.

2.4 Structural damage identified

Similar to the pathological manifestations, some of the main types of damage observed in the bridges and viaducts of this study are illustrated in Figures 9 to 12.



Figure 9. Absence of lateral guard-rail



Figure 10. Damaged drain causing infiltration and moisture spots between the beams



Figure 11. Deformed elastomeric bearing



Figure 12. Extreme erosion around the foundation

Figure 13 quantifies the principal damage types found in the analyzed set of structures. It was verified that 92 bridges had damaged and/or nonexistent drains. Next most prevalent were damaged guardrails (50 SES), followed by breakdowns in stone/concrete masonry (46 SES), as well as the lack or deficiency of bearings (25 SES), and holes in the concrete (20 SES). Other types of damage occurred less frequently.

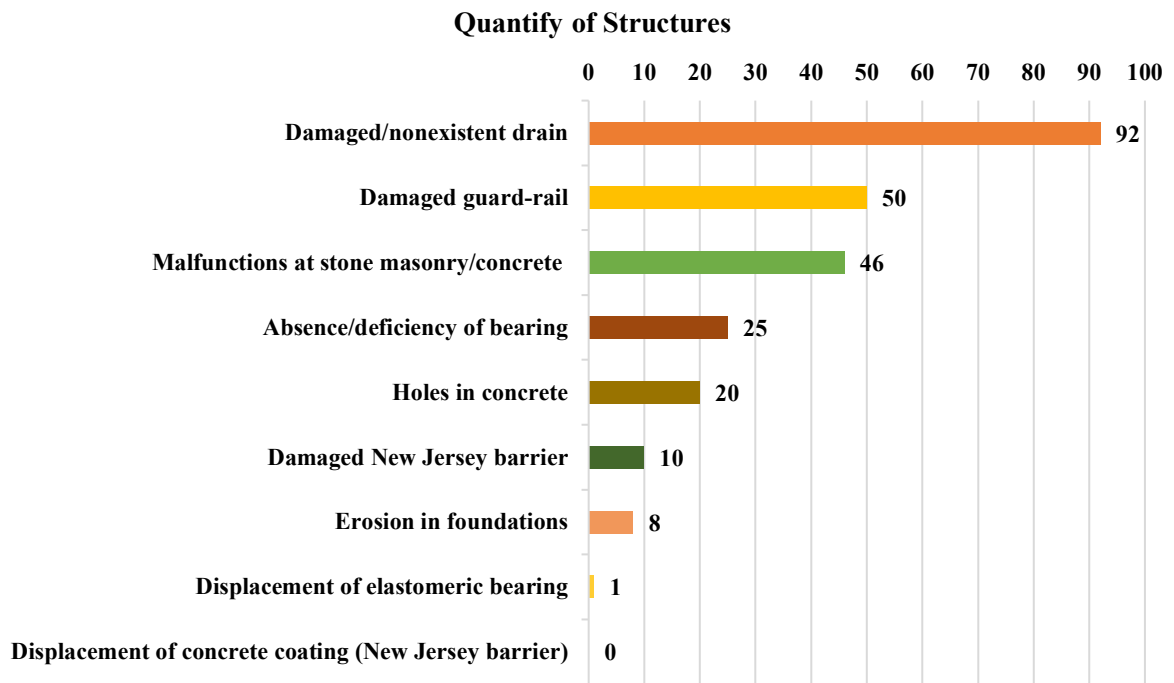


Figure 13. Principal types of structural damage found in the set of structures analyzed

3. Evaluation of stability conditions

3.1 Evaluation by DNIT Standard 010/2004 – PRO

The criteria for evaluating the structural stability conditions considered by DNIT standard 010/2004-PRO are shown in Table 3 below.

Table 3. Relationship between grades assigned and the category of structural problems observed in the survey of road bridges and viaducts

GRADE	DAMAGE / STRUCTURAL INSUFFICIENCY	CORRECTIVE ACTION	STABILITY CONDITIONS	CLASSIFICATION OF BRIDGE CONDITIONS
5	No damage or structural deficiency	Nothing to do	Good	Structure without problems
4	Some damage, but no sign that it is causing any structural deficiency	Nothing to do beyond regular maintenance service	Good	Structure without significant problems
3	There is some damage generating structural insufficiency, but no signs of compromised stability	The recuperation of the structure can be postponed, but the problem must be systematically monitored	Apparently Good	Potentially problematic structure
				Following the evolution of the problems through routine inspections is recommended, in order to detect any worsening of the deficiency in a timely manner
2	There is damage generating significant structural insufficiency in the bridge, but there is still no apparent tangible risk of structural collapse	Recuperation (usually with structural reinforcement) of the structure must be performed in the short term	Tolerable	Problematic structure
				Too much delay in performing recuperation could leave the structure in a critical state, possibly seriously compromising its useful life. Intermediate inspections to monitor the problems are recommended
1	There is damage	Recuperation	Precarious	Critical Structure

	causing severe structural insufficiency of the bridge; the element in question is in critical condition, with a tangible risk of structural collapse	(usually with structural reinforcement) or in some cases, replacement, must be done without delay		In some cases, it may constitute an emergency situation, and recuperation of the structure may be accompanied by special preventive measures, such as: bridge load restriction, total or partial traffic interdiction, provisional shoring, instrumentation with continuous displacement, deformation readings, etc.
--	--	---	--	--

The application of these criteria to the sample studied is shown in Figure 14, which indicates that 156 SES can be classified as potentially problematic (grade 3), or 46.99%. It is important to note that 174 structures were evaluated as having grades between 1 and 3 (critical to potentially problematic), which is equivalent to 52.41% of the sample studied. Only 59 structures (17.77%) received a grade of 5.

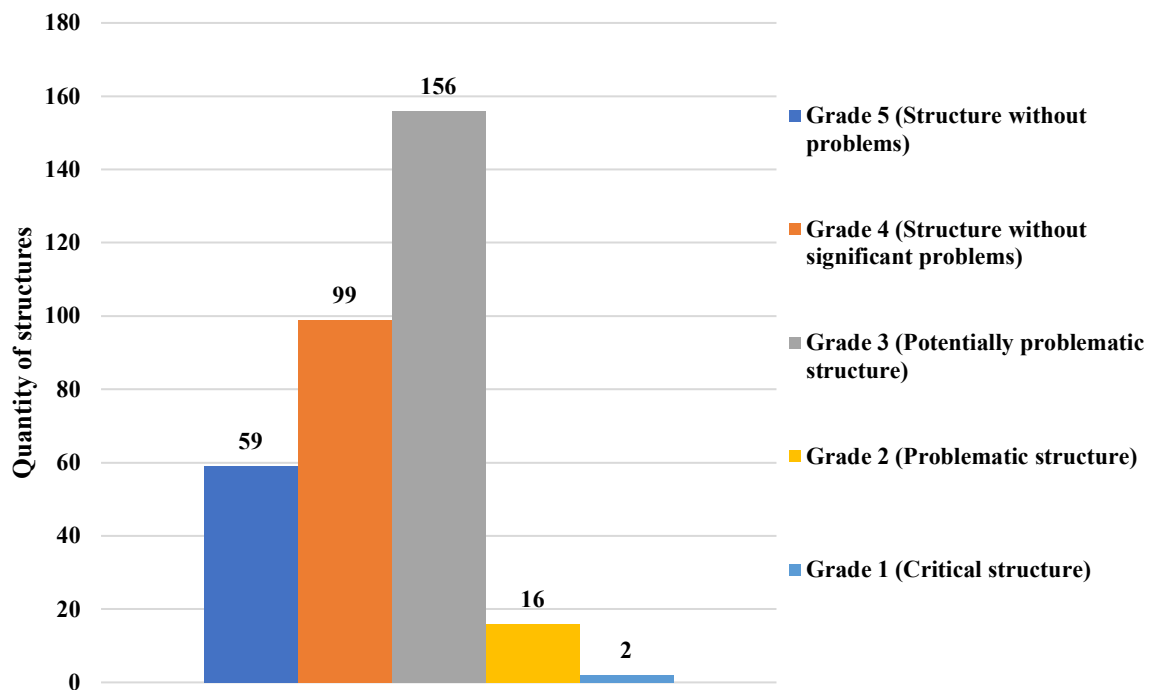


Figure 14. Stability conditions according to DNIT 010/2004-PRO

Table 4 shows the correlation between the construction period and the stability conditions. It also shows that 34% of the structures studied were built between 1960 and 1975, meaning that they are over 40 years old, while 8% are almost 70 years old.

Table 4. Construction period vs. stability condition according to DNIT standard

Construction Period	Total (BR-101, BR-104, BR-110, BR-116, BR-232, BR-316, BR-407, BR-408, BR-423, and BR-428)				
	Grade (Stability condition)				
	Grade 5	Grade 4	Grade 3	Grade 2	Grade 1
1940 to 1960	0	7	14	5	1
1960 to 1975	5	34	67	7	0
1975 to 1985	2	20	28	4	0
1985 to 2000	1	5	3	0	1
After 2000	45	21	17	0	0
Unidentified	6	12	27	0	0
Total	59	99	156	16	2

3.2 Evaluation by NBR 9452/2016

The structural evaluation according to NBR 9452/2016 followed the criteria shown in Table 5. In Table 6 it can be seen that, according to these criteria, a grade of 4 was most common, attributed to 116 bridges. A grade of 5 was obtained by 107 SES, followed by grade 3 (87), grade 2 (20) and grade 1 (2). By these criteria, the 113 structures built between 1960 and 1975 had scores different from those obtained by the criteria of the DNIT standard.

Table 5. Classification of SES condition according to structural, functional, and durability parameters

GRADE	CONDITION	STRUCTURAL CHARACTERIZATION	FUNCTIONAL CHARACTERIZATION	DURABILITY CHARACTERIZATION
5	Excellent	The structure presented satisfactory conditions, with only irrelevant and isolated defects	The SES presents security and comfort to users	SES is in perfect condition and routine maintenance should be provided
4	Good	The structure has a small degree of damage, but in areas that do not compromise structural safety	The SES has minor damages that do not cause discomfort or insecurity to the user	SES presents a few small anomalies, which may compromise its useful life in a region of low environmental aggressiveness
3	Average	There are damages that may cause some structural deficiency, but there are no signs of compromising the stability of the structure. It is recommended to follow up on the problems. Interventions may be necessary in the	The SES causes user discomfort, with defects that require medium-term action	SES has a few small and few anomalies that compromise its useful life, in a region of moderate to high environmental aggressiveness, or SES has many moderate anomalies that compromise its useful life, in a region of low environmental

		medium term		aggressiveness
2	Bad	There are damages that compromise the structural safety of the SES, but without imminent risk. It may evolve to structural collapse. SES needs significant interventions in the short term	SES with functionality visibly compromised and user security risks, requiring short term interventions	SES has moderate or many pathological manifestations, which compromise its useful life in a region of high environmental aggressiveness
1	Critical	There are damages that cause serious structural insufficiency in the SES. There are structural elements in critical condition, with tangible risk of structural collapse. The SES requires immediate intervention and may require load restriction, total or partial traffic ban, provisional shoring, and associated instrumentation	The SES does not present functional, usable conditions	The SES is in a state of high deterioration, indicating a problem of structural and/or functional risk

Table 6. Construction period vs. structural condition using standard NBR 9452

Period of Construction	TOTAL				
	Structural Condition				
	Grade 1	Grade 2	Grade 3	Grade 4	Grade 5
1940 to 1960	1	4	8	8	6
1960 to 1975	0	8	38	54	13
1975 to 1985	0	4	16	24	10
1985 to 2000	1	1	3	1	4
After 2000	0	0	3	16	64
Unidentified	0	3	19	13	10
Total	2	20	87	116	107

3.3 Considerations on the analyses made by the DNIT and ABNT standards

Both standards used in this study assign a classification grade from 1 to 5 for stability conditions. The DNIT 010/2004-PRO Standard also includes concepts, inspection types, the necessary qualifications for inspectors, and the minimum frequency of surveys that allow some evaluation criteria to be defined. However, the recent revision of NBR 9452 (ABNT, 2016), in addition to adopting the concepts and guidelines contained in the DNIT standard, introduced greater flexibility by including structural, functional, and durability parameters. These parameters made inspections and classification criteria of bridges and viaducts in Brazil more realistic.

It is worth highlighting that the two standards made the diagnosis of the main pathological manifestations possible without significant differences in the evaluation of damages and other anomalies in the sample bridges.

On the other hand, when analyzing stability conditions, a considerable difference was observed in the results obtained by each of the two standards, as can be seen in Table 7.

Table 7. Structural condition (Standard DNIT 010/2004-PRO) vs. Structural condition (NBR 9452/2016)

GRADE	DNIT 010/2004 – PRO STANDARD		STANDARD 9452 (ABNT, 2016)	
	SES	%	SES	%
5	59	17.77	107	32.23
4	99	29.82	116	34.94
3	156	46.99	87	26.21
2	16	4.82	20	6.02
1	2	0.6	2	0.6

Even considering that inspections were carried out visually, depending essentially on the experience and judgment of the inspector, the information in Table 7 shows that, with regard to grades 1 and 2, referring to structures in the worst conditions, there were no differences in the results obtained through the two standards.

However, results related to the other grades assigned (3, 4 and 5) show that analysis by NBR 9452 leads to values representing significantly better structural conditions, when compared to those obtained by the DNIT Standard. This means that several bridges and viaducts in this study that may have poor durability conditions and functionality assessments but have satisfactory structural conditions. It also means that these structures can be used without reaching the ultimate state limit. The opposite situation was also verified: bridges and viaducts classified without durability and functionality problems (grades 4 and 5) that had a low structural condition classification.

In general terms, it is possible to affirm that the new version of the ABNT standard that introduces greater variability in the evaluation parameters and applies them to a larger quantity of the elements that make up a bridge, guarantees a more consistent and more realistic evaluation than the DNIT standard, which scores only five elements and is therefore a more conservative evaluation. This is evident in the case of a Special Engineering Structure without major breakdowns that can have one of the elements evaluated with a low rating, and therefore will have the final technical grade correspond to the lowest value among those received all of the

elements. This produces a conservative final assessment that does not represent the actual situation of the bridge.

In this sense, NBR 9452 (ABNT, 2016), even though it also bases its final evaluation on the lowest individual grade, introduces a greater amount of parameters for judgment and therefore is less conservative, because it determines the grades through a more comprehensive analysis. This standard also allows for a more comprehensive and realistic diagnosis of the structure, which is a breakthrough in Brazil, which lacks methods and literature to assess the safety of existing bridges, unlike other countries where sophisticated analyses are used, including probabilistic methods.

4. CONCLUSIONS AND RECOMMENDATIONS

The significant occurrence of structural accidents, some of a serious nature, involving the Brazilian Special Engineering Structures at the federal, state, and municipal levels, is a concrete fact that can be verified through simple observation of the news media. It is possible to conclude that the vulnerability of such structures is directly associated with the environmental aggressiveness of certain regions. Erosion processes at foundations and lack of proper maintenance also contribute to reduced safety and the need for large and costly repairs.

This study sought to contribute to the production of knowledge on this subject, which still lacks specialized literature in Brazil, based on the case study presented, showing a panorama of the current situation of the federal highway network bridges in Pernambuco, and which also represents the situation the bridges in the entire Brazilian road network.

This study showed that a key factor contributing to the occurrence and evolution of damages is the fact that many of these bridges were designed and built during times when the standards did not take into account concepts aimed at guaranteeing greater durability, and there was no knowledge of the performance of the materials used in constructions. In addition, there was a progressive evolution to the flow and weight of vehicles, with significant increase in the mobile loads transmitted to the structures, which were not originally planned for such values. These facts, coupled with the lack of conservation policies and strategies, have accelerated the evolution of the pathological problems, structural damage, and deficiency of functionality of the Brazilian Special Engineering Structures.

This study also showed that the lack of a database containing the cadastral information necessary for the management of Brazilian road network bridges has made the elaboration of precise diagnoses difficult and hindered the adoption of adequate measures to solve the structural and functional problems based on their respective priorities, since a lot of necessary information cannot be found in the SGO of the DNIT.

Even so, this work makes some recommendations that, if adopted, would contribute to the minimization of many of the problems identified in the sample studied which are repeated in other Special Engineering Structures in Brazil. The recommended interventions are shown below in order of priority, according to the frequency of occurrence found during the inspections performed. Most of these recovery and reinforcement interventions are not very complex and do not entail great costs.

- Restoration of the superstructure drainage system, due to the fact that 88.25% of the bridges analyzed had infiltrations and efflorescence in the deck concrete and 27.71% had damaged and/or destroyed drains.
- Recuperation with the application of a concrete layer over the bridge deck, since 52.71% of the sample bridges showed concrete displacement.
- Treatment and/or replacement of corroded reinforcements, which were found in 51.81% of the structures inspected.

- Replacement of damaged or destroyed New Jersey barriers and guardrails, observed in 18.07% of the bridges studied.
- Correction of joint failures, many caused by differential pressure and erosion, found in 16.26% of the bridges. In such cases, it is necessary to carry out geotechnical and hydrological studies to verify the safety of the foundations and the flow section, to determine the necessity of reinforcement and protection against erosion.
- Replacement of damaged expansion joints, responsible for the appearance of pathological manifestations and structural damage in 47.29% of the studied structures.
- Replacement of damaged support units responsible for changes in the transmission of the forces on the bridge deck to the mesostructure, occurring in 7.53% of the bridges.
- Correction of miscellaneous damages such as holes in the concrete, small cracks, and displacements in secondary elements of most bridges surveyed.

The recommendations above should be the focus of projects prepared by specialized professionals and executed by companies with experience in recovery and reinforcement of bridge structures. In the most problematic bridges (those with grades 1 and 2), the first step should be a numerical analysis to measure structural safety and define the need and type of reinforcement.

Another issue that must be considered of fundamental importance in guaranteeing the safety of bridges and viaducts in Brazil is the implementation of management systems at the federal, state, and municipal levels that will allow for the registration of structures, routine inspections, advanced monitoring techniques, and the definition of intervention priorities. Budget resources must also be guaranteed to enable conservation actions to take place before damage develops and worsens exponentially, as it currently occurs.

It must not be forgotten that the Brazilian road network continues to expand, making it necessary to design high quality projects that, in addition to concepts and materials adequate to guarantee a longer useful life, also include appropriate devices to facilitate inspections and preventive maintenance.

Finally, it is possible to conclude that the results obtained from this research, even though referring only to the federal road network in Pernambuco, show the current conservation situation of the Brazilian highway Special Engineering Structures as a whole, and are consistent with studies performed by other authors that analyzed much smaller samples of bridges.

5. ACKNOWLEDGEMENTS

The authors are grateful to the Polytechnic School of the University of Pernambuco, as well as to the National Department of Transportation Infrastructure (DNIT) for allowing access to data and providing information on the bridges studied in this research project.

6. REFERENCES

Associação Brasileira de Normas Técnicas (2016), *NBR 9452: inspeção de pontes, viadutos e passarelas de concreto - procedimento*. Rio de Janeiro.

Cunha, A. A. (2011), *Estudo das patologias em obras de arte especiais do tipo pontes e viadutos estruturados em concreto*. 152p. Final course project (Bachelor's in Civil Engineering) – Universidade Estadual de Goiás, Goiânia.

Departamento Nacional de Infraestrutura de Transportes (2004). *Norma DNIT 010/2004 – PRO: inspeções em pontes e viadutos de concreto armado e protendido – procedimento*. 1.ed. Rio de Janeiro.

Meyer, K. F., *Passarelas e pontes para dutos*. 2. ed. Belo Horizonte: RONA. 243p.

Structural and functional conditions of bridges and viaducts on federal highways in Pernambuco

Milani, C. Kripka, M. Pravia, Z. (2015), *Monitoramento de pontes*. Revista infraestrutura urbana. PINI: São Paulo, 16.ed, 2011. Available at: <<http://infraestruturaurbana.pini.com.br/solucoes-tecnicas/16/artigo260592-1.aspx>>. Accessed on: 12 Apr. 2015.

Silva, C. J. G. (2016), *Uma amostra das condições estruturais e funcionais de pontes e viadutos das rodovias federais de Pernambuco*. Master's Dissertation, Universidade de Pernambuco.

Vitório, J. A. P.; Barros, R. M. M. C. de. (2013) *Análise dos danos estruturais e das condições de estabilidade de 100 pontes rodoviárias no brasil*. In: Congresso da Associação Portuguesa Para a Segurança e Conservação de Pontes, 3, 2013, Porto. Anais... Porto, 9p.

Evaluation of pathological problems associated with carbonation and sulfates in a concrete tower with more than 50 years in service

E. E. Maldonado-Bandala^{1*}, D. Nieves-Mendoza¹, J. L. Vela-Jiménez², P. Castro-Borges³.

*Corresponding author: claytonjgsilva@gmail.com

DOI: <http://dx.doi.org/10.21041/ra.v8i1.284>

Received: 14/12/2017 | Accepted: 22/12/2017 | Published: 31/01/2018

ABSTRACT

This work presents and discuss the results of a corrosion inspection, as well as a repair proposal for the external walls of a reinforced concrete tower which is in the southern coast of the Veracruz state. The inspection included a drone guided damage survey together with physical, chemical, mechanical and electrochemical tests that allowed the concrete characterization and corrosion damage. The governing deterioration mechanism of the structure was carbonation of concrete. However, the sulfate emission in this industrial environment was reflected on the compressive resistance, cracks and delaminations. These conditions were taken into account on the proposed actions for repairing and extending the service life of the structure.

Keywords: inspection, tower, reinforced concrete, diagnosis, service life.

Cite as: E. E. Maldonado-Bandala, D. Nieves-Mendoza, J. L. Vela-Jiménez, P. Castro-Borges (2018), “*Evaluación de problemas patológicos asociados a carbonatación y sulfatos en una torre de concreto con más de 50 años de servicio*”, Revista ALCONPAT, 8 (1), pp. 94 – 107, DOI: <http://dx.doi.org/10.21041/ra.v8i1.284>

¹Facultad de Ingeniería Civil, Universidad Veracruzana, Circ. Gonzalo Aguirre Beltrán s/n, Zona Universitaria, C.P. 91000, Xalapa, Veracruz, México.

²Consortio RNC S.A. de C.V. Esteban Mascareñas 44, Col Mártires de Chicago C.P. 91090, Xalapa, Veracruz, México.

³Centro de Investigación y de Estudios Avanzados del IPN Unidad Mérida, Antigua Carretera a Progreso Km. 6, 97310 Mérida, Yucatán, México; Tels. (999) 942-94-00. Fax: (999) 981-29-23

Legal Information

Revista ALCONPAT is a quarterly publication of the Latinamerican Association of quality control, pathology and recovery of construction- International, A. C., Km. 6, antigua carretera a Progreso, Mérida, Yucatán, C.P. 97310, Tel.5219997385893, alconpat.int@gmail.com, Website: www.alconpat.org

Editor: Dr. Pedro Castro Borges. Reservation of rights to exclusive use No.04-2013-011717330300-203, eISSN 2007-6835, both awarded by the National Institute of Copyright. Responsible for the latest update on this number, ALCONPAT Informatics Unit, Ing. Elizabeth Sabido Maldonado, Km. 6, antigua carretera a Progreso, Mérida, Yucatán, C.P. 97310.

The views expressed by the authors do not necessarily reflect the views of the publisher.

The total or partial reproduction of the contents and images of the publication without prior permission from ALCONPAT International A.C. is not allowed.

Any discussion, including authors reply, will be published on the third number of 2018 if received before closing the second number of 2018.

Evaluación de problemas patológicos asociados a carbonatación y sulfatos en una torre de concreto con más de 50 años de servicio

RESUMEN

En este trabajo se presentan y discuten los resultados de la inspección por corrosión, y una propuesta de reparación de los muros exteriores de una torre de concreto reforzado localizada en la costa sur del estado de Veracruz. La inspección incluyó un levantamiento de daños con un dron, y ensayos físicos, químicos, mecánicos y electroquímicos que permitieron caracterizar el concreto y los daños por corrosión. El mecanismo gobernante de la corrosión en la estructura estudiada fue la carbonatación. Sin embargo, la emisión de sulfatos en ese ambiente industrial se reflejó en la resistencia a la compresión, grietas y delaminaciones. Las condiciones anteriores fueron contempladas en las acciones propuestas de reparación para extender su vida de servicio.

Palabras clave: inspección; torre; concreto reforzado; diagnóstico; vida de servicio.

Avaliação de patologias associadas com carbonatação e sulfatos em uma torre de concreto com mais de 50 anos de serviço

RESUMO

Este artigo apresenta e discute os resultados da inspeção de corrosão e uma proposta para reparar as paredes exteriores de uma torre de concreto armado localizada na costa sul do estado de Veracruz. A inspeção incluiu uma pesquisa de danos com um drone e testes físicos, químicos, mecânicos e eletroquímicos que permitiram a caracterização de danos de concreto e corrosão. O mecanismo governante de corrosão na estrutura estudada foi a carbonatação. No entanto, a emissão de sulfatos neste ambiente industrial foi refletida na resistência à compressão, fissuras e delaminações. As condições acima foram contempladas nas ações de reparo propostas para ampliar sua vida útil.

Palavras-chave: inspeção; torre; concreto armado; taxa de corrosão; diagnóstico; vida útil.

1. INTRODUCTION

As part of a recent reform of the energy sector in Mexico, the federal government is required to purchase unproductive properties and buildings from the private sector. Many of these have been abandoned for decades and exhibit high degrees of degradation due in part to accelerated corrosion phenomena resulting from lack of maintenance and exposure to aggressive environments.

Corrosion of reinforced concrete structures is a serious problem, particularly in industrial environments. It can manifest as intense pathological signs which can lead to critical problems in function, safety, excessive rehabilitation and service costs and loss of appearance; indeed, depending on the degree of damage, it can put human life at risk (Helene, 2003; Sulaimani 1992, Andrade 1992; del Valle et al., 2006).

Many of the properties to be acquired by the federal government are petroleum industry installations. Restoring these to productive levels of functioning will require rehabilitation. The causes for corrosion-related failures will need to be investigated as well as the complex relationship between the physical, chemical and mechanical properties of the concrete and steel reinforcement.

The present study responds to the need to rehabilitate and return to operation reinforced concrete towers in petroleum industry installations in the southern portion of the state of Veracruz, Mexico. These are a vital asset in this industry, which is economically significant in the region. The towers were evaluated with an emphasis on durability. This involved destructive and non-destructive assays, visual inspection using an aerial drone, and electrochemical, chemical and mechanical tests. These evaluations are discussed and a structural diagnosis presented highlighting the mechanisms that intensified corrosion. The final objective is to identify the corrective measures needed to extend the use life of these existing assets.

2. INSPECTION PLAN

2.1 Preliminary inspection

A survey was done of the structure, the exposure environment and damages. Due to the tower's structural complexity and dimensions, images were taken of its elements. Visual survey was done and images taken using an aerial drone (Phantom 4), following programmed schemes as indicated in the DURAR Manual (Troconis del Rincón et al., 1997).

2.2 Detailed inspection

Premature failures in concrete structures are mainly due to lack of quality control and incorrect construction, repair and rehabilitation procedures (DURACON, 2007). A series of trials and measurements are needed to collect data to identify the causes and the proper stage of prevention. This data is used for problem evaluation, and to define the nature and mechanism of corrosion in the case at hand.

2.2.1 *Electrochemical Evaluation*

Steel position was detected with a wall scanner and electrochemical measurements taken. Current measurement (E_{corr} vs. Cu/CuSO_4) was done following the guidelines in ASTM C876-09 (2009) and NMX-C-495-ONNCCE-2015 (2015). Corrosion rate (i_{corr}) was measured with the polarization resistance technique, using a GECOR 10 (Feliú et al., 1993) and according to NMX-C-501-ONNCCE-2015 (2015). The resulting data served to clearly define points of active corrosion in the structure.

2.2.2 *Physicochemical Evaluation*

Cores were extracted from the structure to directly test concrete quality and its potential to corrode the reinforcement. Assays were done of carbonation depth (NMX-C-515-ONNCCE-2016, 2016), chloride concentration (ASTM C114-05, 2005), and sulfate chemical attack. Concrete resistance to simple compression was tested with a hardened concrete core test (NMX-C-083-ONNCCE 2010, 2010).

3. RESULTS AND DISCUSSION

The tower in question is exposed to an aggressive environment, classified as B2 according to the Federal District Complementary Technical Guidelines (Normas Técnicas Complementarias de Distrito Federal - NTC-DF). This classification is based on its location in the midst of large bodies of marine waters: Laguna de Pajaritos is 700 m north and the Coatzacoalcos River is 600 and 2700 m east. It is also exposed to air containing industrial gases originating in a petrochemical complex immediately to the south (Figure 1). In addition, climate in the zone is humid tropical with a rainy season from June to September. Rainfall is highest during August and

September. Annual rainfall percentage varies from 6 to 10.5% compared to the driest month of the year.

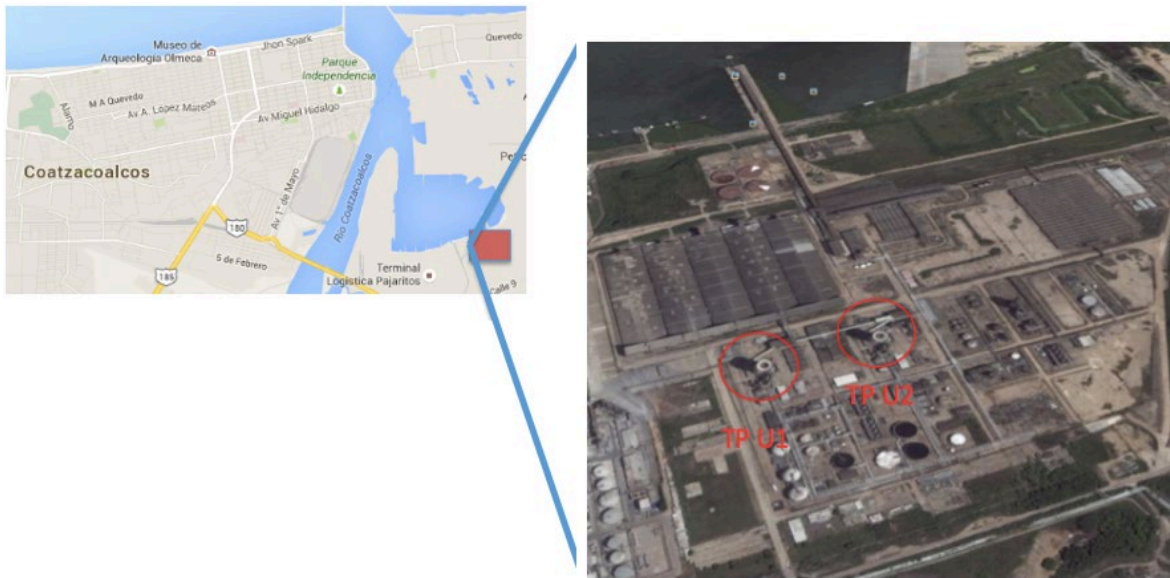


Figure 1. Tower location, indicated as “U2”.

The studied structure is a cylindrical tower (23 m diameter x 70+ m high). The walls are 30+ cm thick and built of concrete reinforced with AISI 1018 steel. Aggregate is silicate sand and thick quartz gravel. Based on its Mohs scale value (7) and the prevalence of SiO_2 in its chemical structure, quartz has high hardness. However, aggregate particle shape is rounded, providing weak traction in the concrete mass. Fifty years of service and its location in an industrial-marine environment have caused the tower to develop a combination of almost imperceptible and quite evident damage.

3.1 Visual inspection with drone

An aerial drone was used to facilitate damage survey due to structural complexity, limited access to high areas and time concerns. An autonomous mission was designed using a flight plan based on sequential GPS points along the tower’s four vertical surfaces (north, east, south and west). Drone cruise speed was controlled such that high quality images were taken in areas with visible structural damage. These were converted into two-dimensional maps and areas with the greatest visible damage marked (Figure 2).

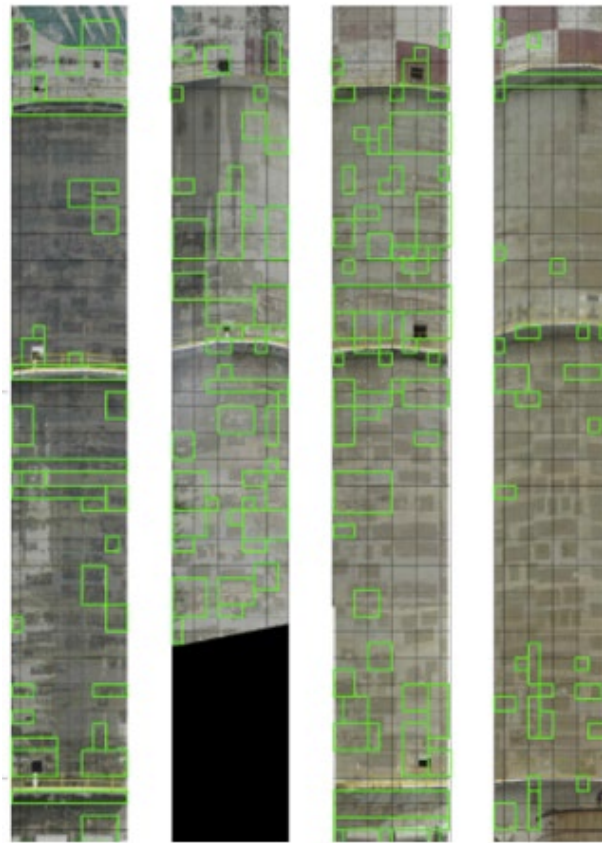


Figure 2. Two-dimensional map of drone images. Areas of major visible damage delimited by green lines.

Previous, localized repairs are clearly visible in the images. Since these were probably not done adequately, they may have accelerated deterioration processes in the concrete-steel system (Figure 3 and 4). There are also areas of concrete detachment and spalling, exposed steel reinforcement, diminished section of the reinforcement and cracks ranging in length from approximately 0.50 m to 5.00 m and in width from 3 mm and up.



Figure 3. Exposed steel reinforcement, corrosion, concrete spalling and multiple rectangles indicating the sites of previous localized repairs.



Figure 4. Detail of localized repairs in which the more recent concrete has separated from the original concrete, causing occasional spalling and anodic zones favoring formation of corrosion cells.

Twelve study zones were then located on the structure and analyses done at these locations: linear polarization resistance using a guard ring to restrict the current (Andrade et al., 2004); half-cell potentials; and chemical tests to measure the carbonation profile and chlorine and sulfate concentrations. A test was also done of resistance to compression and the cover thickness measured with a wall sensor. Test zones were assigned keys indicating their locations (Table 1).

Table 1. Test zone nomenclature.

Classification	-	Height of test	-	Test point or zone number
U2 (Tower)		Np (ground level) P1 (catwalk 1) P2 (catwalk 2) P3 (catwalk 3)		01-12
For example: Tower - Catwalk 1- Test Zone 01 = U2-P1-P01				

3.2 Detailed Inspection

3.2.1 Resistance to simple compression ($f'c$)

Overall $f'c$ values were less than 250 kg/cm^2 (Table 2), and in test zone U2-P1-P04 values were less than 50% of the recommended value (350 kg/cm^2 ; NTC-DF, 2008). These values are indicated for exposure to a B2 environment, that is, member surfaces in contact with the soil and exposed to aggressive exterior environments.

Table 2. Results of electrochemical, chemical and physical tests.

Location Code	U2-NP-P01	U2-P1-P02	U2-P1-P03	U2-P1-P04	U2-P1-P05	U2-NP-P06
Orientation	West	South	South	South	South	North
Height from base of structure (m)	0	16	16	16	16	0
Resistance to Simple Compression f_c (kg/cm ²)	246.09	---	181.30	114.92	---	
	Minimum resistance for concretes exposed to sulfates = 350 kg/cm² (NTC-DF, 2008)					
Chloride Concentration at 3 cm depth (% pp concrete weight)	---	---	0.05	0.039	---	0.079
	Chloride Threshold = 0.11% pp concrete (P. Castro-Borges, 2013) in marine environment					
Chloride Concentration at 3 cm depth (% pp in concrete weight)	---	---	0.65	0.41	---	0.81
	Maximum admissible concentration = 0.45 % pp concrete (Andrade et al. 1998)					
Sulfates Concentration at 3 cm depth (% pp concrete)	19.35 13.37	---	21.77	46.09	---	---
Corrosion Potential (mV vs. Cu/CuSO ₄)	>-200	>-200	>-200	<-350	>-200	>-200
Corrosion rate (μA/cm ²)	0.1 – 0.5	> 1	0.1 – 0.5	> 1	> 1	0.1 – 0.5
	Moderate	Very High	Moderate	Very High	Very High	Moderate
Average cover (mm)	30.5	38	34.5	34.5	28	36
	Minimum cover in B2 environment = 45 mm (NTC-DF, 2008)					
Average rebar diameter (mm)	17.9	17.9	16.9	19.5	19.6	24.9

Location Code	U2-NP-P07	U2-NP-P08	U2-P2-P09	U2-P2-P10	U2-P3-P11	U2-P3-P12
Orientation	South	East	East	South	South	East
Height from base of structure (m)	0	0	45	45	60	60
Resistance to Simple Compression f_c (kg/cm ²)	164.57	186.89	---	---	---	---
	Minimum resistance for concretes exposed to sulfates = 350 kg/cm² (NTC-DF, 2008)					
Chloride Concentration at	0.03	---	0.037	---	0.032	---

3 cm depth (% pp concrete weight)	Chloride Threshold = 0.11% pp concrete (P. Castro-Borges, 2013) in marine environment					
Sulfates Concentration at 3 cm depth (% pp concrete)	0.38	---	0.25	---	0.30	---
	Maximum admissible concentration = 0.45 % pp concrete (Andrade et al. 1998)					
Depth of Carbonation (mm)	11.11	13.42	---	---	---	---
Corrosion Potential (mV vs. Cu/CuSO ₄)	-200 a - 350	>-200	>-200	-200 a - 350	>-200	>-200
Corrosion rate (μA/cm ²)	0.1 – 0.5	0.5 – 1	> 1	> 1	0.5 – 1	0.5 – 1
	Moderate	High	Very High	Very High	High	High
Average cover (mm)	39	50	22	36.5	30.5	27.3
	Minimum cover in B2 environment = 45 mm (NTC - DF, 2008)					
Average rebar diameter (mm)	21.1	20.3	20.9	30.6	22.5	20.4

3.2.2 Depth of Carbonation

In some samples the depth of carbonation was notable. For example, in U2-P1-P04 a clear colorless zone was visible after phenolphthalein application (Figure 5). This indicates a considerable drop in concrete pH that extends to the depth of the rebar (Table 2). Severe damage is also present from cracks running parallel to the wall surface.

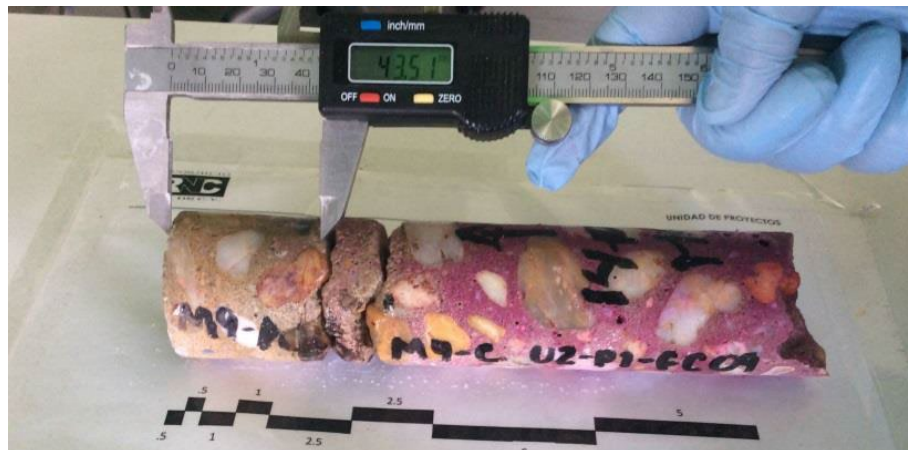


Figure 5. Depth of carbonation in U2-P1-P04. Note depth of damage and cracks parallel to the surface.

3.2.3 Sulfates concentrations

At the concrete surface, this parameter varied from 0.25 to 1.0% pp concrete content, and at 3 cm depth it varied from 0.50 to 0.80% pp concrete content (Figure 6). These are considered high values since the limit is 0.40% pp concrete content. Nearby sources of high sulfate levels include marine waters, industrial gases and the water in adjacent cooling towers. Sulfate attack of concrete components can cause formation of ettringite and plaster.

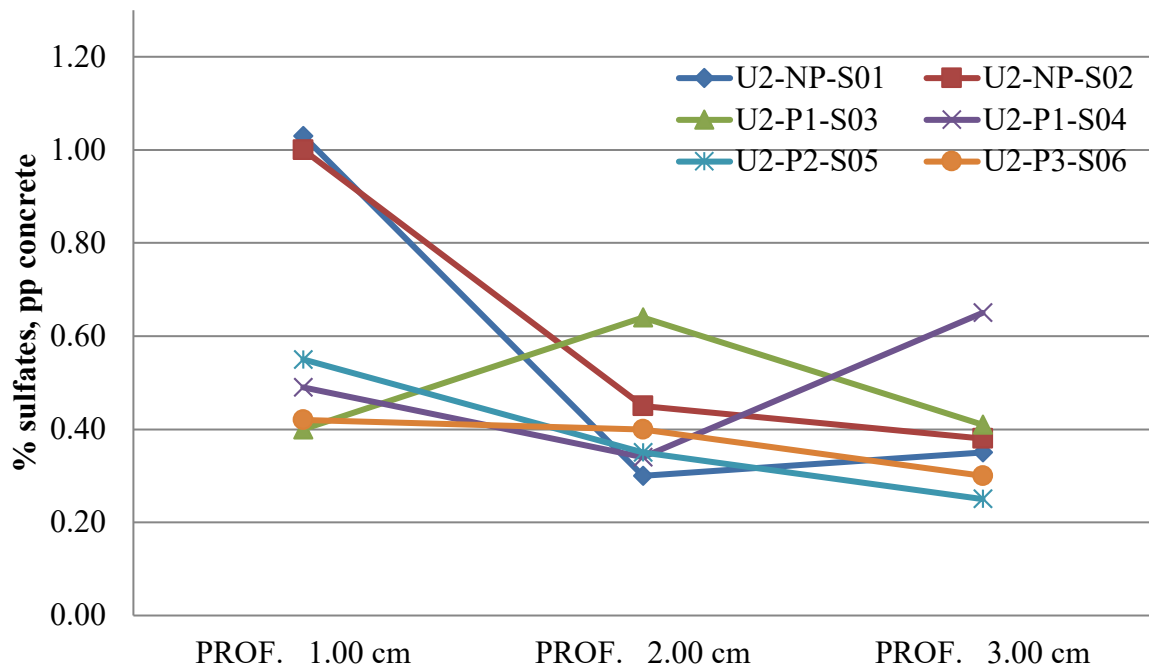


Figure 6. Sulfate concentration in concrete samples by depth. All tested areas exceeded the 0.40% pp concrete threshold, indicating sulfates damage. (PROF = DEPTH)

3.2.4 Chlorides concentration

Chlorides levels have not reached concentrations which could cause corrosion problems in the steel reinforcement and therefore do not seriously threaten structure integrity (Table 2) (Troconis et al., 1997; DURACON, 2006; DURACON, 2007).

3.2.5 Corrosion rate

Non-destructive tests of corrosion rate were run even though areas of exposed steel were quite evident and rebar corrosion was obvious. Values for this parameter were moderate to very high in most cases (Table 2), with values near $5 \mu\text{A}/\text{cm}^2$ (Figure 7).

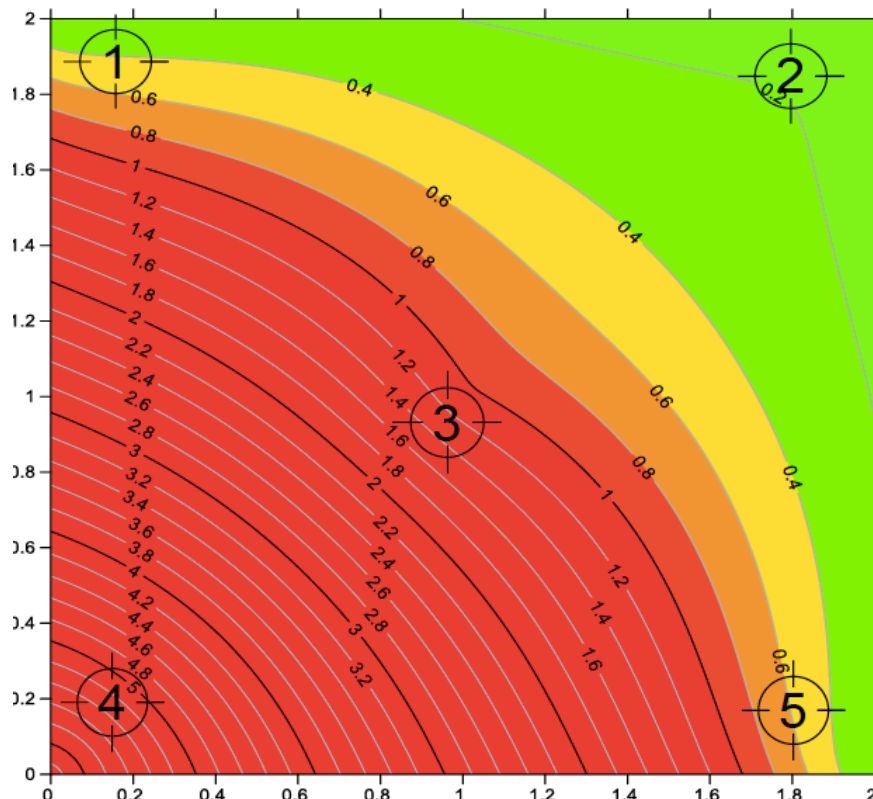


Figure 7. Corrosion rate isovalues for study zone U2-P1-P04; most values are very high.

The very high corrosion rate values may have been caused by localized repairs done with uncompacted materials, which cause cracks and spalling between the new and pre-existing concrete. This is a very common effect at the concrete-steel interface in real structures. It arises from the “top-bar” effect in which adherence to the steel reinforcement decreases in the cover, particularly in thick concrete with inadequate compaction (P.R. Jeanty et al., 1988; A. Castel, 2006). It can also result from corrosion caused by galvanic current within the macrocell. This is caused by an electric connection between rebar exposed to different electrochemical surroundings, that is, passive steel in recently repaired zones and active steel in carbonated zones (J. Gulikers and M. Raupach, 2006; J. Warkus and M. Raupach, 2006). High galvanic currents result which lead to high corrosion levels according to RILEM recommended levels (A. Nasser et al., 2010).

System electrolyte characteristics are vital to identifying the elements needed for aggressive agent contamination and thus to understanding the corrosion mechanisms occurring in the studied structure. The studied concrete tower is located inside a petrochemical plant and adjacent a series of cooling towers. The main mechanism for lowering water temperature in these towers is partial evaporation, which causes a gradual decrease in the quality of the circulating water. It also leads to a continuous increase in chemical compound concentration within the condenser system, and constant emission of sulfate solutions.

Sulfate ion ingress and low compression resistance values are two important conditions that can induce degradation of structural properties in the studied structure. Sulfate attack is known to be quite complicated (E.F. Irassar, 2009), although there are some principal factors that affect the evolution of concrete properties, such as sulfate solution concentration, exposure to high temperatures and low concrete pH (J. Skalny, 2002). All three of these factors were present in the studied structure. Indeed, the sulfates concentration considerably exceeded the proposed maximum concentration (C. Andrade, 1998), possibly leading to formation of ettringite and plaster. This could have accelerated concrete degradation as the products of concrete hydration

and the sulfate ion solution caused expansion and cracking (C. Yu et al., 2015; F. Bellmann et al., 2006). After exposure to soluble sulfates a concrete matrix can soften or its overall porosity increase, thus reducing structure durability.

3.3 Rehabilitation-reinforcement proposal

After the inspection, recommendations were made to immediately begin repair, rehabilitation and reinforcement. A general description is provided below, but a full account is contained in the corresponding executive report. Increasing the structure's residual use life will require that the entire tower be addressed to prevent the creation of zones vulnerable to galvanic effects.

Preliminaries

Deteriorated and/or contaminated concrete should only be removed from anodic zones. Steel rebar needs to be cleaned and the substrate prepared following official guidelines (NMX-C-518-ONNCCE-2016, 2016). If deemed necessary after evaluation, rebar should be replaced.

Stage 1

The high corrosion rate results suggest the presence of zones in which loss of steel reinforcement section is advanced. In places where the decrease in original nominal diameter exceeds 10% the structure needs to be reinforced through substitution of the damaged rebar with rebar of the original diameter and with the same yield point (f_y) to meet applicable regulations (NMX-B-457-CANACERO-2013, 2013). Repair sequence and geometry must meet the guidelines in the Rehabilitar network manual (Helene, 2003).

Stage 2

Due to the structure's geometrical condition and the difficulty of building centering and applying spray concrete at high altitudes, section recovery is best done using prepared structural repair mortar containing sulfate resistant (RS) Portland cement complying with applicable regulations (NMX-C-414-ONNCCE-2014, 2014; NMX-C-418-ONNCCE-2015, 2015). It will need to be sufficiently fluid to allow for manual application.

Stage 3

To reduce the probability of corrosion in repaired areas, calcium nitrate corrosion inhibitor will need to be applied according to ASTM C494 / C494M-17 (2017).

Stage 4

Low resistance to compression in the structure's concrete will require reinforcement of the base with carbon fiber reinforced polymer (CFRP) up to the catwalk 1 (P1) level. This system will increase confinement, and resistance to shear force and external loads (e.g. winds and earthquakes), without compromising structure ductility (ACI-440R-07, 2007).

Stage 5

A chloride-impermeable anti-carbonation covering will need to be applied with the capacity to bridge cracks and including chemical components complying with ASTM C494 / C494M-17 (2017). If cracks appear they should be covered since these are the primary point of contaminant ingress.

4. CONCLUSIONS

Use of an aerial drone for inspection of reinforced concrete is a powerful tool allowing visual examination of otherwise inaccessible areas.

Carbonation is the primary mechanism of corrosion in the studied structure. The high CO₂ concentration and high relative humidity in the surrounding environment have reduced concrete pH and generated depassivation of the steel reinforcement.

Sulfate emissions in the surrounding industrial environment and their sulfate deposition on the structure's concrete walls has caused a notable decrease in mechanical resistance. This is clearly visible in the form of cracks and spalling.

Previous localized repairs accelerated corrosion damage in adjacent zones by creating galvanic cells.

Low mechanical resistance values in the concrete and high corrosion rate values in different zones of the structure have compromised its structural integrity. This can pose a safety risk for personnel working in the area and therefore requires immediate rehabilitation and reinforcement.

The five-stage repair proposal presented here can be expanded into a full structural repair executive project.

5. REFERENCES

A. Castel, T. Vidal, K. Viriyametanont, R. François, “*Effect of Reinforcing Bar Orientation and Location on Bond With Self-Compacting Concrete*”, ACI Struct. J. 3, Vol. 4 (2006) 559–567.

A. del Valle, J. Perez, A. Torres, M. Madrid, “*Evaluación del Puente Pajaritos: Una Estructura de Concreto de 50 Años en el Ambiente Agresivo del Golfo de México*” Ingeniería de Construcción, Vol (21) 1, (2006)

A. L. Sulaimani, J. Kaleemullah, M. Bsulbul, A. Rasheeduzzafar, “*Influence of Corrosion and Cracking on Bond Behavior and Strength of Reinforced Concrete Members*”. ACI structural Journal. (1992) pp. 220-231.

A. Nasser, A. Clement, S. Laurens, A. Castel, “*Influence of Steel-Concrete Interface Condition on Galvanic Corrosion Currents in Carbonated Concrete*”, Corros. Sci. Vol. 52 (2010) 2878–2890, <https://doi.org/10.1016/j.corsci.2010.04.037>

ACI 440R-07 Report on Fiber-Reinforced Polymer (FRP) Reinforcement for Concrete Structures, American Concrete Institute (2007)

ASTM C114-05, *Standard Test Methods for Chemical Analysis of Hydraulic Cement*, ASTM International, West Conshohocken, PA, (2005) DOI: <https://doi.org/10.1520/C0114-05>

ASTM C494 / C494M-17, *Standard Specification for Chemical Admixtures for Concrete*, ASTM International, West Conshohocken, PA, 2017. DOI: https://doi.org/10.1520/C0494_C0494M-17

ASTM C876-09, *Standard Test Method for Corrosion Potentials of Uncoated Reinforcing Steel in Concrete*, ASTM International, West Conshohocken, PA, (2009) DOI: <https://doi.org/10.1520/C0876-09>

C. Andrade, “*Manual de Inspección de obras dañadas por corrosión de armaduras*” CSIC (1998)

C. Andrade, “*Vida útil de las Estructuras de Hormigón Armado: Obras Nuevas y Deterioradas*” Seminario Internacional EPUSP/FOSROC sobre patología das estruturas de concreto-Uma Visao moderna. Anis. San Paulo. (1992)

C. Andrade, C. Alonso, J. Gulikers, R. Polder, R. Cigna, Vennessland, M. Salta, A. Raharinaivo, B. Elsener “*Thest Metod for On-Site Corrosion rate Measurement of Steel Reinforcement in Concrete by Means of the Polarization Resistance Method*” Material and Structures/Matériaux et Constructions. Vol 37 (2004) pp. 623-643. DOI: <https://doi.org/10.1007/BF02483292>

- C. Yu, W. Sun, K. Scrivener “*Degradation Mechanism of Slag Blended Mortars Immersed in Sodium Sulfate Solution*” *Cem. Concr. Res.*, Vol. 72 (6) (2015), pp. 37-47.
<https://doi.org/10.1016/j.cemconres.2015.02.015>.
- Cem. Concr. Res.*, Vol. 39 (3), (2009), pp. 241-254
- DURACON Collaboration, O. Trocónis de Rincón and coauthors. “*Durability of concrete structures: Duracon, an Iberoamerican Project. Preliminary results*”. Building & Environment. Elsevier Science LTD Publication. Vol 41 (7). (2006). pp. 952-962.
- DURACON Collaboration, O. Trocónis de Rincón and coauthors. “*Effect of the Marine Environment on Reinforced Concrete Durability in Iberoamerican Countries: DURACON Project/CYTED*”. Corrosion Science. Elsevier Science LTD Publication. Vol. 49 (7). (2007). pp. 2832-2843. <https://doi.org/10.1016/j.corsci.2007.02.009>.
- E. F. Irassar “*Sulfate Attack on Cementitious Materials Containing Limestone Filler – A Review*” *Cem. Concr. Res.*, Vol. 39 (3), 2009, Pages 241-254.
<https://doi.org/10.1016/j.cemconres.2008.11.007>.
- F. Bellmann, B. Möser, J. Stark “*Influence of Sulfate Solution Concentration on the Formation of Gypsum in Sulfate Resistance Test Specimen*” *Cem. Concr. Res.*, Vol. 36 (2) (2006), pp. 358-363.
<https://doi.org/10.1016/j.cemconres.2005.04.006>.
- J. Gulikers, M. Raupach, “*Numerical Models for the Propagation Period of Reinforcement Corrosion – Comparison of a Case Study Calculated by Different Researchers*”, *Mater. Corros.* Vol. 57 (8) (2006) 618–627. <https://doi.org/10.1002/maco.200603993>
- J. Skalny, J. Marchand, I. Odler, “*Sulfate Attack on Concrete*” Spon Press, New York (2002)
- J. Warkus, M. Raupach, “*Modelling of Reinforcement Corrosion – Corrosion With Extensive Cathodes*”, *Mater. Corros.* Vol. 57 (12) (2006) 920–925. <https://doi.org/10.1002/suco.201200003>
- NMX-B-457-CANACERO-2013, *Industria Siderúrgica – Varilla Corrugada de Acero de Baja Aleación para Refuerzo de Concreto – Especificaciones y Métodos de Prueba*, CANACERO (2013)
- NMX-C-083-ONNCCE 2010, *Industria de la Construcción – Concreto – Determinación de la Resistencia a la Compresión de Especímenes – Método de Ensayo*, ONNCCE, México DF, (2010)
- NMX-C-414-ONNCCE-2014, *Industria de la Construcción – Cementantes Hidráulicos – Especificaciones y Métodos de Ensayo*. ONNCCE, México DF, (2014)
- NMX-C-418-ONNCCE-2015, *Industria de la Construcción – Cementos Hidráulicos – Determinación del Cambio de Longitud de Morteros con Cemento Hidráulico Expuestos a una Solución de Sulfato de Sodio*. ONNCCE, México DF, (2015)
- NMX-C-495-ONNCCE-2015, *Industria de la Construcción - Durabilidad de Estructuras de Concreto Reforzado - Medición de Potenciales de Corrosión del Acero de Refuerzo sin Revestir, Embebido en Concreto - Especificaciones y Método de Ensayo*. ONNCCE, México DF, (2015)
- NMX-C-501-ONNCCE-2015, *Industria de la Construcción - Durabilidad de Estructuras de Concreto Reforzado - Medición de Velocidad de Corrosión en Campo - Especificaciones y Método de Ensayo*. ONNCCE, México DF, (2015)
- NMX-C-515-ONNCCE-2016, *Industria de la Construcción – Concreto Hidráulico – Durabilidad – Determinación de la Profundidad de Carbonatación en Concreto Hidráulico – Especificaciones y Método de Ensayo*. ONNCCE, México DF, (2016)
- NMX-C-518-ONNCCE-2016, *Industria de la Construcción - Durabilidad de Estructuras de Concreto Reforzado – Procedimientos de Preparación y Limpieza de Superficies para Reparación*. ONNCCE, México DF, (2016)
- NTC DF *Normas Técnicas Complementarias para Diseño y Construcción de Estructuras de Concreto* México DF (2008)
- O. Troconis de Rincón y Miembros de la Red DURAR. *Red Temática XV.B. Durabilidad de la Armadura. Manual De Inspección, Evaluación y Diagnóstico de Corrosión en Estructuras de*

Hormigón Armado, CYTED Maracaibo. Venezuela. (1997).

P. Castro-Borges, M. Balancán-Zapata, A. López-González, “*Analysis of tools to evaluate chloride threshold for corrosion onset of reinforced concrete in tropical marine environment of Yucatán, México*”. *Journal of Chemistry*, (2013), Article ID208619, Hindawi Publishing Corporation, <http://dx.doi.org/10.1155/2013/208616>, 8p.

P. Helene, F. Pereira (2003), *Manual de Rehabilitación de Estructuras de hormigón. Reparación, Refuerzo y Protección*. Rehabilitar Red Temátca XV.F CYTED. Primera edición .

P.R. Jeanty, D. Mitchell, M.S. Mirza, “*Investigation of Top Bar effects in Beams*”, *ACI Struct. J.* Vol.85 (3) (1988) 251–257.

Paweł Regucki, R. Krzyzyska, Z. Szeliga, H. Jouhara, “*Mathematical Model of Sulphate ion Concentration in a Closed Cooling System of a Power Plant*” *Thermal Science and Engineering Progress* Vol.4 (2017) 160–167. <https://doi.org/10.1016/j.tsep.2017.09.012> .

S. Feliú, J.A. González, V. Feliú, Jr S. Feliú, M.L. Escudero, I. Rz Maribona, V. Austiín, C. Andrade, J.A. Bolaño, F. Jiménez F. (1993), *U.S. Patent No. 5.259.944*. (1993)